The amazing osteoclast

Towards an *in vitro* 3D
co-culture model of bone

Stefan J. A. Remmers

The amazing osteoclast

Towards an *in vitro* 3D co-culture model of bone

Stefan J. A. Remmers

The amazing osteoclast

Towards an *in vitro* 3D co-culture model of bone

PROEFSCHRIFT

ter verkrijging van de graad van doctor aan de Technische Universiteit Eindhoven, op gezag van de rector magnificus prof.dr.ir. F.P.T. Baaijens, voor een commissie aangewezen door het College voor Promoties, in het openbaar te verdedigen op dinsdag 14 maart 2023 om 16:00 uur.

door

Stefan Johannes Abraham Remmers

geboren te Tilburg

Dit proefschrift is goedgekeurd door de promotoren en de samenstelling van de promotiecommissie is als volgt:

voorzitter:	prof. dr. M. Merkx
1e promotor:	prof. dr. K. Ito
2e promotor:	dr. S. Hofmann
leden:	prof. dr. J. de Boer
	dr. J.J.C. Arts
	prof. dr. P. Habibovic - *Maastricht University*
	prof. dr. J. Klein-Nulend - *Academisch Centrum voor Tandheelkunde Amsterdam*
	dr. ing. J. J. J. P. van den Beucken - *Radboud Universiteit Nijmegen*

Het onderzoek of ontwerp dat in dit proefschrift wordt beschreven is uitgevoerd in overeenstemming met de TU/e Gedragscode Wetenschapsbeoefening.

Summary

Bone is a highly dynamic tissue with both mechanical and metabolic functions. As the mechanical demands placed upon bones change, bones adapt and optimize their structure and strength by removing obsolete or damaged tissue and producing new or stronger tissue when and where needed. The cells responsible for bone remodeling are the bone forming osteoblasts, the bone resorbing osteoclasts, and the regulating osteocytes. In healthy tissue, bone resorption and formation are in equilibrium. In diseases such as osteoporosis this equilibrium is disturbed, leading to pathological changes that affect the bone's mechanical functionality. Many treatment options are available for osteoporosis, but the degenerative nature of osteoporosis still cannot be undone, highlighting the need for accurate, reproducible, and translatable model systems to study the cellular and molecular mechanisms underlying bone remodeling and bone disease.

Because bone remodeling is a 3D process involving both osteoblasts and osteoclasts, a 3D *in vitro* co-culture would be well-suited for studying bone remodeling. 3D osteoblast-osteoclast co-cultures have been in development for many years but are routinely analysed using destructive techniques. Earlier, a 3D *in vitro* model in which mesenchymal stromal cells differentiated into osteoblasts and deposited mineralized matrix onto silk-fibroin scaffolds was developed where mineralized matrix deposition was monitored over time using micro-computed tomography (Melke et al., 2018). The model was shown to be capable of monitoring formation over time but did not include osteoclasts and was therefore not capable of monitoring resorption over time. This model was used as the foundation of the work reported in this thesis.

The aim of this thesis was to develop a human *in vitro* 3D osteoblast-osteoclast co-culture model in which both bone formation and resorption could be monitored over time.

To develop this model, we first assessed the base of knowledge available on osteoblast-osteoclast co-cultures. A systematic review was conducted identifying all available osteoblast-osteoclast co-cultures. Their methods were analyzed and extracted into two

databases, which resulted in a comprehensive interactive systematic map. This systematic map provided an unprecedented amount of information on cells, culture conditions and analytical techniques used in literature for osteoblast-osteoclast co-cultures. Simultaneously, this map highlighted the large variation and lack of consensus on various methodological aspects of osteoblast-osteoclast co-cultures.

Due to the complexity and difficulties of analyzing of 3D cultures, we first needed to be able to reliably obtain functional osteoclasts in 2D. The findings of the systematic map were applied to investigate the effect of seeding density and osteoclastic culture medium supplement concentration on osteoclastogenesis and osteoclastic resorption. This gave valuable insight into the cells' requirements for differentiation and resorption and provided the foundations necessary to translate 2D *in vitro* osteoclastogenesis and resorption to a 3D environment.

Then, the learnings from our work on osteoclasts were combined with earlier work on silk-fibroin scaffold mineralization to develop a human *in vitro* 3D osteoblast-osteoclast co-culture model, in which we were able to quantify, localize and visualize both formation and resorption in parallel over time using micro-computed tomography. Finally, this model was further developed into a model in which remodeling was in a state of equilibrium. Here we showed that the response of the model could be tuned towards showing an excess of either resorption or formation by applying corresponding stimuli. Although the stimuli used in this study were not based on physiological conditions or disease models, they confirmed that the 3D co-culture model in equilibrium can respond to biochemical stimuli, which manifests as a quantifiable effect on resorption and formation. The model presented in this thesis can be used as an *in vitro* co-culture model of human bone remodeling and can be further developed for various applications in fundamental research, drug development and personalized medicine.

To summarize, this thesis provides an unprecedented amount of readily accessible information on osteoblast-osteoclast co-cultures, culminating in the development of a human *in vitro* 3D osteoblast-osteoclast co-culture model of bone remodeling in which formation and resorption can be monitored over time non-destructively. The model is capable of pronouncing states of near-equilibrium, resorption, and formation after application of the corresponding stimuli. The 3D osteoblast-osteoclast co-culture model presented in this thesis can be used as an *in vitro* co-culture model of human bone remodeling and can be further developed for various applications in fundamental research, drug development and personalized medicine.

Contents

Chapter 1

General Introduction

1.1 Bone tissue and remodeling

At first glance, our bones may appear like static structural elements of our body that no longer change after reaching adulthood. This could not be further from the truth. Bone is a highly dynamic tissue with both mechanical and metabolic functions. As the mechanical demands placed upon bones change, bones adapt and optimize their structure and strength by removing obsolete or damaged tissue and producing new or stronger tissue when and where needed. Examples thereof are spaceflight-induced reduction in bone mineral density in astronauts (Sibonga, 2013), or exercise-induced increase in bone mineral density in athletes (Bellver et al., 2019).

The cells directly responsible for bone remodeling are the bone forming osteoblasts and bone resorbing osteoclasts (Fig 1.1). These cells are closely linked, and together form the basic multicellular units (Frost, 1969). The process of bone remodeling is regulated by osteocytes. Osteocytes are the regulators of bone remodeling and comprise about 90 to 95 % of all cells in bone (Parfitt, 1977). They form an intricate inter-cellular network of filopodia through so-called canaliculi, that can sense and react to interstitial fluid flow caused by biomechanical changes in their local environment (Bonewald, 2011; Klein-Nulend et al., 2013). Osteoclasts differentiate from circulating blood monocytes. These monocytes are attracted to the site of resorption though biochemical signalling by osteocytes and differentiate near or at the bone surface into osteoclasts to remove old or damaged bone. These cells are believed to be short-lived (Parfitt, 1994) and disappear after their job is completed. Recently however, new evidence has disputed the long-standing expected lifespan of approximately 2 weeks, suggesting that the *in vivo* lifespan can be extended by supplying new nuclei (Jacome-Galarza et al., 2019) and that osteoclasts can relocate by de- and refusing into osteomorphs (McDonald et al., 2021). Tightly coupled to resorption, bone lining cells clean and prepare the resorbed surface for bone formation (Everts et al., 2002). Osteoprogenitor cells derived from mesenchymal stromal cells are recruited to the site of bone formation most notably from nearby capillaries and canopies through chemotaxis (Dirckx et al., 2013; Kristensen et al., 2014). After differentiating into osteoblasts that can live for up to 200 days (Manolagas and Parfitt, 2010), these cells deposit new mineralized matrix to repair the bone tissue. During the process of bone formation, some osteoblasts entomb themselves into lacunae within the mineralized matrix and transition to become new osteocytes (Bonewald, 2011). In healthy tissue, bone resorption and formation are in equilibrium, with the bone strength and structure optimized to meet the demands placed upon the body. In diseases such as osteoporosis this equilibrium is disturbed, leading to pathological decrease in bone mineral density that adversely affect the bone's mechanical functionality (Feng and McDonald, 2011).
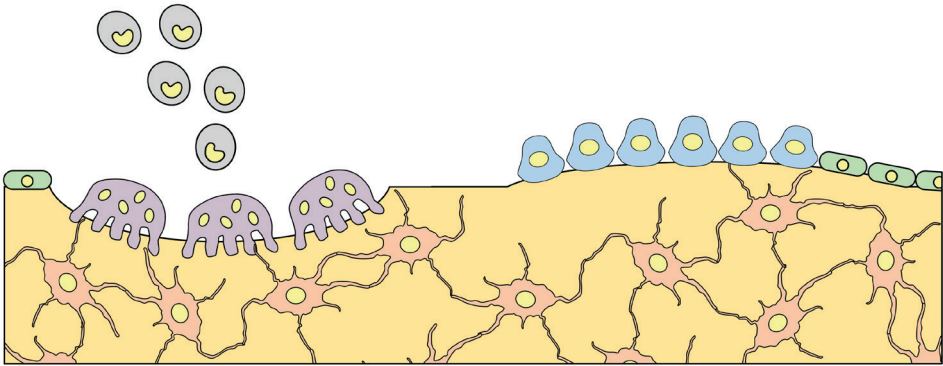
Fig. 1.1. **Bone remodeling.** *Osteoclasts (purple) are the bone resorbing cells derived from blood-borne monocytes (grey). Monocytes travel to the site of activity and differentiate into multinucleated osteoclasts through cell-fusion. Osteoblasts (blue) are the bone forming cells. During bone formation, some osteoblasts become entombed in the newly-formed matrix and become osteocytes (orange), which have a regulating role. Others become lining cells (green) with a role in coupling resorption and formation.*

Many of the biochemical players in these processes have been identified and studied (Deschaseaux et al., 2010; Matsuo and Irie, 2008; Sims and Gooi, 2008), and are being targeted by treatment options for osteoporosis (Bellido, 2014; Matsuo and Irie, 2008). Regrettably, these treatment options are not yet capable of reversing the degenerative nature of the disease, in most cases merely slowing the progression thereof. This indicates that there is a need for more accurate, reproducible, and translatable model systems to study the cellular and molecular mechanisms underlying bone remodeling and bone disease, which could be used to find better drug targets.

1.2   Bone models

In a preclinical setting, available options to study bone remodeling are limited to the use of either animal models or *in vitro* cell culture experiments. Animal models are frequently used for studies on bone disease and drug development and are considered a fundamental part of preclinical research. Using animals raises many ethical concerns (3R principles to reduce, refine and replace the use of animals) and is generally more time-consuming and expensive than *in vitro* research. While animal physiology is similar to that of humans, the differences are often large enough to result in poor translation of results from animal studies to human clinical trials (Burkhardt and Zlotnik, 2013; Contopoulos-Ioannidis et al., 2003).

While *In vitro* cell-culture models do not share the same ethical concerns, the use of animal cells can still lead to a different response compared to human cells (Jemnitz et al., 2008). The most substantial advantages of *in vitro* cell culture models are that they open up the

possibility to use cells of human origin, both from healthy human donors or even from diseased patients (Jemnitz et al., 2008; Langhans, 2018). Most cell culture experiments are conducted with a single cell type. These are perfect for thoroughly studying that particular type of cell but are limited to the degree in which they can be used to study interaction between different cell types. Because bone formation and resorption occur simultaneously and both osteoblasts and osteoclasts are known to interact with each other through paracrine signalling (Matsuo and Irie, 2008), a co-culture of both osteoblasts and osteoclasts is generally considered the best way to mimic bone remodeling *in vitro* (Owen and Reilly, 2018). Many types of co-culture exist (Goers et al., 2014; Paschos et al., 2015; Zhu et al., 2018), but only a direct co-culture within the same microenvironment allows the two-way signalling necessary for real-time interaction and thus the ability to affect both formation and resorption in real time.

1.3   Osteoblast-osteoclast co-culture models

Osteoblast-osteoclast co-culture models have been used in some form for over forty years. The development of these models progressed slowly because the precise origin of the osteoclast was long unknown. T.J. Chambers in 1982 was the first to co-culture isolated rat osteoclasts with osteoblasts in an attempt to reverse their quiescence through direct cell contact (Chambers, 1982). At that time, osteoclasts could only be obtained by isolation from fragmented (animal) bones. Six years later, Takahashi cultured mouse spleen cells and osteoblasts together and published the first account of osteoclastogenesis in osteoblast-osteoclast co-cultures (Takahashi et al., 1988). Their methods were used by virtually all others in the next decade, although at this point the purpose of the osteoblast-osteoclast co-cultures was merely to generate osteoclasts. Using the co-culture as a model for bone remodeling became possible only after the discovery in 1999 by Suda (Suda et al., 1999) that Receptor Activator of Nuclear Factor Kappa Ligand (RANKL) and Macrophage Colony Stimulating Factor (M-CSF) were the necessary and sufficient cytokines required for differentiating cells from the monocyte/macrophage lineage into functioning osteoclasts (Simonet et al., 1997; Teitelbaum, 2000; Udagawa et al., 1990). From that point onward, osteoclasts could be generated without osteoblasts. At the same time, osteoblast-osteoclast co-cultures started to develop from tools for osteoclastogenesis into models in which the interaction with and function of osteoblasts were studied as well.

Most *in vitro* cultures are conducted in 2D monolayer (Amizuka et al., 1997; Marino et al., 2014), because this is usually easier to conduct and analyse, cheaper and less time consuming, while still providing useful data. However, *in vivo* bone remodeling is a three-dimensional process where cells likely respond differently than in 2D (Edmondson et al.,

2014; Li and Kilian, 2015). Therefore, quantification of bone formation or resorption in co-culture *in vitro* should ideally be done in a 3D environment (Owen and Reilly, 2018). Many groups have done 3D osteoblast-osteoclast cultures in the last 15 years, mostly using hydrogels (Heinemann et al., 2011) or scaffolds (Papadimitropoulos et al., 2011). Due to the additional complexity of the 3D environment, analytical techniques for measuring formation or resorption are commonly destructive in nature, using for example Alizarin Red mineralized nodule staining (Rossi et al., 2018) or Scanning (Hayden et al., 2014) and Transmission (Domaschke et al., 2006) electron microscopy for surface metrology.

Instead of using end-point destructive techniques for each timepoint, ideally the same cultures are monitored over time to detect and localize remodeling events in both three-dimensional space and time. Micro-computed tomography, a variant of the commonly used CT scan, is an X-ray-based scanning technique that has proven effective for detecting mineralized tissue and was recently used to monitor bone remodeling in animal models (Brouwers et al., 2008; Schulte et al., 2011a, 2011b) and *in vitro* bone formation on scaffolds (Hagenmüller et al., 2007).

Many materials have been used as scaffolds for bone tissue engineering including metals, ceramics, bioactive glasses and polymers (Bose et al., 2012; Wu et al., 2014). Silk fibroin in particular has been shown to be a biomaterial well-suited for bone tissue engineering, because of its remarkable mechanical properties, easy processing, tunable degradation, and excellent biocompatibility (Hagenmüller et al., 2007; Kasoju and Bora, 2012; Melke et al., 2016). Osteoblast-mineralized silk-fibroin scaffolds are a prime candidate for developing a 3D *in vitro* osteoblast-osteoclast co-culture model suitable for longitudinal monitoring, as they were shown to not only result in a mineralized scaffold, but also a collagenous matrix deposited between the pores (Melke, 2019; Melke et al., 2018) correlating with mineralized tissue deposition, both of which are sequentially deposited (first type I collagen, which in turn is mineralized with calcium phosphate) in bone tissue *in vivo* (de Wildt et al., 2019).

However, much is still unknown about osteoclasts. Their limited availability, complex manner of differentiation, high between-donor variation (Flanagan and Massey, 2003; Husch et al., 2021) and short lifespan (Manolagas and Parfitt, 2010; Parfitt, 1994) make it challenging to study them. Additionally, there is no consensus on the various parameters of *in vitro* research such as seeding densities, medium composition and supplement concentrations, despite their known impact on obtaining meaningful numbers of functionally competent osteoclasts *in vitro* (Kozbial et al., 2019; Mather, 1998; Remmers et al., 2021; Shahdadfar et al., 2005).

1.4   Outline of this thesis

The **aim of this thesis** was to develop a human 3D osteoblast-osteoclast co-culture model in which both bone formation and resorption could be monitored over time. An earlier developed 3D model in which mesenchymal stromal cells differentiate into osteoblasts and deposit mineralized matrix on a silk-fibroin scaffolds was used as the foundation of this work (Melke et al., 2018). This thesis describes the work that was done to study and implement functional osteoclasts into this model.

The current chapter presents a general introduction building up to the relevance and need for a 3D osteoblast-osteoclast co-culture model. In **chapter 2** the lack of consensus on culture conditions for osteoblast-osteoclast co-cultures is highlighted, culminating in a systematic review of all available osteoblast-osteoclast co-cultures, and a systematic map in which all relevant details and experimental conditions are presented in a structured and accessible manner. This systematic map provides an unprecedented amount of information on cells, culture conditions and analytical techniques for using and studying osteoblast-osteoclast co-cultures.

Due to the complexity and difficulties of analyzing of 3D cultures, we first needed to be able to reliably obtain functional osteoclasts in 2D. **Chapter 3** describes how the findings of the systematic map were applied to investigate the effect of seeding density and supplement concentration on osteoclastogenesis and osteoclastic resorption, providing the context and foundations necessary to translate *in vitro* osteoclastogenesis and resorption to a 3D environment.

In **chapter 4**, we applied all that was learned to combine earlier work on silk-fibroin scaffold mineralization with our work on osteoclasts to develop a 3D osteoblast-osteoclast co-culture, in which we were able to quantify, localize and visualize both osteoblastic and osteoclastic activity in parallel over time using micro-computed tomography. This model was developed further in **chapter 5**, where we showed that the response of the model can be tuned towards formation, resorption and equilibrium by applying different seeding densities and different culture media.

The results obtained in this thesis are discussed in **chapter 6** and provide a solid foundation of readily accessible knowledge invaluable for anyone venturing into the realm osteoblast-osteoclast co-cultures and describe our path to understanding and manipulating the amazing osteoclast to develop an *in vitro* 3D co-culture model of bone.

Chapter 2

Osteoblast-osteoclast co-cultures: A systematic review and map of available literature

2.1 Abstract

Drug research with animal models is expensive, time-consuming and translation to clinical trials is often poor, resulting in a desire to replace, reduce, and refine the use of animal models. One approach to replace and reduce the use of animal models is to use *in vitro* cell-culture models.

To study bone physiology, bone diseases and drugs, many studies have been published using osteoblast-osteoclast co-cultures. The use of osteoblast-osteoclast co-cultures is usually not clearly mentioned in the title and abstract, making it difficult to identify these studies without a systematic search and thorough review. As a result, researchers are all developing their own methods, leading to conceptually similar studies with many methodological differences and, as a consequence, incomparable results.

The aim of this study was to systematically review existing osteoblast-osteoclast co-culture studies published up to 6 January 2020, and to give an overview of their methods, predetermined outcome measures (formation and resorption, and ALP and TRAP quantification as surrogate markers for formation and resorption, respectively), and other useful parameters for analysis. Information regarding these outcome measures was extracted and collected in a database, and each study was further evaluated on whether both the osteoblasts and osteoclasts were analyzed using relevant outcome measures. From these studies, additional details on methods, cells and culture conditions were extracted into a second database to allow searching on more characteristics.

The two databases presented in this publication provide an unprecedented amount of information on cells, culture conditions and analytical techniques for using and studying osteoblast-osteoclast co-cultures. They allow researchers to identify publications relevant to their specific needs and allow easy validation and comparison with existing literature. Finally, we provide the information and tools necessary for others to use, manipulate and expand the databases for their needs.

2.2   Introduction

Bone is a highly dynamic tissue with mechanical and metabolic functions that are maintained by the process of bone remodeling by bone forming osteoblasts (OBs), bone resorbing osteoclasts (OCs), and regulating osteocytes. In healthy tissue, bone resorption and formation are in equilibrium, maintaining the necessary bone strength and structure to meet the needs of the body. In diseases such as osteoporosis and osteopetrosis this equilibrium is disturbed, leading to pathological changes in bone mass that adversely affect the bone's mechanical functionality (Feng and McDonald, 2011).

Studies on bone physiology, bone disease and drug development are routinely performed in animal models, which are considered a fundamental part of preclinical research. The use of animals raises ethical concerns and is generally more time consuming and expensive than *in vitro* research. Laboratory animals are also physiologically different from humans. Their use in pre-clinical studies often leads to poor translation of results to human clinical trials (Burkhardt and Zlotnik, 2013; Contopoulos-Ioannidis et al., 2003) and subsequent failure of promising discoveries to enter routine clinical use (Montagutelli, 2015; Thomas et al., 2016). These limitations and the desire to reduce, refine and replace animal experiments gave rise to the development of *in vitro* models (Holmes et al., 2009; Owen and Reilly, 2018). Over the last four decades, significant progress has been made towards developing OB-OC co-culture models.

The development of *in vitro* OB-OC co-cultures started with a publication of T.J. Chambers in 1982 (Chambers, 1982), where the author induced quiescence of isolated tartrate resistant acid phosphatase (TRAP)-positive rat OCs with calcitonin and reversed their quiescence by co-culturing them with isolated rat OBs in direct contact. At that time, studies involving OCs resorted to the isolation of mature OCs by disaggregation from fragmented animal bones. The first account of *in vitro* osteoclastogenesis in co-culture was realized in 1988 when Takahashi and co-authors (Takahashi et al., 1988) cultured mouse spleen cells and isolated mouse OBs in the presence of 1α,25-dihydroxyvitamin D3 and found TRAP-positive dentine-resorbing cells. The herein described methods were used and adapted to generate OCs for the following decade. Most of the studies published until this point in time used co-cultures as a tool for achieving osteoclastogenesis, as opposed to a model for bone remodeling. At that time, a co-culture of OBs with spleen cells or monocytes was the only way of generating functional OCs *in vitro*. It wasn't until 1999 that Suda (Suda et al., 1999) discovered Receptor Activator of Nuclear Factor Kappa Ligand (RANKL) and Macrophage Colony Stimulating Factor (M-CSF) as the necessary and sufficient proteins required for differentiating cells from the monocyte/macrophage lineage into functioning OCs (Simonet et al., 1997; Teitelbaum, 2000; Udagawa et al., 1990).

This discovery marked the start of co-culture models developed for studying bone remodeling.

In recent years, many research groups have ventured into the realm of OB-OC co-cultures with the intent of studying both formation and resorption, but each group seems to be individually developing the tools to suit their needs resulting in many functionally related experiments that are methodologically completely different. In addition, the use of such methods is often not clearly stated within title and abstracts. Simple title/abstract searches such as 'OB + OC + co-culture' show only a fraction of available studies using OB-OC co-cultures. Finding and comparing different co-culture approaches and their results is thus complicated which forces each group to develop and use their own methods.

The aim of this study was to conduct a systematic review of all OB-OC co-cultures published up to January 6, 2020. With this systematic review, we aimed at identifying all existing OB-OC co-culture studies and analyze these within two comprehensive databases, allowing researchers to quickly search, sort and select studies relevant for their own research. Database 1 contains all OB-OC co-culture studies in which at least one relevant primary outcome measure was investigated (formation and/or resorption) or secondary outcome measure (alkaline phosphatase (ALP) and/or tartrate resistant acid phosphatase (TRAP) quantification as surrogate markers for formation and resorption, respectively) (S1_File_Database_1). A sub-selection of studies that investigated these relevant outcome measures on both OBs and OCs in the co-culture was included in Database 2, accompanied by additional details on methods, culture conditions and cells (S2_File_Database_2). The collection of the two databases will further be referred to as a systematic map. The complete systematic map can be accessed through the following DOI: https://doi.org/10.1371/journal.pone.0257724

2.3   Methods

For this systematic map a structured search protocol was developed using the SYRCLE protocol format (de Vries et al., 2015). The protocol and search strings were made publicly available before completion of study selection via Zenodo (S. J. A. Remmers et al., 2020) to ensure transparency of the publication. In short, three online bibliographic literature sources were consulted with a comprehensive search query and the resulting publications were combined and screened using a four-step procedure (Fig. 2.1): 1) identification of OB-OC co-cultures, 2) identification of relevant outcome measures, 3) categorization in Databases 1 and 2 (Fig. 2.2), 4) search for additional articles in the reference lists of studies included in Database 2 and relevant reviews.

Screening step 1

Pubmed	Embase	Web of Science
1964	2709	3014

Combined — 7687

Not Primary 813 | **Primary Studies** 6874

Duplicates 2949 | **Unique studies** 3925

Screening step 2

Not OB-OC co-cultures 3231 | **OB-OC co-cultures** 694

No Fulltext 1 | **Not English** 35 | **No relevant OM** 406 | **Relevant OM** 252

Database 1 — 255

Screening step 3

Not both studied 178 | **OB + OC studied** 77

One relevant OM 38 | **Both relevant OM** 39

Database 2 — 39

Screening step 4

Reviews	DB2 screening
10	39

Primary Studies 29 | **Primary Studies** 37

Combined — 66

Unique studies — 59

OB-OC co-cultures — 3

Relevant OM — 3

2

Fig. 2.1. *Flow diagram of systematic literature search and screening*. Screening step 1: Hits from 3 online bibliographic literature sources were combined, primary studies were selected, and duplicates were removed. Title and abstracts were screened for the presence of OB-OC co-cultures. Screening step 2: OB-OC co-cultures were screened in full text for relevant outcome measures. All studies in which at least one relevant outcome measure was studied were included into Database 1. Screening step 3: Papers in which both cell types were studied with relevant outcome measures were included into Database 2. Screening step 4: Papers included into Database 2 and reviews were screened for potentially missing relevant studies and identified studies were screened in the same manner as above. Each screening step is marked with a separate background color. Each selection step within the screening steps is marked with a colored header. Blue header: used as input for the review. Grey header: selection step. Red header: excluded studies. Yellow header: Database as presented in this systematic map. Abbreviations: outcome measures (OM), Database 2 (DB2), osteoblast (OB), osteoclast (OC).
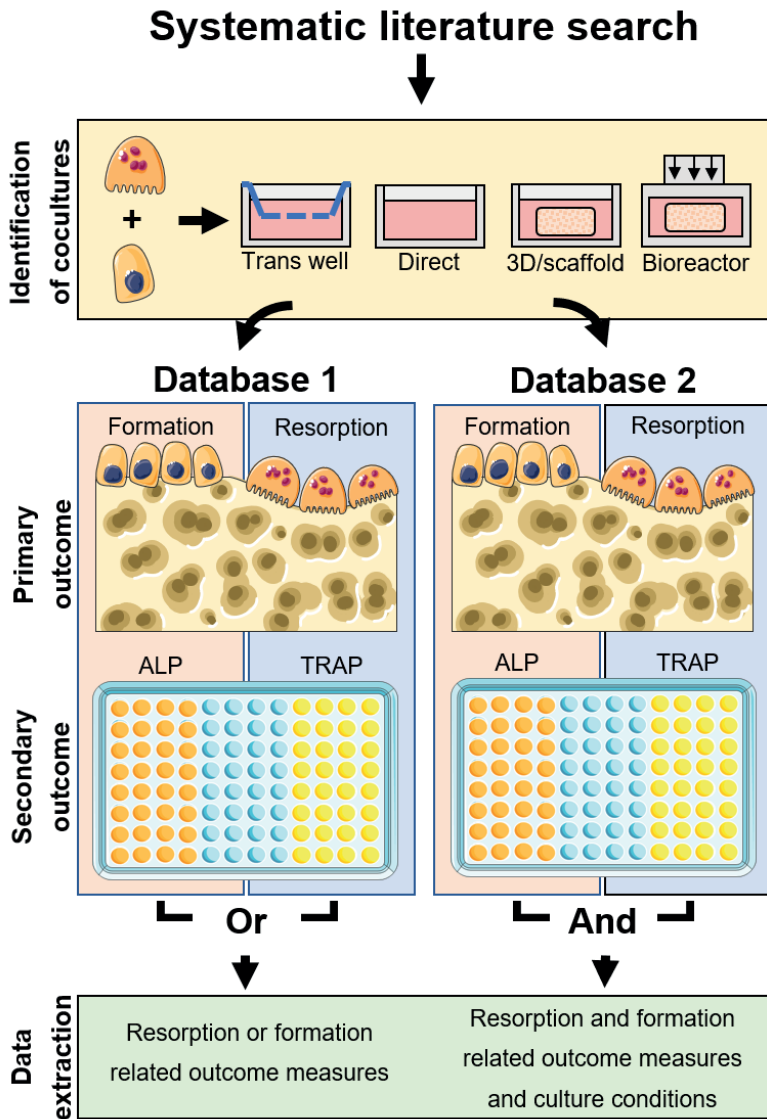
Fig. 2.2. *Schematic overview of Databases 1 and 2.* All identified studies were searched for OB-OC co-cultures, where co-culture was defined as OB and OC being present simultaneously and able to exchange biochemical signals. In addition to direct-contact cultures, cultures such as transwell cultures, 3D or scaffold cultures and bioreactor cultures were allowed as well. OB-OC co-culture studies which used relevant outcome measures were included into Database 1. Of these, only the relevant outcome measures were analyzed. All studies where relevant outcome measures were used for both OB and OC were included into Database 2 as well. Of these, cells and culture conditions were analyzed. The figure was modified from Servier Medical Art, licensed under a Creative Common Attribution 3.0 Generic License (http://smart.servier.com, accessed on 2 July 2021).

2.3.1 Database Search

The online bibliographic literature sources Pubmed, Embase (via OvidSP) and Web of Science were searched on January 6, 2020 with a predefined search query consisting of the following components: ([OBs] OR ([OB precursors] AND [bone-related terms])) AND ([OCs] OR ([OC precursors] AND [bone-related terms])) AND [co-culture], where each component in square brackets represents a list of related thesaurus and free-text search terms. The full search strings can be found via Zenodo (S. J. A. Remmers et al., 2020). The results of all three searches were combined. Conference abstracts and duplicates were removed using the duplicate removal tools of Endnote X7 and Rayyan web-based systematic review software (Ouzzani et al., 2016). The entire screening and data collection process was performed independently by two researchers.

2.3.2 Screening step 1: Identification of OB-OC co-cultures

This step was performed to identify and extract OB-OC co-cultures from the complete list of studies identified from the three online bibliographic literature sources after automatic removal of conference abstracts and duplicates. Using Rayyan web-based systematic review software (Ouzzani et al., 2016), the titles and abstracts were screened for the presence of primary studies using OB-OC co-cultures. Reviews, theses, chapters, and conference abstracts that were not automatically detected were excluded at this point. Potentially relevant reviews were saved separately to serve as an additional source of studies that could have been missed by the systematic search.

In the selection process, co-culture was defined as the simultaneous (assumed) presence of OBs and OCs (or OB-like and/or OC-like cells) within the same culture system at a moment during the described experiment such that the cells were able to communicate either via soluble factors in the medium and/or direct cell-cell contact. Both primary cells and cell lines of any origin were admitted including heterogeneous cell populations if these were clearly defined and expected to result in a biologically relevant number of the desired cell type. The presence of progenitor cells (such as monocytes or mesenchymal stem/stromal cells) was allowed only if these were either verified or expected to differentiate into OBs and/or OCs. Studies using a single animal or human donor for both cell types were allowed, but only if the two (progenitor) cell types were at one point separated, counted, and reintroduced in a controlled manner. Trans-well systems (no physical contact but shared medium compartment with or without membrane), scaffolds (3-dimensional porous structure of any material including decellularized matrix), and bioreactor culture systems (culture exposed to physical stimuli such as rotation, mechanical loading or fluid flow) were included. Conditioned media experiments were

excluded because these do not allow real-time two-way exchange of cell signals. Explant cultures, organ cultures and other *ex vivo* cultures were excluded, except when these were used solely to generate decellularized matrix.

When the study used any type of OB-OC co-culture as defined above, the study was included. When, based on the title and abstract, it was possible that there was a co-culture but this was not described as such, the full-text publication was screened.

2.3.3   Screening step 2: Identification of relevant outcome measures in the co-culture experiments

This step was used to identify co-cultures that specifically investigated relevant outcome measures related to bone remodeling: formation or resorption (primary outcome measures), or quantitative measurements of activity markers ALP or TRAP in a dedicated assay (secondary outcome measures). The primary outcome measures of resorption and formation were chosen because these are the processes that are directly affected in bone diseases. Formation/resorption measurement was defined as any method that directly measures the area or volume of (tissue) mineralization by OBs or resorption by OCs or any method that measures by-products or biochemical markers that directly and exclusively correlate to formation/resorption respectively. The secondary outcome measures of ALP and TRAP were included because these are regarded as viable alternatives for the direct measurement of formation and resorption. The measurement of ALP and TRAP was defined as the detection of either the enzymatic activity or the direct quantification of these proteins present. Polymerase Chain Reaction (PCR) and Immuno-histological stainings (with or without image analysis) were not considered relevant outcome measures. The full texts of the studies identified in screening step 1 were screened for experimental techniques and outcome measures. Studies in which for at least one of the cell types a relevant outcome measure was used were selected to be used in Database 1 (S1_File_Database_1). Publications written in languages other than English with no translation available and publications where the full text could not be found were excluded at this point.

2.3.4   Screening step 3: Categorization within Database 1

This step made the distinction between studies from screening step 2 on how OBs or OCs were studied in each publication. Each study was categorized into one of five categories within Database 1: 1) A relevant outcome measure was measured in both OBs and OCs in

the co-culture. These studies were also included in the in-depth screening for Database 2 (S2_File_Database_2). 2) and 3) Both cell types were studied, but relevant outcome measures were only measured in OCs or OBs respectively. 4) and 5) Only OCs or OBs respectively were studied in co-culture, the other cell type was neglected.

2.3.5   Screening step 4: Review and reference list screening

To find additional studies that may have been missed during bibliographic searches, relevant review articles and studies labeled as category 1 were screened for additional unique relevant publications. Identified publications were screened as before.

2.3.6   Database 1 generation and analysis – All co-cultures with relevant outcome measures

All information related to the relevant outcome measures was collected and organized in Database 1. For resorption, additional information on the resorbed substrate, the methodological procedure and quantification of results was collected. For formation, additional information on the type of analysis, the methodological procedure and quantification of results was collected. For both ALP and TRAP, additional information on the mechanism of the biochemical assay, whether it was conducted on lysed cells or supernatant, and information regarding the quantification was collected. In addition, the following information was collected, whether: the authors described their setup as a model specifically for remodeling, the experiment was conducted in 3D, the experiment applied bioreactors, more than 2 cell types were cultured simultaneously, the culture used a trans-well setup, the culture used PCR and components in the supernatant of the culture were analyzed by ELISA or a similar quantification method. Finally, a column for additional remarks was introduced for details that did not fit in another column. Studies where the authors are color coded in pink were those found through screening step 4. Studies categorized as category 1 in screening step 3 were selected for use in Database 2 and had their title color coded in orange.

2.3.7   Quality assessment and scripting

Database 1 only reports the methods used for analyzing relevant outcome measures, and not the data obtained from them or the results described in the publication. Quality assessment in Database 1 is thus limited to assessing the completeness of the necessary

elements of the collected methodological details, to the extent that the description of used methods is complete enough to be properly represented in Database 1 and related tables. Publications in which information was missing are here represented as 'not reported' if no information was provided, 'reference only' if no information was provided but another study was referenced, and 'undefined kit', when a commercial kit was used but the content or methodology was not further described. Instances of missing information can easily be identified in figures, tables and databases, but were not further used in this systematic map. Studies where information was missing were still used for other analyses for which the corresponding provided information was present.

A script was written in Excel Visual Basics programming language to analyze Database 1 and extract relevant statistical information on the collected information. On sheet 2 "Data" of the Database 1 excel file, the descriptive statistical data and collected information are presented in the form of lists and tables and together with a button to re-run the analysis based on the reader's requirements. The script is integrated within the excel file and can be used only when the file is saved as a 'macro-enabled' file (.xlsm).

2.3.8 Database 2 generation and analysis – All co-cultures in which both cell types had relevant outcome measures.

Additional information was collected from studies in which relevant outcome measures were studied on both OBs and OCs (Category 1 studies). The species (Jemnitz et al., 2008), origin (cell line or primary) and cell type (Owen and Reilly, 2018) of both the OBs and OCs, seeding numbers, densities (Bitar et al., 2008) and ratios (Jolly et al., 2018) were collected or calculated. The culture surface (bio-)material (Jones et al., 2009), sample size, culture duration, medium refreshing rate, environmental conditions and pre-culture duration (De Vries et al., 2015) were collected if available. The medium components (Kyllönen et al., 2013) and supplements were extracted, as well as medium components of any monoculture prior to the co-culture. Finally, the tested genes of all studies applying PCR and any proteins studied with ELISA or other supernatant analyses executed on the co-culture were noted.

2.3.9 Quality assessment and scripting

In Database 2, the culture conditions, cells and materials used are reported, and not the data obtained from them or the results described in the publication. Quality assessment in Database 2 is thus limited to assessing the completeness of the necessary elements of

the collected methodological details, to the extent that the description of used methods is complete enough to be properly represented in Database 2 and related figures and tables. Publications in which information was missing are here represented as 'not reported' (NR) if no information was provided, or 'reference only' if no information was provided but another study was referenced. If studies were missing information critical to reproduce the outcome measures (for example seeding ratio's, culture surface material, medium or supplement information, critical steps in analyses), the cells in the database missing this information were labeled in red. If the missing information was not critical for the outcome measures but necessary for replication of the study (for example sample size, medium refresh rate, control conditions), the cells were labeled in orange.

Three scripts were written using Excel Visual Basics programming language to analyze and process Database 2. One script counts all instances of cells labeled as 'missing info' and present this number in two dedicated columns (missing critical or non-critical info). One script counts the frequency of occurrence of all (co-)authors and years of publication. Finally, one script analyzes this database and extracts relevant descriptive statistical data on the collected information. On sheet 2 "Data" of the Database 2 excel file, the statistical data and collected information are presented in the form of lists and tables together with the buttons to re-run the analyses based on the reader's requirements. The scripts are integrated within the excel file and can be used only when the file is saved as a 'macro-enabled' file (.xlsm).

2.4   Results

2.4.1   Search results

From three online bibliographic literature sources, 7687 studies were identified (Pubmed: 1964, Embase via OvidSP: 2709, Web of Science: 3014). 6874 studies remained after removing conference abstracts, and 3925 unique studies remained to be screened after duplicate removal.

2.4.2   Studies included into Database 1 and 2

After screening step 1, 694 studies remained as OB-OC co-cultures. A list of these studies is available as a supplementary file (S4_File_List of all OB-OC co-cultures). Screening step 2 further excluded one study because of missing full text, 35 studies because they were in a language other than English and 406 studies because no relevant outcome measure was used. The qualifying 252 studies were included in Database 1. Screening step 3 revealed

that in 77 of the 252 studies in Database 1 both the OB and OC were studied. In 39 of these, both OB and OC were studied using relevant outcome measures. These 39 studies were included in Database 2.

Screening step 4 identified 34 unique studies from the reference lists of the included 39 studies of Database 2, and identified another 25 unique studies from the 10 identified review publications. These additional 59 studies were screened as described previously and resulted in an additional 3 OB-OC co-cultures with only relevant outcome measures measured on one cell type, resulting in a total of 255 studies with relevant outcome measures on at least one cell type for Database 1, and still 39 studies in which relevant outcome measures were studied in both cell types for Database 2. A detailed overview of the search and selection process is shown in Fig. 2.1.

2.4.3   Publications per year

The publications included in Database 1 were published between 1983 and 2019, with a peak in publications around the year 2000, followed by a slight but steady increase until now (Fig. 2.3a). The peak roughly coincides with the discovery that M-CSF and RANKL were both necessary and sufficient to induce osteoclastic differentiation in monocytes in 1999 (Suda et al., 1999). The included publications in Database 2 span the time between 1997 and 2019, with only 8 publications before 2010 (Fig. 2.3b). This coincides with the progress in development of *in vitro* co-cultures of OBs and OCs, moving beyond co-cultures with OBs to generate OCs, and moving towards co-cultures of OBs and OCs to study for example cell-cell interactions (Owen and Reilly, 2018).
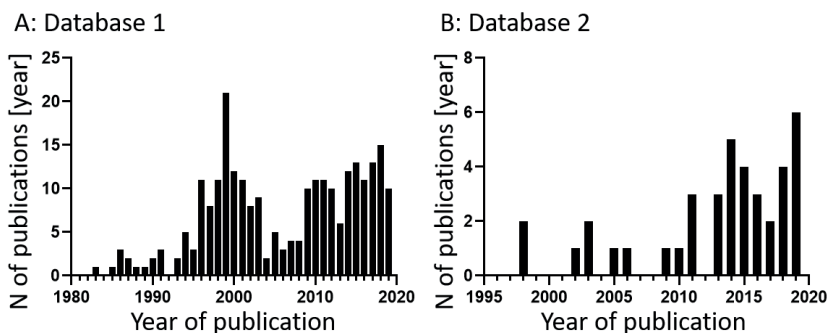

Fig. 2.3. **Relevant publications per year. (A)** All 255 publications that contain relevant outcome measures counted by year ranging from 1983 to 2019 (Database 1). **(B)** The 39 selected publications of Database 2 counted by year ranging from 1998 to 2019 (Database 2).

2.4.4   Database 1 results

Database 1 provides an overview of all OB-OC co-culture studies published until January 6, 2020 in which at least one relevant outcome measure was studied. Of the 255 studies included, resorption was analyzed in 181 studies, formation was analyzed in 37 studies and both were analyzed in 16 studies. ALP was analyzed in 42 studies, TRAP was analyzed in 61 studies and both were analyzed in 22 studies (Table 2.1).

2.4.4.1   Resorption

Out of all 255 OB-OC co-culture publications included in Database 1, resorption was studied directly on 188 occasions in 181 studies and quantified 142 times (Table 2.2 + Table 2.3). In some publications, more than one material or method of analysis for resorption was used. Different materials in the same publication were counted as different studies, resulting in a counted number of studies that is higher than the actual number of publications.

Most studies used discs or fragments of either bone or dentine, visualizing resorption pits directly or after contrast enhancement with stainings. Resorption on bone fragments was quantified using radioimmunological assays measuring the release of *in vivo* pre-labeled ^{3}H-proline or type I collagen telopeptide. Synthetic resorbable discs or coatings on culture plates will further be referred to as 'osteologic' plates or discs. Their exact composition is usually not revealed. Resorption of osteologic plates reveal the translucent culture plate, while unresorbed areas are less translucent and can be contrast-enhanced with for example von Kossa's method, facilitating image analysis.

Hydroxyapatite (HA) and other calcium phosphates were used in the form of discs, films, coatings, or scaffolds and were analyzed using various types of microscopy, both with and without prior staining. Resorption of ECM or nodules produced by OBs and scaffolds mineralized by OBs were investigated with transmission electron microscopy (TEM), light microscopy after staining, 2-photon Second Harmonic Generation microscopy (Hikita et al., 2015), supernatant phosphate levels, or with an ELISA for C-terminal telopeptide (CTx) or N-terminal telopeptide (NTx), which are bone turnover marker more commonly used for testing urine and serum samples.

2.4.4.2   Formation

Out of all OB-OC co-cultures included in Database 1, formation was studied directly 39 times in 37 studies and quantified 29 times (Table 2.4). In some studies, more than one

method of measuring, analyzing and quantifying formation was used. In those cases, all methods are counted as individual studies. The methods were divided into 5 types: nodule analysis, volume analysis, surface analysis, supernatant analysis and 3D scans.

*Table 2.1. **Combinations and frequencies of primary and secondary outcome measures.** This table can be referenced to identify the number of studies using any combination of primary and secondary outcome measures. All 255 studies that investigate at least one of the primary or secondary outcome measures are represented exactly once in this table. Each study is represented by a combination of primary outcome measures (horizontal) and secondary outcome measures (vertical). Marginal totals of each row and column are counted under 'total' with the grand total in the bottom-right cell.*

Combinations of primary and secondary outcome measures in each study		Primary outcome measures				
		No resorption or formation	Resorption only	Formation only	Resorption and formation	Total
Secondary outcomes	No ALP or TRAP	0	151	14	9	174
	ALP only	16	0	2	2	20
	TRAP only	23	9	3	4	39
	ALP + TRAP	14	5	2	1	22
	Total	53	165	21	16	255

➔ *Table 2.2. **Occurrences of resorption on different types of substrates and subsequent analyses.** Each column signifies a different material used as a substrate for measuring resorption. The first rows show how many instances of each material were included into this systematic map in total, and how many times the results were quantified. The final column shows incremental totals per material type or analysis type. This table consists of two sections. The top section shows in what form or shape the corresponding materials were used as a substrate for resorption. The bottom section shows the techniques that were used to study the resorption described on the materials described in the top section. Each individual study is represented exactly once in the top section of the table to signify the type and form of the substrate used, and exactly once in the bottom section of the table to signify the method used to analyze the resorption that occurred on these substrates. This required the selection of the most 'important' part of the methods used. In the cases where first a staining was used followed by microscopy, only the staining is listed. Only in those cases where resorption was investigated directly with a microscope without prior staining, the type of microscopy is listed. 'Mineralized' = A priori mineralized matrix by other cells.*

		Materials used as a resorbable substrate for measuring resorption										
Shapes, structures and types of materials used as resorbable substrate for analysis of resorption.		Dentine	Bone	HA	Silk	Collagen	CaP	PLLA	Chitosan	Osteologic	Mineralized	Not reported	Per-row total
Per-material total number of studies		76	66	6	5	2	4	1	1	19	6	2	188
Per material quantified studies		55	52	3	4	1	4	0	0	17	4	2	142
Shape or structure of	Discs	76	63	2			2			13			156
	Films			2	4			1	1				8
	Coatings			2			1						3
	Scaffolds				1	1					3		5
	Hydrogels					1							1
	ECM										2		2
	Nodule										1		1
	Fragments		3										3
	Substrates						1						1
	Plates									6			6
	Not reported											2	2
Analysis techniques for analyzing resorption on resorbable substrates.		Dentine	Bone	HA	Silk	Collagen	CaP	PLLA	Chitosan	Osteologic	Mineralized	Not reported	Per-row total
Staining	Toluidine Blue	36	19										55
	Haematoxylin	16	2										18
	Eosin		1										1
	H&E		1										1
	Alum / Coomassie Blue		1										1
	TRAP	1											1
	Von Kossa						2			4	1		7
Microscopy	Phase contrast						1			4			5
	SEM	12	37	5	3		1			1			59
	TEM					1					1		2
	2-Photon										1		1
	Atomic force				1			1	1				3
	Reflected light	8	2										10
	Dark field									1			1
	Light microscopy									6			6
Other	Assay				1								1
	Immuno-assay		3								3	1	7
	MicroCT				1					1			2
	Reference only	2											2
	Not reported	1		1						2		1	5
	Total per material	76	66	6	5	2	4	1	1	19	6	2	188

Table 2.3. **Supernatant resorption techniques.** *This table presents five resorption analyses that can be measured in the culture supernatant and not on the material itself. They are presented separately because they were done in addition to 'regular' analyses.*

Supernatant Analysis techniques per material used for analysis of resorption.		Dentine	Bone	HA	Silk	Collagen	CaP	PLLA	Chitosan	Osteologic	Mineralized	Not reported	Per-row total
Supernatant analysis	NTx	1									2		3
	CTx										1	1	2
	ICTP		1										1
	Phosphate release					1					2		3
	Radioactive proline release		2										2

Table 2.4. **Occurrences of different methods of formation detection and subsequent analyses.** *Each column signifies a different type of analysis used for measuring formation. The first rows show how many instances of each type of analysis were included into this systematic map in total, and how many times the results were quantified. The final column shows marginal totals per row of each row. This table consists of two distinct sections, each starting with a row showing all analysis types for convenience. The first section lists defining characteristics of studies such as using films, scaffolds, hydrogels or pellets, or using a technique to first stain tissue, and then releasing and measuring the released dye. Not each study had such defining characteristics, and the total of section one does not add up to 39 studies. Section two shows either which materials was measured, or which technique was used for measuring formation. Each instance of formation is represented in section two of this table exactly once.*

		Type of analysis used to measure formation					
	Technique	Scan	Nodule analysis	Supernatant analysis	Surface analysis	Volume analysis	Per-row Total
	Total	3	20	6	5	5	39
	Quantified	3	12	6	3	5	29
Measured	Scaffold	2	1	1	3	2	9
	Film	1		1	1	2	5
	Hydrogel					1	1
	Pellet		1			1	2
	Dye release		5				5
	Analysis	Scan	Nodule analysis	Supernatant	Surface analysis	Volume analysis	Per-row Total
Staining	H&E				1		1
	Von Kossa		2		1		3
	Alizarin Red		16				16
	Lentiv. Fluor.		1				1
Assay	Calcium					3	3
	Ca + P					2	2
	CICP			6			6
Scan	SEM		1		3		4
	microCT	3					3
Per-analysis Total		3	20	6	5	5	39

The most common method to quantify formation was investigating mineralized nodule formation by staining techniques and/or imaging. Alizarin Red staining could be quantified by releasing the dye from the minerals using acetic acid, followed by spectrophotometry (Schroder et al., 2012). Surface analysis was to study mineralization on scaffolds, films, or particles. Scaffolds were stained and/or imaged, and the area of matrix deposition was visualized or quantified. Volume analysis was used to describe the measurement of mineralized tissue components calcium and phosphate, which were released after destruction of the matrix. The types of formation measurement above are destructive methods, requiring sacrifice of the samples.

Non-destructive methods include supernatant analysis to describe the measurement of Collagen type I C-terminal propeptide (CICP), a byproduct of collagen deposition, in cell culture supernatant. 3D scanning by μCT quantified the three-dimensional structure of mineralized matrix.

2.4.4.3   *TRAP measurements as a surrogate marker of osteoclastic resorption*
Out of all OB-OC studies in Database 1, the predominant OC marker TRAP (Hayman, 2008) was studied 63 times in 61 publications (Table 2.5). TRAP can be measured intracellularly or excreted into the medium, either by measuring its enzymatic phosphatase activity directly, or by quantifying the amount of TRAP molecules present. TRAP release was studied both on cell lysate and on supernatant, and in some cases on both. The most frequently used method to study TRAP activity was using 4-nithophenylphosphate (pNPP). Others used the fluorophore Naphthol ASBI-phosphate (Vaughan et al., 1971) which shows specificity for TRAP isoform 5b (Janckila et al., 2001). Naphtol ASMX phosphate (Davidov, 1967) and an otherwise undisclosed diazonium salt function in a similar manner. Enzyme linked Immunosorbent Assay (ELISA) was used to detect TRAP using conjugated enzymes or fluorophores. Others used a kit to detect TRAP, but no description of the assay other than the manufacturer were given.

2.4.4.4   *ALP measurements as a surrogate marker of osteoblastic tissue formation*
Bone turnover marker ALP was studied in 42 publications (Table 2.6). ALP was most frequently measured using pNPP as substrate which is converted by ALP itself. Enzyme Immuno Assays (EIA) and ELISAs are immunoenzymatic assays (Lequin, 2005) that label ALP molecules with a detectable substrate or other enzymes. Others used a kit to measure ALP, but no description of the assay other than the manufacturer were given.

Table 2.5. **TRAP measurement techniques and analyses.** *Each column in this table signifies a different technique to measure TRAP. This table consists of two distinct sections. The first section shows the number of studies that used each technique, and whether these were used on (lysed) cells or on culture supernatant. The second section shows with which method of analysis the TRAP content was analyzed. If one study measured TRAP on both cells and supernatant, then that study is represented twice in both sections resulting in a higher count of occurrences than number of studies that analyzed TRAP. In all other cases, each study is represented once in each section.*

Type	pNPP	N-ASBI-P	N-ASMX-P	ELISA	Diazonium salt	Undefined kit	Reference	Not reported	Total
Total	33	5	1	9	1	9	4	1	63
Lysed cells	29	5	1	1		3	2		41
Supernatant	6			7	1	6	2		22
Reference only				1					1
Not reported						1		1	2
Analysis	pNPP	N-ASBI-P	N-ASMX-P	ELISA	Diazonium salt	Kit	Reference	Not reported	Total
absorbance	33		1	8		6	2	1	51
Fluorescence		5							5
Reference only	2			1	1		2		6
Not reported						4			4

Table 2.6. **ALP measurement techniques and analysis.** *Each column signifies a different technique to measure ALP. The first rows show the occurrence of each technique and whether these were used on (lysed) cells, or on culture supernatant. The final three rows show with which method of analysis the ALP content was measured. In a single study ALP can be measured with the same technique on both cell lysate and culture supernatant, resulting in a higher count of occurrences than number of studies that analyzed ALP.*

		ALP measurement techniques				
	Type	pNPP	EIA	ELISA	Undefined kit	Total
Substrate	Total	26	8	1	7	42
	Lysed cells	19	1		6	26
	supernatant	8	7	1	2	18
Detection	absorbance	25	8	1	3	37
	Reference only	2				2
	Not reported				5	5

2.4.5 Database 2 results

While Database 1 provides an overview of all reported methods to study the relevant outcome measures (resorption, formation, TRAP and ALP), Database 2 provides more experimental details such as culture conditions used for co-cultures.

2.4.5.1 Osteoblasts

Database 2 included 39 studies. Table 2.7 presents the cell types at the start of the co-culture. Most studies used human primary cells. Almost half of the studies started the co-culture with OBs, the others started with progenitor cells. As a result of ambiguous isolation methods and nomenclature which is subjective and can evolve over time (Lindner et al., 2010), some cell descriptions in Table 2.7 might refer to identical cell populations. This systematic map reflects the nomenclature used by the authors or extrapolated from the description and does not further interpret the provided information.

Except for the oldest 6 studies that used chicken and rat cells, all studies used human or mouse cells, most of which were primary cells. While the studies using rat and mouse cells mostly directly introduced OBs (either isolated as such or differentiated before seeding), those that used human cells predominantly introduced progenitor cells (Lindner et al., 2010). Those that used primary OBs purchased expandable human OBs (Clarke et al., 2013) or used OBs (Kadow-Romacker et al., 2013), undefined expanded bone cells (Hammerl et al., 2019), or differentiated MSCs (Bongio et al., 2016) from bones obtained during a surgical procedure. OB Seeding densities ranged from 0.9×10^3 cells/cm^2 to 60×10^3 cells/cm^2 with a mean of 11×10^3 cells/cm^2 (N = 26) in 2D (Fig. 2.4a) and from 0.3×10^3 cells/cm^3 to 7×10^3 cells/cm^7 with a mean of 15×10^6 cells/cm^3 (N = 6) in 3D (Fig. 2.4d).

*Table 2.7. **Osteoblast origins and occurrences.** From Database 2, the origin of the cells that were used as OB was extracted. Each column represents a different cell type of OB-like cells or their precursors. Each row represents a different source of cells, differentiating between both the origin species and whether the cells are primary cells or cell lines. Incremental totals are presented in the last row and column.*

Cell Origin	Osteoblasts	Mesenchymal stem cells	Mesenchymal stromal cells	Stromal cells	Stromal vascular Fraction	Osteoprogenitor cells	Per-row Total
Human primary	4	9	2	6	1		22
Human cell line	1						1
Mouse primary	3	2					5
Mouse cell line	4						4
Rat primary	3					1	4
Chicken primary				2			2
Reference only	1						1
Total	16	11	2	8	1	1	39
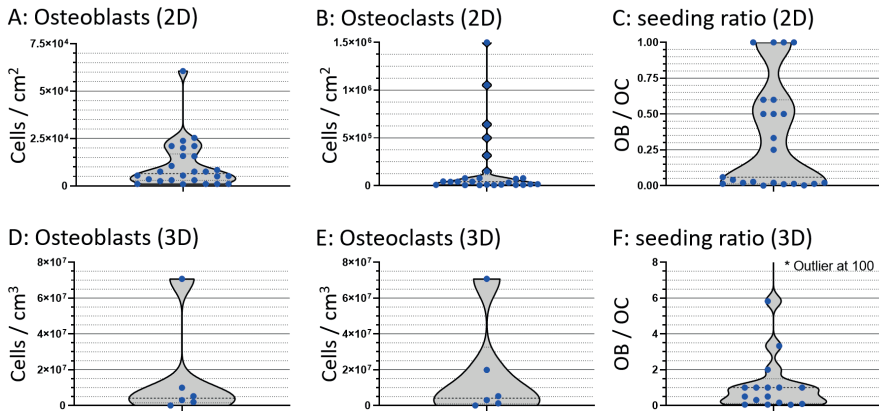
Fig. 2.4. ***Seeding densities and seeding ratios.*** *Violin plots of 2D and 3D seeding ratios of OB **(A+D)**, OC **(B+E)** and respective seeding ratios in co-cultures **(C+F)**. Values are calculated based on reported seeding numbers of the cells or precursors thereof per surface are or volume. No distinction was made between different (precursor) cell types in these figures, resulting in a considerable spread in data that could be attributed to proliferation and cell fusion after seeding The ranges along the Y-axis are not the same for each figure. Each seeding density of each study is represented by a blue dot.*

2.4.5.2 Osteoclasts

Out of the 39 studies in Database 2, 20 used human primary cells, the others used animal primary cells or any type of cell line for resorption (Table 2.8). Cultures were mostly initiated with OC progenitors: 16 studies introduced monocytes, 11 introduced mononuclear cells, the rest used other precursors.

The 6 oldest included studies used chicken and rat cells, all others used mouse or human cells. With only one exception combining a mouse ST-2 cell line with human monocytes (Domaschke et al., 2006), all studies used cells of exclusively a single species for the OB and OC source. Only one study claimed to introduce OCs directly into co-culture but failed to provide any information regarding the cell source and was therefore ignored from further investigation.

The OC seeding density ranged from 5×10^3 cells/cm^2 to 15×10^6 cells/cm^2 with a mean of 190×10^3 cells/cm^2 (N = 25) in 2D (Fig. 2.4b) and from 20×10^3 cells/cm^3 to $70*10^6$ cells/cm^3 with a mean of 17×10^6 cells/cm^3 (N = 6) in 3D (Fig. 2.4e). Seeding ratios of OB:OC in 2D varied highly and ranged from 1:1500 to 1:1 (Fig. 2.4c). seeding ratios of OB:OC in 3D ranged from 100:1 to 1:25 (Fig. 2.4f).

2.4.5.3 Co-culture medium composition and culture conditions

The behavior of cells is highly dependent on their environment, of which the biochemical part is predominantly determined by the culture medium composition. The main components of typical culture media are a base medium, fetal bovine serum (FBS) and specific supplements such as OB and OC supplements. 8 different base (or complete) media were reported (Fig. 2.5a), with αMEM and DMEM accounting for approximately 80% of all studies. FBS content ranged from 0% to 20%, with most studies using 10% (Fig. 2.5b). Those without supplemented FBS used forms of complete media of which the composition was not described, but possibly including a type of serum or equivalent serum-free supplements.

*Table 2.8. **Osteoclast origins and occurrences.** From Database 2, the origin of cells used as OC was extracted. Each column represents a different cell type of OC-like cell or a precursor. Each row represents a different source of cells, differentiating between both the origin species and whether the cells are primary cells or cell lines. Incremental totals are presented in the last row and column.*

Cell Origin	Monocytes	Mononuclear cells	Macrophages	Osteoclast precursors	Osteoclasts	Spleen cells	Total
Human primary	10	6	1	3			20
Human cell line	4						4
Mouse primary	2		2	2			6
Mouse cell line			2				2
Rat primary		3				1	4
Chicken primary		2					2
Reference only					1		1
Total	16	11	5	5	1	1	39
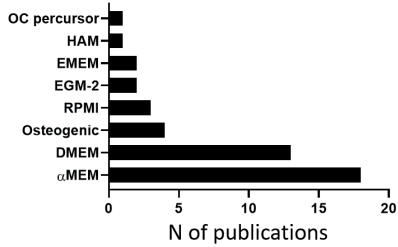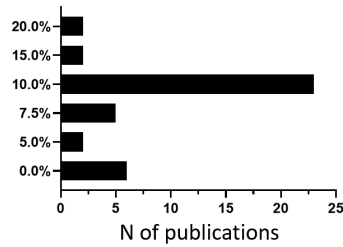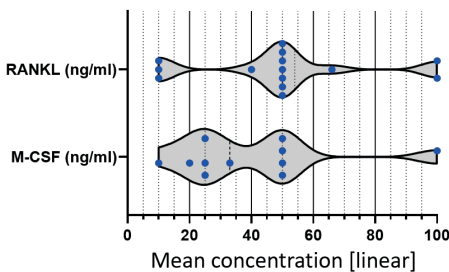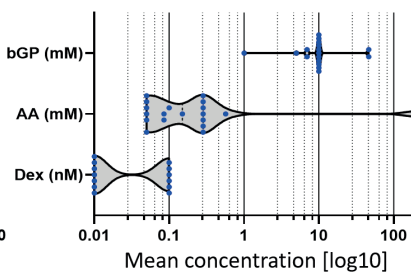
*Fig. 2.5. **Medium components used by studies in Database 2. (A)** The occurrence of all identified base and complete media used during the co-culture phase of each study. **(B)** Serum concentrations during the co-culture phase of each study. **(C)** OC supplements administered during the co-culture phase of each study. Please note that the x-axis has a linear distribution. **(D)** Osteogenic supplements during the co-culture phase of each study. Please note that the x-axis has a logarithmic scale. Individual concentrations or molarities are shown as blue dots.*

M-CSF concentration was reported in 11 studies and ranged from 10 ng/ml to 100 ng/ml with a mean of 39,82 ng/ml (Fig. 2.5c). RANKL concentration was reported in 14 studies and ranged from 10 ng/ml to 100 ng/ml with a mean of 49 ng/ml. OB supplements were recalculated to molarity if necessary (Fig. 2.5d). Ascorbic Acid (AA) (also referred to as ascorbic acid-2-phosphate, L-ascorbic acid or L-ascorbate-2-phosphate) concentration was reported in 19 studies and ranged from 0.05 mM to 0.57 mM, with a mean of 0.18 mM and one outlier at 200 mM that was disregarded for this calculation. Dexamethasone was used in 13 studies and was used in 2 different molarities: 6 times at 10^{-7} M and 7 times at 10^{-8} M. β-Glycerophosphate (βGP) concentration was reported in 17 studies, and ranged from 1 mM to 46 mM, with a mean of 13 mM.

2.5 Discussion

In recent years, many research groups have ventured into the realm of OB-OC co-cultures with the intent of studying both formation and resorption. Due to a lack of standardization within the field and the difficulty of finding publications based on methods instead of results, each group seems to be individually developing the tools to suit their needs resulting in many functionally related experiments that are methodologically different. The use of OB-OC co-cultures is usually not clearly mentioned in the title and abstract, making it difficult to find these studies without a systematic search and thorough review. The aim of this study was to generate a systematic map to give an overview of existing osteoblast-osteoclast co-culture studies published up to 6 January 2020, and present their methods, predetermined outcome measures and other useful parameters for analysis in 2 databases which can be filtered, sorted, searched and expanded.

The Database 1 contains all OB-OC co-culture studies in which at least one relevant primary outcome measure (formation and/or resorption) or secondary outcome measure (ALP and/or TRAP quantification) was investigated (S1_File_Database_1). A sub-selection of studies that have relevant outcome measures investigated on both OBs and OCs in the co-culture are shown in Database 2, accompanied by additional details on methods, culture conditions and cells (S2_File_Database_2).

2.5.1 Resorption

Most studies in Database 1 investigating resorption did so in 2D cultures using a resorbable substrate such as bone, dentine, or synthetic osteological discs. This is not unexpected, as these three options are either the actual *in vivo* material (bone), a similar

material with excellent properties for studying resorption (dentine) (Boskey, 2007), or a material designed specifically for the purpose of studying resorption (osteologic discs or coated wells). Dentine is a component of ivory, usually obtained from elephants (Armour et al., 2001), hippo's (Buckley et al., 2002) or sperm whales (Lalande et al., 2001). Regulations regarding ivory are strict and the material is rare, making it difficult to obtain. One crucial advantage of using dentine over bone is related to the native structure of dentine itself: it does not contain canaliculi and has fewer other irregularities, providing more contrast between the native structure and resorption pits to accurately visualize them (Boskey, 2007; Rumpler et al., 2013). The advantages of bone over dentine are that bone is the actual tissue of interest, it can be obtained from many different species in relevant quantities and sizes, it can be prelabeled *in vivo* with radioactive markers such as ^{3}H-proline (Teti et al., 1991), and could be used in conjunction with cells from the same species or even same animal, although the latter was not observed in this map. Synthetic osteologic discs have the advantage of being produced in a uniform manner and should show little sample-to-sample variation compared to discs made from animal tissue or hand-made discs. Using well plates with thin osteologic coatings has the advantage that once the coating is resorbed the translucent well below is revealed, which facilitates imaging with light microscopes. Combined with certain stainings, it makes quantifying resorbed area using conventional light microscopy easier.

It is believed that the deposition of collagen type I by osteoblasts is a vital step in the formation of mineralized tissue (de Wildt et al., 2019), and similarly could play a role in the resorption thereof. When using collagen-based materials, techniques such as NTx (Rossi et al., 2018) and CTx (Krishnan et al., 2014) can be used. These bone turnover markers are used in the clinic and can quantify resorption by analyzing the liberated collagen fragments in the supernatant (Shetty et al., 2016). It is possible to generate the to-be-resorbed material *in vitro* by OBs (Krishnan et al., 2014), even within the same experiment. This simulates a bone remodeling environment that is a step closer to the physiological process of bone remodeling versus only resorption, although *in vivo* the order is typically reversed: first, ECM is resorbed by OC, then new ECM is deposited by OB (Delaisse, 2014). However, the process of creating a mineralized matrix may introduce a variation in substrate size even prior to initiating the co-culture (S. Remmers et al., 2020).

Because most studies were conducted in 2D, most resorted to using various types of 2D microscopy to analyze resorption, usually after staining to increase contrast. This can facilitate the quantification of resorbed area using image analysis software but is usually limited to a quantification of surface area, whereas resorption is a three-dimensional process. While methods exist to reconstruct a set of stereoscopic 2D images into 3D height maps (Chan et al., 2004), these were not identified within the studies in either database of

this systematic map. Instead, one could also consider techniques that can directly quantify the resorbed volume. Examples are 2-photon microscopy for thin samples and micro computed tomography (μCT) (Hagenmüller et al., 2007). Due to the non-destructive nature of μCT, it is well suited to monitor mineralized volume change over time within the same samples over a longer period of time (Hagenmüller et al., 2007; Melke et al., 2018; S. Remmers et al., 2020). Registering consecutive images can even show both formation and resorption events within the same set of images of the same sample if both mineralizing OBs and resorbing OCs were present (S. Remmers et al., 2020). The usefulness of such a monitoring tool is however dependent on the envisaged resolution versus the corresponding potential cell-damage caused by radiation exposure (Kraehenbuehl et al., 2010; Yang et al., 2012), and requires the use of sterile scannable culture vessels, which poses some practical constraints. While μCT in this map is predominantly used on 3D samples, one study used it to quantify the thickness of mineralized films and combined that data with a surface metrological analysis (Hayden et al., 2014).

Overall, the golden standard (bone and dentine discs) remains the most-used method to study 2D resorption, although alternatives such as osteological coatings offer new and easy ways of quantification. Compared to 2D cultures however, 3D cultures are under-represented in this systematic map. Only 24 studies were labeled as 3D co-cultures in Database 1, the first being published only in 2006 (Domaschke et al., 2006). From these we learn that studying 3D resorption remains a challenge, with the only identified viable options for quantification being μCT imaging and supernatant analysis techniques such as NTx and CTx.

2.5.2 Formation

Bone formation is a multi-step process in which properly stimulated OBs lay down a framework of type I collagen, which in turn is mineralized with calcium phosphate (de Wildt et al., 2019). No single method of measuring formation confirms the occurrence of each step in this process, instead relying on the assumption that the confirmed presence of one step indicates the presence of the entire process.

With most studies being 2D co-cultures, it is no surprise that most formation analyses were stainings. Of these, Alizarin Red is particularly interesting due to the possibility of quantifying the amount of bound dye, which correlates to the amount of calcium (Schroder et al., 2012). A risk when using this method on larger samples is that it is not certain how far both dye application and dye extraction penetrate the material. This

should not affect relative comparisons between different sample groups but could lead to underestimations of calcium deposition. By completely lysing the samples and directly measuring the exact amount of calcium or phosphate (Hayden et al., 2014a; Loomer et al., 1998) this risk could be avoided, at the cost of not gaining information on the distribution of calcium or phosphate through the sample.

The two types of non-destructive formation measurements, CICP and μCT, are coincidently well-suited for the analysis of three-dimensional co-cultures. Because of their non-destructive nature, they can be used to measure the same sample repeatedly and prior to destructive techniques. CICP measurements (Boanini et al., 2015) have no negative effects on the co-culture, requiring only a culture supernatant sample. The use of μCT leads to both quantification and visualization of mineralization within the same sample over time but needs some consideration because the same constraints described for resorption apply here as well.

Overall, 2D nodule stainings were the most frequently used method to measure formation. Combined with Alizarin Red dye release these provide an easy way to quantify mineralization, though CICP supernatant analysis and μCT techniques provide a non-destructive alternative that can also be used for 3D co-cultures.

2.5.3   ALP and TRAP

ALP and TRAP are the two major markers for indirectly quantifying OB and OC activity that were included into Database 1. ALP makes phosphates available to be incorporated into the matrix (Golub and Boesze-Battaglia, 2007) and TRAP has been associated with migration and activation of OC (Sheu et al., 2003). Their presence is not conclusive proof that formation and resorption are occurring because ALP is expressed already in differentiating MSCs (Kim et al., 2012) and TRAP is expressed on monocytes as well (S. Remmers et al., 2020). Still, there is a correlation between their presence and that of OB and OC activity. These enzymes can be measured both after lysis of the cells or within the culture supernatant. The former allows the quantification of enzyme per DNA content when combined with a DNA assay, whereas the latter allows the monitoring of relative enzyme release over time. The most frequently used methods are the pNPP-based methods where ALP and TRAP directly convert a substrate into a measurable compound. Naphthol-based methods (Vaughan et al., 1971) rely on a similar principle, and show an increased specificity for TRAP isoform 5B in particular (Janckila et al., 2001). The main advantage of these methods is that they use the inherent enzymatic activity of ALP and TRAP, reducing the complexity and cost of the assay. However, the reliance on the inherent enzymatic activity of the enzymes is also a practical limitation as inherent activity

can be affected by for example freeze-thaw cycles and long-term storage, which is a likely occurence when monitoring ALP or TRAP release over time. A workaround would be to analyze the samples directly after collection. Another risk is that both ALP and TRAP are phosphatases. Assays that rely on their inherent phosphatase activity may show cross-reactivity of other phosphatases, although this can largely be mitigated by controlling the pH during the test.

Immunoenzymatic assays such as ELISA (Engvall and Perlmann, 1971) detect the presence and not the activity of these enzymes instead. These methods have the capacity to detect low protein concentrations because each individual protein can be labeled with an excess of new enzymes each capable of converting substrate. In the case of TRAP, ELISA kits exist that are specific for TRAP isoform 5b which is expressed almost exclusively in OCs (Halleen et al., 2006), whereas isoform 5a is also expressed by macrophages and dendritic cells (Halleen et al., 2002). While in a co-culture with pure populations of OB and OC this distinction would not be relevant, macrophages, macrophage-like cells and macrophage precursors (Young et al., 2015) can be used as precursors for OCs (Hikita et al., 2015), and thus express isoform 5a in co-culture. Whether this negatively affects the results is another matter that can only be determined by comparison between the two assay types.

To conclude, pNPP based methods are the most frequently used methods for detecting ALP and TRAP due to their affordability and simplicity. However, immunoenzymatic detection methods are more sensitive and specific, and do not rely on the intrinsic enzymatic activity of ALP and TRAP which can be affected by freeze-thaw cycles, long-term storage, and could show cross-reactivity with other phosphatases.

2.5.4   Osteoclasts

Osteoclastic resorption is an integral part of *in vivo* bone maintenance. Old and damaged bone tissue is resorbed and replaced by OBs with new bone tissue. There is a clear preference in the studies identified for Database 2 for using human cells to generate OCs, most notably monocytes and mononuclear cells. These have in the past two decades proven to be a reliable and relatively straight-forward precursor population for OCs (Owen and Reilly, 2018), they can be obtained from human blood donations, and are thought to be better representatives for studying human physiology than cells of animal origin (Burkhardt and Zlotnik, 2013; Contopoulos-Ioannidis et al., 2003).

The choice of using precursors versus differentiated OCs is forced sharply into one direction because of both biological and experimental limitations. The extraction of OCs

from bone is possible but cumbersome, requires access to fresh bone material and generally does not yield relevant numbers of OCs. Generating OCs from circulating precursors is easier. However, OCs have an average life span of approximately 2 weeks (Manolagas, 2000; Parfitt, 1994), some of which would already be lost if OCs would be created prior to the actual experiments. In contrast to most cells, differentiation happens by fusion of several precursors into a single OC. Fused multinucleated OCs can become large and hard to handle without being damaged. For those reasons they are usually differentiated from precursors within the actual experiments.

Thanks to the discovery of M-CSF and RANKL being sufficient to induce osteoclastic differentiation (Suda et al., 1999), OCs can currently be obtained *in vitro* without the need for OBs. Where in the past researchers used spleen cells for this, the studies included in this systematic map predominantly use (blood-derived) mononuclear cells, monocytes, or macrophages as precursor cells.

There are *caveats* and risks associated with each cell source. Animal cells introduce a between-species variation and can respond differently than human cells (Jemnitz et al., 2008). Human donor cells tend to exhibit large between-donor variation compared to cell lines (Susa et al., 2004) and the number of cells acquired is limited and variable (Yang et al., 2018). The large variation between donors again highlights the need for patient-specific disease models instead of generic bone models. By using cells of a single diseased donor, the reaction of that patient's cells on potential treatment options can be studied. Immortalized cell-lines are more practical than primary cells but result in immortal OC-like cells. While these can greatly reduce between-experiment and between-lab variation, they are also physiologically less relevant. While these risks and characteristics do not discredit any source as a viable source of OCs for any experiment, the results of the corresponding studies should be interpreted with these characteristics in mind.

2.5.5 Osteoblasts

OBs are the bone forming cells, and together with bone resorbing OCs they keep the bone mass and bone strength in equilibrium. The preference for the use of human primary cells identified in the studies included in Database 2 can be explained by the good availability of donor material, expandability of OB precursors, and because human cells better reflect human physiology than cells from other species (Burkhardt and Zlotnik, 2013; Contopoulos-Ioannidis et al., 2003). The choice of OB progenitors versus OBs is not as crucial here as it is with OCs. MSCs, the most commonly used precursors, have a tri-lineage potential (Pittenger et al., 1999) and differentiate into OBs on a 1-1 ratio. The advantage of osteoprogenitors such as MSCs is that these are capable of extensive

proliferation before differentiation. Using progenitors allows studying osteoblastogenesis in addition to bone formation. When the effect of an intervention on mineralization but not osteogenesis is under investigation, care must be taken that the intervention is not applied before differentiation has been achieved.

The advantage of directly introducing OBs instead of precursors, whether obtained directly from primary material or pre-differentiated *in vitro*, is that these do not need to be differentiated within the experiment anymore, and any experimental conditions affect only mature OBs and not osteoblastogenesis in parallel. OBs or to-be-differentiated MSCs isolated from bone marrow or orthopedic surgery are the most common source of primary human OBs. Healthy human donor OBs are scarce because these persons rarely undergo bone surgeries or get bone biopsies. Whether the use of OBs from diseased donors affects experimental results needs to be elucidated. On the other hand, using patient cells to create a personalized *in vitro* disease model is the first step towards personalized medicine, especially if all cells are of that same patient. Finally, the risks of using animal cells the introduction of a between-species variation. While none of these risks directly discredit any of the methods obtaining OBs, the results must be interpreted with these risks and characteristics in mind.

2.5.6 Culture conditions

The success of a cell-culture experiment is dependent on the culturing conditions. For many cell-types, optimal culture conditions have been established. During co-culture experiments however, the needs of two or more cell types need to be met. Medium components and factors may be needed in different concentrations, as they can be beneficial to one cell type but inhibitory to the other (Vis et al., 2020).

There is a clear preference for medium based on DMEM and αMEM, but many factors influence the choice of base medium. Base media are chosen based on the intended cell type, recommendations by a manufacturer or supplier of either cells or medium, preferred effect on cells, interaction with other supplements, and earlier experience. These factors make direct comparison of experimental results within literature virtually impossible. Additionally, none of the studies mentioned why they specifically chose the base media they used.

Another variable in medium composition is FBS (or FCS). It is known to have batch-to-batch- and between-brand differences (van der Valk et al., 2018) which can impact the results of an experiment tremendously. However, no study explains why each type and concentration of FBS was chosen.

When osteoblastic or osteoclastic supplements were used, the concentrations were within the same orders of magnitude in all studies, except for AA. Only 2 studies used all 5 of the supplements indexed in this study (AA, βGP, Dexamethasone, M-CSF and RANKL) and many combinations of supplements have been registered in this map. OC supplements RANKL and M-CSF are both necessary and sufficient for osteoclastogenesis (Suda et al., 1999). However, OBs can produce RANKL and M-CSF themselves to trigger differentiation (Takahashi et al., 1988) and therefore the supplements are not necessarily required in co-culture. Each osteoblastic supplement contributes to a specific function. Dexamethasone upregulates osteogenic differentiation, βGP acts as a phosphate source, and AA is a co-factor involved in collagen synthesis (Langenbach and Handschel, 2013). Depending on the type of (progenitor) cells introduced, the aim of the experiment and other methodological details, their inclusion could be necessary. Finally, many studies used or omitted specific supplements related to their research question regarding the activity of OBs or OCs or used less common supplements for differentiation such as vitamin D3, human serum or Phorbol 12-myristate 13-acetate.

What is seldom addressed however, is the compromise that must be made in choosing the right supplements and concentrations. Adding too high doses of supplements could cause an excess of these signals in the culture medium, effectively overshadowing any other ongoing cell-signaling over the same pathway by other cells. This is of critical importance when the goal is not to achieve only OB and/or OC activity, but a self-regulating system with experimental conditions or interventions that are expected to affect this system. Here, it may be beneficial to experiment with lower concentrations of factors, supplemented only during critical phases of the cells' development or differentiation.

The choice of medium in a co-culture is most likely going to be a compromise and must be based on the exact research question to be addressed, where the advantages and disadvantages of base media and supplements for both cell types are carefully weighed.

2.5.7 Seeding densities and seeding ratios

Using the correct seeding densities plays a major role in proliferation and cell function of OBs (Bitar et al., 2008; Wiedmann-Al-Ahmad et al., 2002) and osteoclastic differentiation (Motiur Rahman et al., 2015). The seeding densities reported in this map show an enormous spread. Many factors could have influenced these numbers. For example, some studies report the numbers prior to expansion, others expand the cells in (co-)culture. Similarly, the percentages of relevant precursor cells in heterogenous cell populations can vary widely. The cell numbers present and OB:OC ratio most likely even change during a co-culture due to ongoing cell-division, differentiation, fusion and different expected life

spans and corresponding cell death. Regrettably, the available documentation of exact cell numbers introduced is often lacking, and open to some interpretation.

Animal type, cell type, cell line versus primary cells and even passage number may also directly influence the choice of seeding densities in addition to various experimental choices. At the same time, the purpose of the experiment and more specifically the purpose of the cells and type of interaction or result required should determine the necessary seeding density. The combination of all these factors suggests that there in fact is no ideal seeding density, and that the best seeding density for a certain experiment can only be determined by taking all the above factors into account, learning from others that did similar experiments, and most importantly verifying assumptions and predictions in the lab.

Looking at the cell seeding ratio, here reported as number of seeded OB/OB-precursors per seeded OC/OC-precursor, outliers can be normalized against their seeded counterparts. In 2D studies, there are never more OBs/OB-precursors than OCs/OC-precursors. At most, they are seeded at a 1:1 OB:OC ratio. Even though in human bone tissue the ratio of OB:OC is estimated to be approximately 7:1 (Gruber et al., 1986), higher OC numbers than OB numbers are seen. OB precursors can still proliferate, whereas OC precursors usually still need to fuse together to form mature OC or OC-like cells. In 3D we do not see the same trend, with ratio's ranging from 1:20 to 100:1. These differences are again affected by the same factors that influence individual OB and OC seeding densities, further enhanced by the extra layer of complexity that are inherent to 3D cultures. As with the individual seeding densities, these factors prevent us from determining an ideal seeding ratio.

2.5.8   Limitations

While the authors took great care to construct a series of search queries fine-tuned for each of the three online bibliographic literature sources, the authors cannot be certain that all relevant OB-OC co-cultures have been included into the two databases. The search was limited by the necessary addition of a 'co-culture' search element. Co-culture studies without any indication thereof in the title or abstract simply cannot be identified through the initial search. To compensate for this, screening step 4, searching through identified reviews and publications included into Database 2, was executed. Publications in languages other than English were excluded because none of the researchers involved in data curation and analysis were fluent in the remaining languages. Consequently, relevant publications might have been excluded based on language.

The quality of reporting in included studies is lacking in many cases. Missing information for reproducing the methods of the studies was identified, and only 13 out of 39 studies included in Database 2 did not miss at least a high-level description of all indexed characteristics.

This systematic map is not intended to provide a definitive answer to the question of how to set up the perfect OB-OC co-culture. Instead, it allows searching through all relevant co-culture studies looking for specific matching experimental characteristics or culture details that may be applicable to one's own research. For this, it contains the possibility to search, sort and filter through many relevant characteristics. This allows one to find relevant studies that may have already (partly) studied one's research question, or that can be used as a guide to design comparable experiments.

2.6   Conclusion

With this systematic map, we have generated an overview of existing OB-OC co-culture studies published until January 6, 2020, their methods, predetermined outcome measures (formation, resorption, ALP and TRAP quantification), and other useful parameters for analysis. The two constructed databases are intended to allow researchers to quickly identify publications relevant to their specific needs, which otherwise would have not been easily available or findable. The presented high-level evaluation and discussion of the major extracted methodological details provides important background information and context, suggestions and considerations covering most of the used cell sources, culture conditions and methods of analysis. Finally, this map includes the instructions for others to expand and manipulate the databases to answer their own more specific research questions.

Chapter 3

3

The effects of seeding density and supplement concentration on osteoclastic differentiation and resorption

3.1 Abstract

Much is still unknown about osteoclasts. Their limited *in vitro* availability, complex manner of differentiation and short lifespan make it challenging to study them. While many studies using osteoclast cultures have been done in the last decades, there is no consensus on the use of various culture parameters for *in vitro* research. The aim of this study was to investigate the effect of monocyte or peripheral blood mononuclear cell (PBMC) seeding density, osteoclastic supplement concentration and priming on the *in vitro* generation of functional osteoclasts, and to explore and evaluate the usefulness of commonly used markers for osteoclast cultures. Morphology and osteoclast formation were analyzed with fluorescence imaging for tartrate resistant acid phosphatase (TRAP) and integrin β3. TRAP release was analyzed from supernatant samples, and resorption was analyzed from culture on Corning® Osteo Assay plates. In this study, we have shown that common non-standardized culturing conditions of monocyte or PBMCs had a significant effect on the *in vitro* generation of functional osteoclasts. We showed how increased supplement concentrations support osteoclastic differentiation and resorption but not TRAP release, while priming resulted in increased TRAP release as well. Increased monocyte seeding densities resulted in more and larger osteoclasts, but not in more resorption or TRAP release. Increasing PBMC seeding densities resulted in more and larger osteoclasts and more resorption, although resorption was disproportionally low compared to the monocyte seeding density experiment. Exploration of commonly used markers for osteoclast cultures demonstrated that Iβ3 staining was an excellent and specific osteoclast marker in addition to TRAP staining, while supernatant TRAP measurements could not accurately predict osteoclastic resorptive activity. With improved understanding of the effect of seeding density and supplement concentration on osteoclasts, more reliable and reproducible osteoclast experiments can ultimately improve our knowledge of osteoclasts, osteoclastogenesis, bone remodeling and bone diseases.

3.2   Introduction

Osteoclasts are bone resorbing cells, that together with bone forming osteoblasts and regulating osteocytes are responsible for bone homeostasis. Monocytes are the main osteoclast precursors (Udagawa et al., 1990), and circulate in the peripheral blood (Henriksen et al., 2012; Kleinhans et al., 2015) as a portion of the peripheral blood mononuclear cells (PBMCs). Monocytes are recruited by osteoblasts and osteocytes (Graves et al., 1999; Kim et al., 2006) towards the site of resorption where they fuse together to form osteoclasts through biochemical signaling receptor activator of nuclear factor kappa-B ligand (RANKL) and macrophage colony stimulating factor (M-CSF) (Takahashi et al., 1999; Teitelbaum, 2000; Yoshida et al., 1990).

Much is still unknown about osteoclasts. Their limited availability, complex manner of attraction and differentiation, high between-donor variation (Flanagan and Massey, 2003; Husch et al., 2021) and short lifespan (Manolagas and Parfitt, 2010; Parfitt, 1994) make it challenging to study them. The use of immortalized cell lines such as murine RAW 264.7 (Collin-Osdoby and Osdoby, 2012) or human THP-1 (Ke et al., 2019) partially mitigates the availability, between-donor variation and lifespan concerns. At the same time however, their unnatural immortality introduces a lifetime deviation from the *in vivo* situation, and they neglect the variation found in patients or healthy donors which ultimately limits translatability of the obtained results. The use of animal cells shares similar concerns for translation towards human health and disease (Burkhardt and Zlotnik, 2013; Contopoulos-Ioannidis et al., 2003). To study human bone remodeling, ideally human primary cells should be used (Owen and Reilly, 2018).

*O*steoclasts are defined as resorbing, multinucleated (≥ 3 nuclei), tartrate resistant acid phosphatase (TRAP) expressing cells with a clearly defined actin ring (Buckley et al., 2005). TRAP, an enzyme secreted in the ruffled border, has been the dominant osteoclast marker for decades and has been linked to lacunar ATP hydrolysis, reactive oxygen species generation, and *in vivo* bone turnover (Hayman, 2008; Hayman et al., 1996; Kaunitz and Yamaguchi, 2008). However, TRAP expression is not exclusive to osteoclasts, as it is expressed in other cells (Hayman et al., 2001) including macrophages (Lord et al., 1990) who share a common monocyte precursor. More recently integrin β3 (Iβ3), an NF-κB-associated cell-surface receptor (Antonov et al., 2011) with a role in actin ring formation (Lee et al., 2015) has been used as an osteoclast marker as well (Barbeck et al., 2017; Nakamura et al., 2007).

While many studies using osteoclast cultures have been done in the last decades, there is no consensus on the various parameters that should be used for *in vitro* research such as seeding densities, medium composition and supplement concentrations (Remmers et al.,

2021). However, it is generally agreed upon that so called 'priming' of monocytes with M-CSF for a certain duration before the addition of RANKL has a beneficial effect on osteoclastogenesis (De Vries et al., 2015; Ross, 2006; Xu and Teitelbaum, 2013) in part because of its stimulatory effect on the expression of various genes including RANKL-related tumor necrosis factor (TNF) (Hayes and Zoon, 1993; Lacey et al., 1998; Yasuda et al., 1998). A recent systematic map of osteoblast-osteoclast co-cultures showed that commonly used seeding densities ranged from 5 to 250 × 10^3 cells/cm^2, and supplement concentrations of RANKL and M-CSF ranged from 10 to 100 ng/mL (Remmers et al., 2021). The large variation is surprising, considering that culture medium content (Mather, 1998; Shahdadfar et al., 2005) and cell seeding density (Kozbial et al., 2019) greatly affect osteoclastogenesis. Combined with the short lifespan of osteoclasts and the complex manner of obtaining them in meaningful numbers, these factors pose significant challenges to the design and execution of cell-culture experiments. A better understanding of the effect of these parameters on osteoclastogenesis, osteoclastic activity and resorption would result in more reliable and reproducible osteoclast experiments, ultimately improving our knowledge of osteoclasts, osteoclastogenesis, bone remodeling and bone diseases.

The aim of this study was to investigate the effect of supplement concentration and seeding density on osteoclastogenesis and functionality. Additionally, we evaluated the usefulness of commonly used tests and markers for osteoclast cultures.

3.3   Materials and Methods

3.3.1   Materials

Two human buffy coats were obtained from Sanquin (Eindhoven, Netherlands) after review and approval of the study by the Sanquin ethics review board. The buffy coats were collected by Sanquin under their institutional guidelines and with written informed consent per Declaration of Helsinki. Fetal Bovine Serum (FBS, batch F7524-500ML / lot BCBV7611) was from Sigma Aldrich / Merck (Zwijndrecht, The Netherlands). RPMI-1640 medium was from Thermo Fisher Scientific (Breda, The Netherlands). Antibiotic/antimycotic (anti-anti) was from Life Technologies (Bleiswijk, The Netherlands). Lymphoprep™ was from Axis-Shield (Oslo, Norway). MACS® Pan Monocyte Isolation Kit was from Miltenyi Biotec (Leiden, the Netherlands). Recombinant human M-CSF and recombinant human RANKL were from PeproTech (London, United Kingdom). Antibody Iβ3 (Orb248939, Mouse monoclonal) was from Biorbyt (Cambridge, United Kingdom). Antibody TRAP (Sc-30833, Goat polyclonal) was from Santa-Cruz

Biotechnology, Inc. (Heidelberg, Germany). Antibody Alexa 488 (715-545-150, Donkey-anti-Mouse IgG H+L) was from Jackson ImmunoResearch (Cambridgeshire, United Kingdom). Antibody Alexa 488 (A11055, Donkey-anti-Goat IgG H+L) was from Molecular Probes (Eugene, OR, USA). Antibody Alexa 350 (A10035, Donkey-anti-Mouse IgG H+L) was from Invitrogen (Waltham, MA, USA). Thin bleach was from the local Jumbo grocery store (Stiphout, Netherlands). All other substances were of analytical or pharmaceutical grade and obtained from Sigma Aldrich / Merck (Zwijndrecht, The Netherlands).

3.3.2   Methods

3.3.2.1   *Monocyte isolation*

Two human peripheral blood buffy coats from two separate healthy donors were obtained from the local blood donation center under informed consent. The buffy coats (±50 mL each) were processed independently in a similar manner as described previously (Bonito et al., 2019; S. Remmers et al., 2020). In short, they were diluted to 180 mL in sodium citrate dissolved in phosphate buffered saline (PBS) (0.6 % w/v) adjusted to pH 7.2 at 4 °C (citrate buffer). PBMCs were isolated by layering onto Lymphoprep™ iso-osmotic medium (30 mL diluted buffy coat onto 16 mL Lymphoprep™) and centrifuging at $800 \times g$ for 30 min (lowest brake and acceleration). The PBMC layer was extracted using sterile Pasteur pipettes and PBMCs were washed 5 × with citrate buffer ($350 \times g$ for 10 min) to remove any remaining Lymphoprep™. PBMCs were used as is for one buffy coat, or further processed to isolate monocytes using the negative selection MACS® Pan Monocyte Isolation Kit as specified by the manufacturers' instructions for the other buffy coat. Here, non-monocytes were labeled with magnetic microbeads and retained in a filter column (size LS) in a magnetic field, while unlabeled cells passed through and were collected to be used as monocytes in this study.

3.3.2.2   *Variation in RANKL and M-CSF supplement concentration*

250×10^3 monocytes per cm^2 (n = 4 per group) were seeded in priming medium (De Vries et al., 2015) (RPMI-1640, 10 % FBS, 1 % Anti-Anti, 50 ng/mL M-CSF) on 24-well Corning® Osteo Assay plates and regular 24-well tissue culture plates in monolayer. Priming medium was replaced after 48 h with base medium (RPMI-1640, 10 % FBS, 1 % Anti-Anti) supplemented with 0, 12.5, 25, 50 or 100 ng/mL of both M-CSF and RANKL. Additionally, one group was seeded without priming medium and cultured directly in medium containing 50 ng/mL of both supplements. Medium was replaced 3 × per week for 2 weeks. All wells received the same medium volume per medium change (1 mL per well).

3.3.2.3   Variation in monocyte/PBMC seeding density

Monocytes were seeded at densities of 125, 150, 175, 200, 225 and 250 × 10^3 cells/cm², and PBMCs were seeded at densities of 250, 300, 350, 400 450 and 500 × 10^3 cells/cm² (n = 4 per group) in priming medium on 24-well Corning® Osteo Assay plates and regular 24-well tissue culture plates in monolayer. PBMCs were seeded at a higher density to partially compensate for the fact that only approximately 20 % of PBMCs are monocytes (Kleiveland, 2015). Priming medium was replaced after 48 h with osteoclast medium (RPMI-1640, 10 % FBS, 1 % Anti-Anti, 50 ng/mL M-CSF and RANKL). Medium was replaced 3 × per week for 2 weeks. All wells received the same medium volume per medium change (1 mL per well).

3.3.2.4   TRAP release quantification

Samples of cell culture supernatant were taken prior to each medium change and stored at -80 °C. 20 µL sample or p-nitrophenol standard in assay buffer (0.1 M sodium acetate, 0.1 % (v/v) Triton X-100 in PBS adjusted to pH 5.5) were incubated for 90 min at 37 °C with 100 µL para-nitrophenylphosphate (pNPP) buffer (1 mg/mL pNPP + 30 µL/mL tartrate solution in assay buffer). Stop solution (100 µL 0.3 M NaOH in ultra-pure water) was used to stop the reaction after 90 min. Absorbance was measured at 405 nm with a Synergy HTX Multi-Mode microplate reader (BioTek, Winooski, United States).

3.3.2.5   Immunofluorescent labelling

The cells cultured in plastic well-plates were fixed in 10 % neutral buffered formalin for 10 min, permeabilized with 0.5 % Triton X-100 in PBS for 10 min, blocked with 10 % horse serum in PBS for 30 min, washed with wash buffer (50 nM Tris pH 7.4, 150 mM NaCl, 5 mM EDTA, 0.05 % NP-40, 0.25 % gelatin). Cells were labeled with one of three marker combinations: TRAP + actin + DAPI with Alexa 488 donkey-anti-goat secondary antibody, Iβ3 + actin + DAPI with Alexa 488 donkey-anti-mouse secondary antibody, or TRAP + Iβ3 + actin with Alexa 488 donkey-anti-goat and Alexa 350 donkey-anti-mouse antibodies. The cells were incubated with primary antibodies for osteoclast markers TRAP and/or Iβ3 overnight at 4 °C (1:100 in wash buffer + 10 % horse serum). The next day, the cells were washed with wash buffer and incubated for 1 h with the respective secondary antibodies (1:300), TRITC-conjugated-Phalloidin (1:200) for actin and DAPI (1:1000) for nuclei in wash buffer. The cells were washed with PBS and imaged with a thin layer of PBS in the wells. Fluorescence images were taken with a Axiovert 200M microscope (Carl Zeiss Microscopy, Oberkochen, Germany).

3.3.2.6   Resorption on Osteo Assay plates

Cells on the Corning® Osteo Assay plates were removed using thin bleach (5 %) for 5 min. The wells were washed with ultra-pure water and dried at 50 °C. Bright field images were taken with a Axio Observer Z1 microscope (Carl Zeiss Microscopy, Oberkochen, Germany). Multiple images were stitched together to cover the complete surface area of the wells. An area of 3 by 5 stitched images completely within the well was cropped and used for image analysis. Images were binarized manually or in small batches using a combination of Matlab R2022a, Ilasik version 1.0 (Berg et al., 2019), and ImageJ (Schneider et al., 2012) with Fiji (Schindelin et al., 2012) to create as accurate as possible binarizations. From these, the percentage of resorption was calculated. Staining was not necessary for this method. An area of 3 by 5 stitched images was selected to improve Ilastik machine learning and binarization results, because light and well-shape artifacts around the edges of the wells obstructed the machine learning algorithm. A pixel classification algorithm was used in Ilastik, where areas of resorption and unresorbed areas were manually labeled to teach Ilastik how to recognize these in the current and subsequent images. The result was visually judged per image, and the algorithm was corrected and reapplied as necessary.

3.3.2.7   Statistical analysis

Quantitative data is represented as mean ± standard deviation (SD) and was analyzed using GraphPad Prism version 8. Data used for statistical analysis was tested for normality using the Shapiro-Wilk normality test and was normally distributed. Resorption data was analyzed with a Student's T-test or a One-Way Analysis of Variances (ANOVA). TRAP release data was compared using a Repeated Measures ANOVA. Bonferroni correction was used to account for multiple *post-hoc* comparisons. Geisser-Greenhouse correction was used to account for unequal variances. Differences were considered statistically significant at a level of $p < 0.05$. Where multiple comparisons were listed as a single difference, only the least significant (highest) p value was listed. Notable significant effects were numbered in the results section and in the figures using unique sequential numbering throughout this study.

3.4 Results

3.4.1 Supplement concentration affected osteoclast generation, TRAP release and resorption in monocytes

Monocytes were cultured in culture media with one of 6 concentrations of RANKL and M-CSF after a common priming phase of 2 days. Fluorescence imaging showed that at 0 ng/mL, minor TRAP expression was detected in monocytes, but Iβ3 expression or multinucleated cells were not (Fig. 3.1a, f, k). TRAP and Iβ3 positive multinucleated cells were detected at 12.5 ng/mL where all Iβ3-positive cells were small. Higher concentrations led to more and larger multinucleated cells (Fig. 3.1b-e, g-j, l-o), but above 25 ng/mL this increase seemed no longer proportional.

TRAP release analysis showed that TRAP release by monocytes increased sharply in all groups until day 7 (Fig. 3.2a). As expected, the 0 ng/mL group stopped releasing TRAP after this initial release that was likely caused by the priming phase. In all other groups, TRAP release continued and increased until the end of culture. Remarkably, TRAP release per well was similar for all concentrations except the 0 ng/mL group. Resorption data showed only resorption after culture with any non-zero concentration of added osteoclastic supplements (Fig. 3.2b). No resorption took place without these supplements, even though all cultures were primed for 2 d. Increasing supplement concentrations resulted in more resorption.

Priming of monocytes resulted in more TRAP release (Fig. 3.2c) and resorption (Fig. 3.2d) compared to the control group without priming. The unprimed group was cultured directly in 50 ng/mL of both supplements and showed considerably less resorption than the primed 50 ng/mL group but similar resorption as the 25 ng/mL group. While the observed difference was substantial, it was not statistically significant. An example of fully imaged Osteo Assay well, the area selected for analysis and the binarized image thereof are shown in Fig. 3.2e – g respectively.

3.4.2 Monocyte seeding density affected osteoclastic differentiation, but not TRAP release or resorption

Monocytes were seeded at 6 densities (125, 150, 175, 200, 225 and 250 × 10^3 cells/cm^2) to investigate how different seeding densities affect multinuclear cell generation, resorption, and TRAP release. TRAP- and Iβ3-positive cells were seen at all seeding densities. The number of large multinucleated cells increased slightly with seeding density, although their size and number of nuclei per cell did seem to increase substantially as monocyte

seeding density increased (Fig. 3.3). Unexpectedly, TRAP release results (Fig 3.4a) suggested that there is very little difference in TRAP release between monocyte seeding densities. Remarkably, there were some significant differences between the 125 and 150 × 10^3 cells/cm^2 groups vs. 200, 225 and 250 × 10^3 cells/cm^2 groups, suggesting that lower seeding densities resulted in higher TRAP release.

Resorption analysis matched these findings and showed that similar amounts of resorption occurred for all monocyte seeding densities (Fig. 3.4b), while increased seeding densities were expected to result in more resorption. The highest amount of resorption was measured in the 150 × 10^3 cells/cm^2 group, one of the lowest seeding densities, although none of the differences between groups were statistically significant.

3.4.3   PBMC seeding density affected multinuclear cell generation and resorption, but hardly affected TRAP release

PBMCs were seeded at 6 densities (250, 300, 350, 400, 450 and 500 × 10^3 cells/cm^2) to investigate how different seeding densities affected multinuclear cell generation, TRAP release and resorption. Fluorescence imaging revealed that TRAP expression was present at all seeding densities (Fig. 3.5g - r). While there were no clearly visible multinucleated TRAP positive cells until a PBMC seeding density of 400 × 10^3 cells/cm^2 (Fig. 3.5j), Iβ3-positive cells were already seen starting at 300× 10^3 cells/cm^2 (Fig. 3.5b). Considering the qualitative nature of immunohistochemistry, this difference was likely a result of chance. Only at the highest seeding density, there was a similar number of large multinucleated cells as observed in the monocyte cultures (Fig. 3.5l + r).

TRAP release showed no large differences between the seeding densities (Fig. 3.6a). On two occasions, the 250 and 300 × 10^3 cells/cm^2 (*11 and *12) groups released significantly more TRAP than higher seeding densities, but these effects were not consistently present. Although remarkably, lower seeding densities seemed to release slightly more TRAP than higher seeding densities. This was in line with the observations made in the monocyte seeding density experiment.

Resorption correlated with seeding density, and gradually increased as seeding density increased (Fig. 3.6b). Despite the high resorption of the 400 × 10^3 cells/cm^2 group with large SD, resorption followed a linear trend that was almost significant ($p = 0.079$). While there were clear differences between the resorption of the seeding densities and a trend is evident, none of these were significant after *post hoc* Bonferroni correction for multiple comparisons.
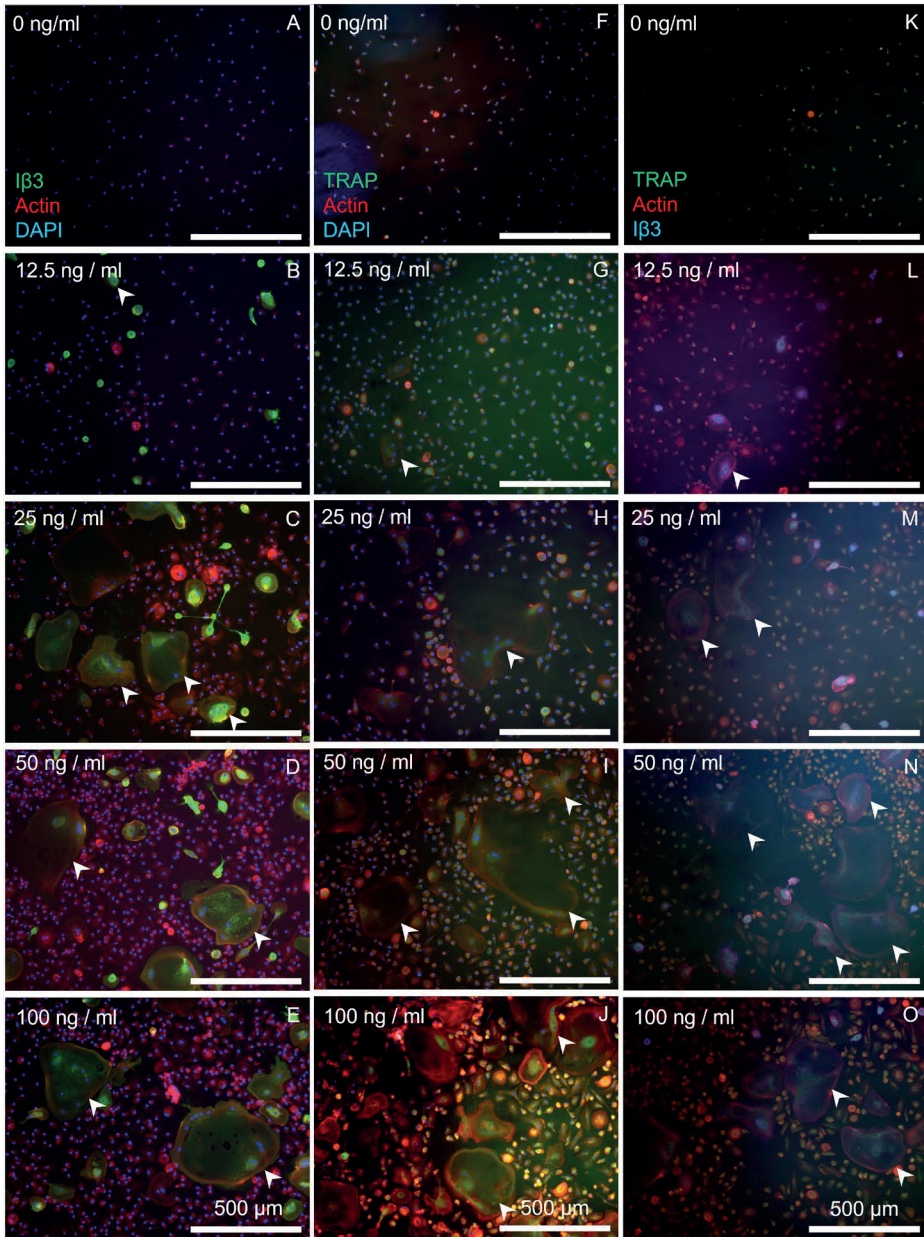
← Fig. 3.1. **The size and number of osteoclasts increases as supplement concentrations increased in monocyte cultures.** *Monocytes were seeded at different densities, cultured, and stained in one of three ways to compare TRAP and Iβ3 stains. (A – E) Iβ3, actin and DAPI staining showed that RANKL and M-CSF are required for Iβ3 expression. At 12.5 ng/mL, Iβ3-positive cells were present, but remain small. At 25 ng/mL and higher, Iβ3-positive cells appeared larger and more numerous. It was not clear if concentrations of 50 and 100 ng/mL result in even more or larger Iβ3-positive cells than at 25 ng/mL. (F – J) TRAP, actin and DAPI staining showed minor TRAP expression at 0 ng/mL but showed no evidence of multinucleated cells. Multinucleated TRAP-positive cells were seen at 12.5 ng/mL, but only at 25 ng/mL they became larger with many more nuclei. Concentrations higher than 25 ng/mL seemed to result in even more TRAP expression. (K – O) TRAP, actin and Iβ3 staining showed combined TRAP-Iβ3 expression predominantly in larger and multinucleated cells. Examples of multinucleated TRAP or Iβ3 positive multinucleated cells were indicated with white arrowheads.*

3
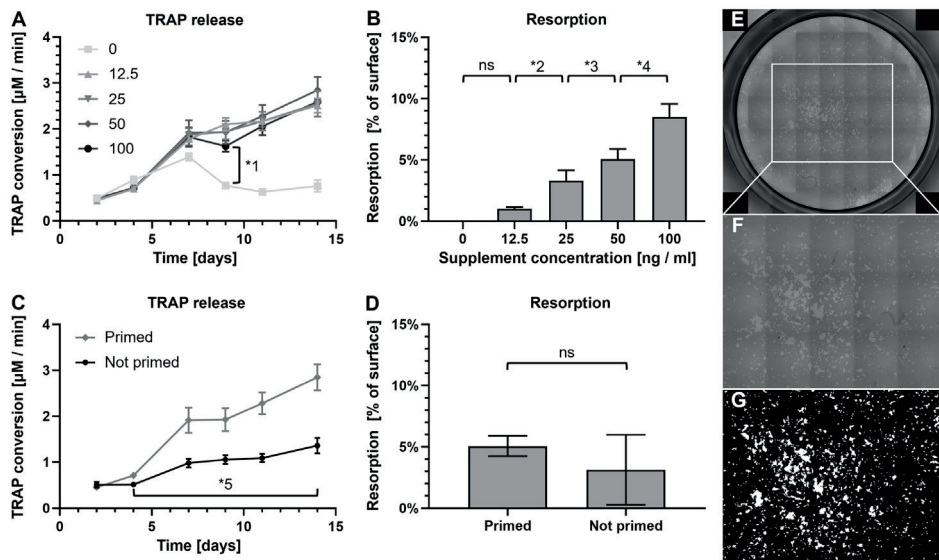
Fig. 3.2. **Supplement concentration affected resorption but not TRAP release in monocyte culture. (A)** *TRAP release increased near-equally in all groups except the 0 ng/mL group, which from day 9 onward deviated from all groups (*1: $p \leq 0.024$). (B) Higher osteoclastic supplement concentrations resulted in more resorption after 14 days, showing a significant linear trend over all data ($p < 0.001$). The difference between 0 and 12.5 ng/mL was not significant (ns) ($p = 0.64$). All other differences were statistically significant (*2: $p = 0.004$, *3: $p = 0.032$, *4 $p < 0.001$). (C) TRAP release of the primed group was significantly higher than that of the not primed group from day 4 onward (*5: $p \leq 0.024$). (D) Resorption analysis shows a substantial but not statistically significant difference of 1.93 percentage points ($p = 0.241$), with a much smaller SD in the primed group compared to the group without priming. (E) Resorption in an Osteo Assay well, imaged with light microscopy and stitched together. The 3 images by 5 images area used for analysis is shown in the white rectangle. Resorption is visible in white / light grey on an unresorbed dark grey background. (F) An enlargement of the area that was used for image analysis. (G) A binarized image of the selected area of interest, which allows easy quantification of the resorbed areas in white and the unresorbed areas in black.*
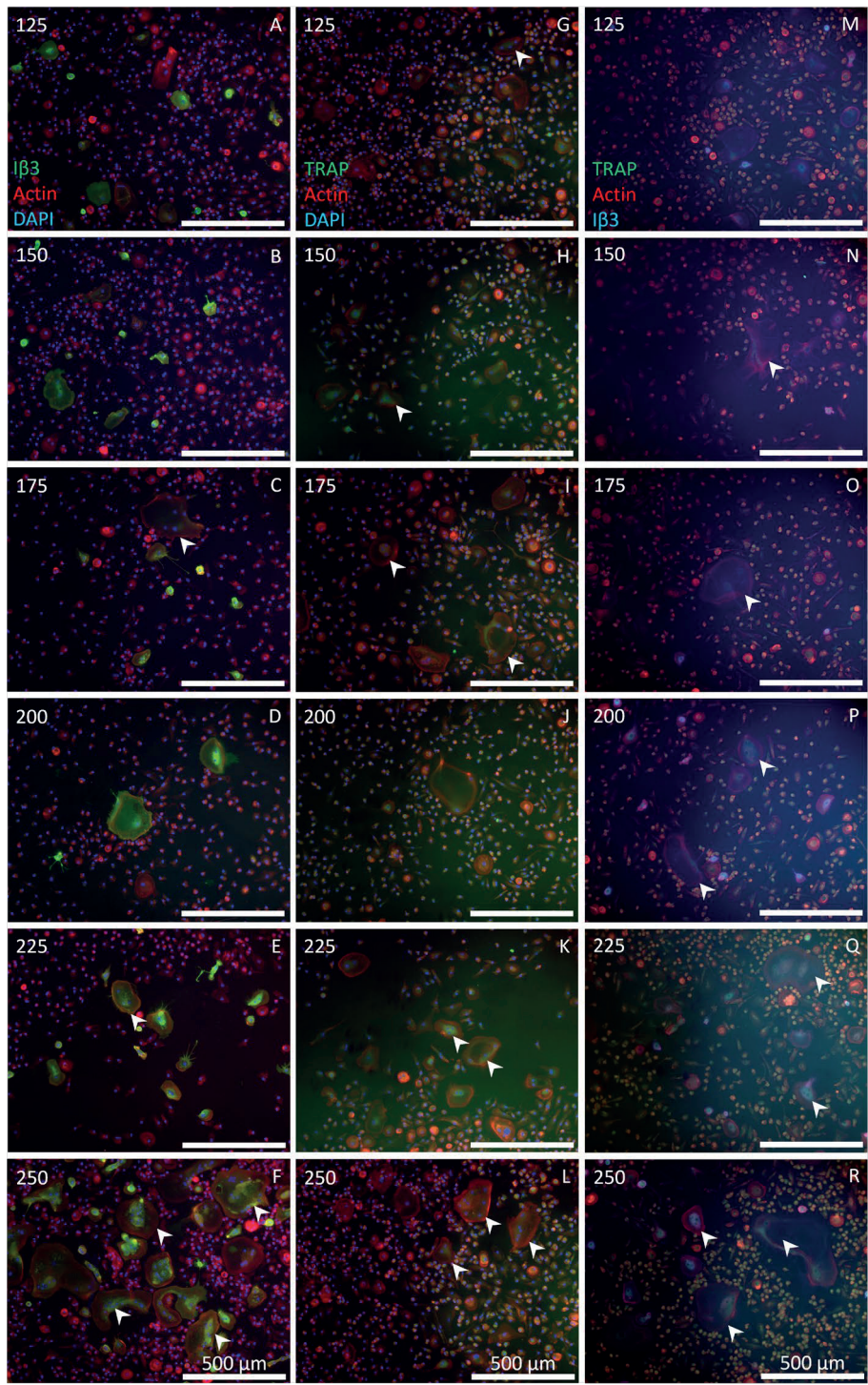
← *Fig. 3.3. **Higher monocyte seeding density led to slightly more and larger osteoclasts.** Monocytes were seeded at different seeding densities and stained in one of three ways. **(A – F)** Iβ3, actin and DAPI staining showed that all seeding densities resulted in Iβ3-positive cells. The size and number thereof increased as seeding density increased. **(G – L)** TRAP, actin and DAPI staining showed that TRAP positive cells were abundant in all seeding densities. While the size of TRAP positive cells increased with seeding density, the number of TRAP positive cells only increased marginally. **(M – R)** TRAP, actin and Iβ3 staining showed that not all TRAP positive cells were also positive for Iβ3. Iβ3 was almost exclusively seen in the larger or multinucleated cells whereas TRAP was also seen in many small mononuclear cells as well. Numbers in the top left corners indicate the monocyte seeding density × 10^3 cells/cm^2. Examples of multinucleated TRAP and / or Iβ3 positive cells are indicated using white arrowheads.*
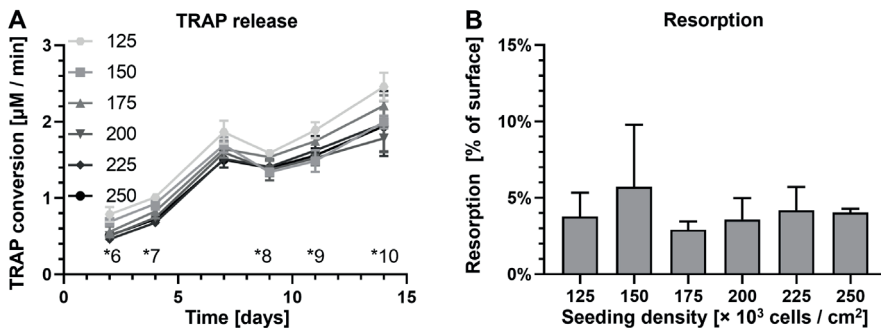
*Fig. 3.4. **Monocyte seeding density hardly affected total TRAP release and did not affect resorption.** **(A)** TRAP release over time increased in all seeding densities and seemed to be higher in the lower seeding densities. There were some significant differences that were inconsistent over time between the groups with one notable exception: the 125 × 10^3 cells/cm^2 group was significantly different from at least one of the 200, 225 and 250 × 10^3 cells/cm^2 groups on all indicated significances (*6 - *10, $p < 0.05$). **(B)** Resorbed surface area at different seeding densities. No significant differences in resorption were observed.*
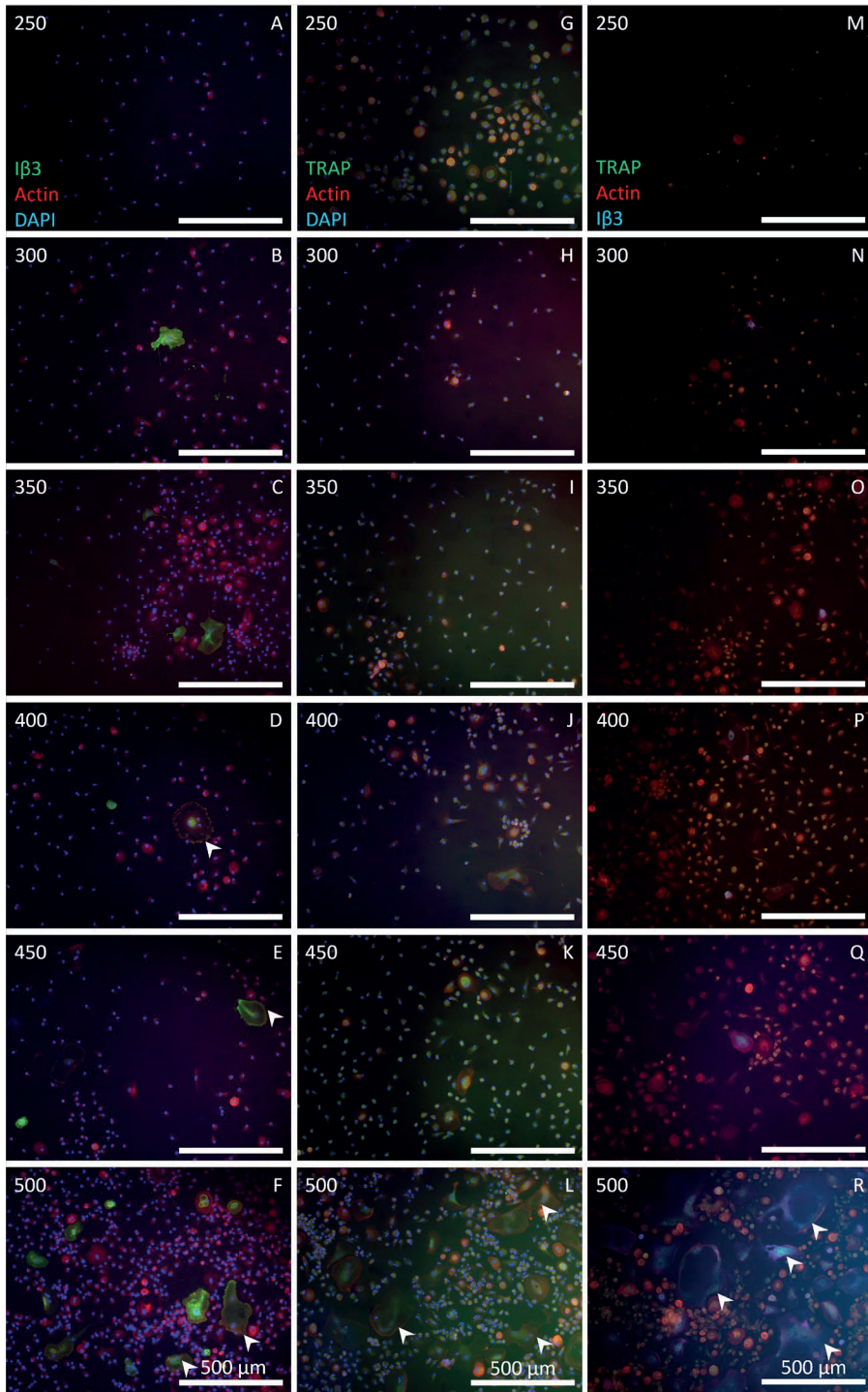
← *Fig. 3.5. **Higher PBMC seeding density led to more osteoclasts.** PBMCs were seeded at different densities and stained in one of three ways. (A – F) Iβ3, actin and DAPI staining showed that all but the lowest seeding density resulted in Iβ3-positive cells. At seeding densities from 300 to 450 × 10³ cells/cm², only few Iβ3-positive cells were seen. Only at the highest seeding density there were many Iβ3-positive cells. (G – L) TRAP, actin and DAPI staining showed that nearly all cells expressed TRAP, but only at a seeding density of 400 × 10³ cells/cm² or higher, larger multinucleated TRAP-positive cells were seen, with their numbers and size increasing at higher seeding densities. (M – R) TRAP, actin and Iβ3 staining showed that not all TRAP positive cells were also positive for Iβ3. Iβ3 was sporadically seen until 450 × 10³ cells/cm², and only at 500 × 10³ cells/cm² Iβ3 was present in many cells. Numbers in the top left corners indicate the PBMC seeding density × 10³ cells/cm². Examples of multinucleated TRAP or Iβ3 positive cells are indicated by white arrowheads.*
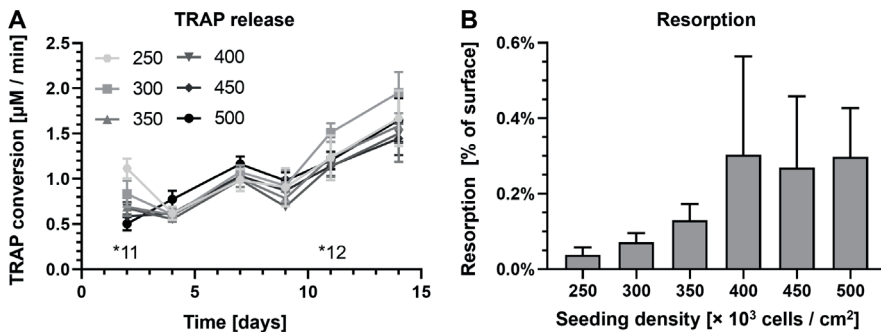
3

*Fig. 3.6. **Increased PBMC seeding densities hardly affected TRAP release but seemed to increase total resorption.** (A) TRAP release over time increased in all seeding densities and seemed to be higher in the lower seeding densities during week 2 of culture. Significant differences were inconsistent over the duration of the culture. *11: 250 vs. 350, 400, 450 & 500 ($p \leq 0.021$). *12: 300 vs. 400 ($p = 0.031$). (B) Increased PBMC seeding densities seemed to lead to increased resorption. The linear trend that is visible is not significant ($p = 0.079$). While some differences were statistically significant, these significances disappeared after correcting for multiple comparisons.*

3.5   Discussion

The limited *in vitro* availability, complex manner of differentiation, high between-donor variation (Flanagan and Massey, 2003; Husch et al., 2021) and short lifespan (Manolagas and Parfitt, 2010; Parfitt, 1994) of osteoclasts and their precursors make it challenging to study them. Furthermore, there is no consensus on parameters such as seeding density (Kozbial et al., 2019) and supplement concentration (Mather, 1998; Shahdadfar et al., 2005) which greatly affect *in vitro* results. In this study, we investigated the effect of supplement concentration and priming in monocyte cultures and seeding density in PBMC and monocyte cultures on osteoclastogenesis, TRAP release over time and osteoclastic resorption and showed that these outcome measures not always tell the same story and may even contradict each other.

3.5.1   Supplement concentration correlated with osteoclastogenesis and resorption.

Concentrations of 25 ng/mL of both supplements were sufficient to achieve the classical osteoclast-like appearance (Buckley et al., 2005), although higher concentrations did not lead to a proportional increase of large multinucleated cells. This is not unexpected, because the typical osteoclast appearance was already reached. Resorption though did show a continuing increasing trend correlating with supplement concentration, confirming that the supplements are not only necessary for differentiation, but also for osteoclastic resorption. Surprisingly, TRAP hardly increased with higher concentrations of supplements, although lack of supplements in the control group ensured a sharp decrease in TRAP release as expected. This matches the findings of Halleen, who proposed that TRAP release is indicative of osteoclast number but not activity (Halleen et al., 2006). This would suggest that while increasing supplement concentration above the threshold of 25 ng/mL not necessarily increases the number of osteoclasts, their size and resorptive capacity still increase. Priming is known to trigger gene expression (Hayes and Zoon, 1993) and benefit osteoclastogenesis (De Vries et al., 2015; Ross, 2006; Xu and Teitelbaum, 2013). Both TRAP release and resorption were lower without priming compared with the same supplement concentrations with priming. This confirmed that priming is a vital step in obtaining functionally competent osteoclasts, and suggests that priming, in contrast to increasing the supplement concentration, does lead to more osteoclasts.

3.5.2 Monocyte seeding density affects osteoclastogenesis, but not TRAP release or resorption after a certain threshold

Osteoclast size and number increased with monocyte seeding density, but remarkably, TRAP release and resorption did not, contrasting the findings of Halleen (Halleen et al., 2006). Resorption between all seeding densities showed no significant differences and TRAP analysis even suggested an inverse relationship between seeding density and TRAP release. These results suggest that there is an optimal seeding density (or range) for these cells which likely was superseded in the lower seeding densities already. What exactly was the limiting factor preventing the increase of TRAP release and resorption is not clear, but there are several possibilities. A seeding density too high could lead to competition for available surface area or specific medium components. Sharing an implicit shortage of available supplements or other media components with more competing cells could result in a lower availability per cell, with a higher proportion of cells not reaching the required threshold to differentiate or resorb. This would mean that commonly accepted culture conditions (Gstraunthaler et al., 1999; Place et al., 2017) might not be suitable for osteoclast cultures at these seeding densities. Lastly, the presence of non-resorbing osteoclasts (Karsdal et al., 2007), or a non-proportional relationship between osteoclast size and resorptive capacity could also have contributed to these findings. While large osteoclasts generally show more resorptive capacity than small ones (Lees et al., 2001), it could be that a large number of small osteoclast-like cells resorbed similar quantities as a lower number of large ones. This was supported by the presence of many slightly enlarged TRAP positive cells in the lower seeding densities, but only relatively few large osteoclasts in the higher seeding densities. These findings suggest that increased seeding densities result in larger but not necessarily more osteoclasts, and that there is a plateau in seeding density above which no increase in osteoclastic resorption is seen anymore, that depending on the donor, could fall within commonly used seeding densities.

3.5.3 PBMC seeding density affects osteoclastogenesis and resorption

PBMCs are commonly used as a monocyte source. However, PBMCs have shown to be able to support osteoclastogenesis independent of external supplements (De Vries et al., 2019; Salamanna et al., 2016). Excluding these cells may result in osteoclasts that are biochemically different from their *in vivo* counterparts, despite showing the correct markers and resorption *in vitro*. In this study, higher seeding densities of PBMCs led to more and larger TRAP- and Iβ3-positive multinucleated cells and a gradual increase in resorption, but not in increased TRAP release. Because osteoclast number and resorption did follow an increasing trend, it is unlikely that there was a competition for surface area

or medium components. While seeding densities were double, the absolute number of monocytes per well was expected to be between 20 and 40 % of those seeded in the monocyte experiment (Kleiveland, 2015), suggesting that the number of monocytes per surface area could still be limiting there. Similarly, non-specific medium components likely were not the limiting factor, but osteoclast supplements could have been considering the absolute difference in monocyte numbers. Resorption increased with seeding density but reached only 10 % of that in the monocyte experiment despite having 20-40 % of the monocytes. This discrepancy could be explained by between-donor variation (Flanagan and Massey, 2003; Susa et al., 2004) or by the spatial constraints inherent to their cell fusion-based differentiation. At lower densities, the relationship between seeding density and resorption is likely closer to exponential than to linear, while the monocyte experiment suggested a maximum effective seeding density. Therefore, we propose that this relationship follows a logistic or S-shaped curve over the full spectrum of seeding densities. These findings suggest that PBMCs can be seeded at much higher densities than monocytes and still see increases in osteoclast formation and resorption, although the total amount of resorption is less-than-proportionate to the number of expected monocytes in the PBMC population.

3.5.4 Method recommendations

This study has shown that fluorescence imaging with either TRAP or Iβ3 effectively labels osteoclasts, although TRAP is expressed in undifferentiated mononuclear cells and monocytes as well (Park et al., 2012; Toyosaki-Maeda et al., 2001). Iβ3 staining appeared to exclusively target osteoclasts in these culture conditions and can thus be just as valuable for identifying osteoclasts (Husch et al., 2021). However, the visual estimation of number and size of osteoclasts did not accurately correlate to resorption, and therefore should not be used to estimate osteoclastic activity. TRAP release was shown to increase with expected osteoclast cell numbers (Rucci et al., 2019), but could not be used as a quantitative marker of resorptive activity, although both supporting and contradicting reports are available of this observation (Husch et al., 2021). While this was unexpected and diminishes the value of TRAP as an osteoclastic activity marker, TRAP still has a vital role as it can be accurately monitored in the cell culture supernatant.

3.5.5 Limitations and future research

The seeding densities of monocytes appeared too high to accurately show the effects of increases in seeding density despite being based on literature. Counting the number of

alive and dead cells in culture supernatant or even further analyzing them with flow cytometry could shed light on what caused the observed plateau in resorption. Quantitative resorption analysis was done using image analysis software, but due to lighting, stitching and contrast artifacts we were not able to accurately analyze complete wells. Instead, a same-size-for-all rectangle in the center of the well was analyzed. This resulted in missed resorption spots along the edges of the wells. Ideally, a method should be developed that can reliably analyze the complete well, possibly through additionally using a staining technique such as von Kossa. Osteoclast cultures show a large between-donor variation (Susa et al., 2004). This means that any concrete number derived from these experiments is valid only for cells from this donor, and other donors should be characterized before use (Buenzli and Sims, 2015).

3.6   Conclusion

In this study, we have shown that common non-standardized culturing conditions of monocyte or peripheral blood mononuclear cells had a significant effect on the *in vitro* generation of functional osteoclasts. We showed how increased supplement concentrations support osteoclastic differentiation and resorption but not TRAP release, while priming resulted in increased TRAP release as well. Increased monocyte seeding densities resulted in more and larger osteoclasts, but not in more resorption or TRAP release. Increasing PBMC seeding densities resulted in more and larger osteoclasts and more resorption, although resorption was disproportionally low compared to the monocyte seeding density experiment. Exploration of commonly used markers for osteoclast cultures demonstrated that Iβ3 staining was an excellent osteoclast marker in addition to TRAP staining, while supernatant TRAP measurements could not accurately predict osteoclastic resorptive activity. With improved understanding of the effect of seeding density and supplement concentration on osteoclasts, more reliable and reproducible osteoclast experiments can ultimately improve our knowledge of osteoclasts, osteoclastogenesis, bone remodeling and bone diseases

Chapter 4

Measuring mineralized tissue formation and resorption in a human 3D osteoblast-osteoclast co-culture model

4.1 Abstract

In vitro tissue engineered bone constructs have been developed, but models which mimic both formation and resorption in parallel are still lacking. In order to be used as a model for the bone remodeling process, the formation and resorption of mineralized tissue volume over time needs to be visualized, localized and quantified. The goal of this study was to develop a human 3D osteoblast-osteoclast co-culture in which 1) osteoblasts deposit mineralized matrix, 2) monocytes differentiate into resorbing osteoclasts, and 3) the formation and resorption of mineralized matrix could be quantified over time using micro-computed tomography (μCT). Mesenchymal stromal cells were seeded on silk fibroin scaffolds and differentiated towards osteoblasts to create mineralized constructs. Thereafter, monocytes were added and differentiated towards osteoclasts. The presence of osteoblasts and osteoclasts was confirmed using immunohistochemistry. Osteoclastic activity was confirmed by measuring the increased release of osteoclast marker tartrate resistant acid phosphatase, suggesting that osteoclasts were actively resorbing mineralized tissue. Resorption pits were visualized using Scanning Electron Microscopy. Mineralized matrix formation and resorption were quantified using μCT and subsequent scans were registered to visualize remodeling. Both formation and resorption occurred in parallel in the co-culture. The resorbed tissue volume exceeded the formed tissue volume after day 12. In conclusion, the current model was able to visualize, localize and quantify mineralized matrix formation and resorption. Such a model could be used to facilitate fundamental research on bone remodeling, facilitate drug testing and may have clinical implications in personalized medicine by allowing the use of patient cells.

4.2   Introduction

Bone consists of three main cell types: bone forming osteoblasts, bone resorbing osteoclasts, and regulating osteocytes. As the mechanical demands placed upon bones change, bones adapt their structure by removing obsolete material or producing new material where it is needed to provide the required strength. This process is made possible by the organization of osteoblasts and osteoclasts into local bone remodeling teams called basic multicellular units (Frost, 1969). While the exact inter- and intracellular mechanisms underlying bone remodeling and bone diseases have not been completely elucidated, many factors and cytokines that play a role in these processes have been identified (Deschaseaux et al., 2010; Matsuo and Irie, 2008; Sims and Gooi, 2008), and are being targeted by treatment options for diseases such as osteoporosis (Bellido, 2014; Matsuo and Irie, 2008). Unfortunately, even with access to various forms of treatment, it is not yet possible to reverse the degenerative nature of osteoporosis, but merely to slow down the progression. In order to elucidate the cellular and molecular mechanisms underlying bone remodeling, as well as to facilitate the development of new and personalized treatments for bone diseases, accurate, reproducible and translatable model systems are needed.

Animal models are considered a fundamental part of preclinical research, but using animals raises ethical concerns and is generally more time-consuming and expensive than *in vitro* research. Although human health and disease are the objects of interest, animals with a similar yet still different physiology are being used, which can lead to poor translation of results from pre-clinical animal studies to human clinical trials, and the failure of highly promising discoveries to enter routine clinical use (Burkhardt and Zlotnik, 2013; Contopoulos-Ioannidis et al., 2003). Those limitations and the desire to reduce, refine and replace animal experiments gave rise to the development of *in vitro* models.

In vitro bone models come with both advantages and limitations. While animal cells are easily accessible and easy to work with, they can respond differently than human cells (Jemnitz et al., 2008). *In vitro* models have the advantage that they can make use of human cells. Many *in vitro* experiments are conducted in 2D monolayer (Amizuka et al., 1997; Marino et al., 2014), which is suitable for the research questions they address. However, *in vivo* bone remodeling occurs in a 3D environment where cells can deposit and resorb quantifiable volumes of mineralized tissue, and where cells likely respond differently than in 2D (Edmondson et al., 2014; Li and Kilian, 2015). Ideally, to study human bone remodeling and quantify bone formation or resorption *in vitro*, primary human cells should be cultured in a 3D environment (Owen and Reilly, 2018). As bone formation and resorption occur simultaneously, a co-culture of both osteoblasts and osteoclasts is required, in particular because it is known that these cells are capable of interacting with

each other through paracrine signalling (Matsuo and Irie, 2008). There are various methods to co-culture cells (Goers et al., 2014; Paschos et al., 2015; Zhu et al., 2018), but only a direct co-culture within the same construct allows a two-way exchange of signalling molecules and access to the same mineralized surface. Functionality of the cells could then be assessed by quantification of the net effect of stimuli on remodeling, as well as the individual effects of resorption and formation.

Recently, 3D osteoclast models (Heinemann et al., 2010; Kleinhans et al., 2015; Perrotti et al., 2009) and 3D osteoblast-osteoclast co-culture models (Hayden et al., 2014; Papadimitropoulos et al., 2011)have been designed to specifically study 3D bone resorption or remodeling using a variety of end-point techniques such as histological imaging, electron microscopy, surface metrology, polymerase chain reaction and various cell marker assays. These studies provided first insights into human bone remodeling but should be improved by quantitatively monitoring bone remodeling over time. Registration of consecutive images similarly to *in vivo* bone studies in mice (Hagenmüller et al., 2007; Schulte et al., 2011a, 2011b) would allow assessing both formation and resorption in parallel, and thereafter separating the contribution of osteoblasts from those of osteoclasts.

The aim of the present study was to establish a 3D co-culture of primary human osteoblasts and osteoclasts on silk fibroin (SF) scaffolds in which 1) osteoblasts first deposit a mineralized bone-like matrix, 2) monocytes are differentiated into resorbing osteoclasts, and 3) the mineralized matrix formation by osteoblasts and the resorption by osteoclasts can be both monitored over time. Such a human *in vitro* model would allow the localization and quantification of formation and resorption events over time to provide a powerful tool for fundamental research on osteoblast-osteoclast interaction and bone remodeling and could have implications for drug development and personalized medicine.

4.3   Materials and Methods

4.3.1   Materials

Dulbecco's modified Eagle medium (DMEM Cat. No 41966) and non-essential amino acids (NEAA) were from Life Technologies (Bleiswijk, The Netherlands). Fetal Bovine Serum (FBS, batch F7524-500ML / lot BCBV7611) was from Sigma Aldrich / Merck. Antigen retrieval citrate buffer, RPMI-1640 medium, poly-L-lysine coated microscope slides and SnakeSkin Dialysis tubing were from Thermo Fisher Scientific (Breda, The Netherlands). Disposable biopsy punches were from Amstel Medical (Amstelveen, the

Netherlands) Trypsin-EDTA (0.25%) and penicillin/streptomycin (P/S) were from Lonza (Breda, The Netherlands). Human bone marrow (healthy male subject, 24 years of age) was from Lonza (Walkersville, MD, USA). The human buffy coat was from Sanquin (Nijmegen, the Netherlands). Lymphoprep™ was from Axis-Shield (Oslo, Norway). MACS® Pan Monocyte Isolation Kit was from Miltenyi Biotec (Leiden, the Netherlands). Recombinant human basic fibroblast growth factor (bFGF), macrophage colony stimulating factor (M-CSF) and receptor activator of nuclear factor kappa-B ligand (RANKL) were from PeproTech (Rocky Hill, NJ, USA). *Bombyx mori L.* Silkworm cocoons were from Tajima Shoji Co., LTD. (Yokohama, Japan). Thin bleach was from the local grocery store. All other substances were of analytical or pharmaceutical grade and obtained from Sigma Aldrich / Merck (Zwijndrecht, The Netherlands).

4.3.2   Methods

4.3.2.1   *Silk fibroin scaffold fabrication*

Silk fibroin (SF) scaffolds were produced as previously described (Meinel et al., 2005; Melke et al., 2018; Nazarov et al., 2004). *Bombyx mori L.* silkworm cocoons were degummed by boiling in 0.2 M Na_2CO_3 in ultra-pure water (UPW) twice for 1 h, rinsed in boiling UPW followed by 10 × washing in cold UPW. The silk was left to dry overnight and was dissolved in 9 M LiBr in UPW (10 % w/v) at 55 °C for 1 h, cooled to RT and filtered through a 5 μm filter. Then, the silk solution was dialyzed against UPW for 36 h using SnakeSkin Dialysis Tubing (molecular weight cut-off: 3.5 kDa) UPW was replaced after 1, 3, 12, 24 and 36 h. Dialyzed silk solution was frozen at -80 °C, lyophilised (Freezone 2.5, Labconco, Kansas City, MO, USA) for 4 d and dissolved to a 17 % (w/v) solution in 1,1,1,3,3,3-Hexafluoro-2-propanol (HFIP). 1 mL silk-HFIP solution was added to 2.5 g NaCl with an average granule size between 250 and 300 μm in a Teflon container and allowed to dry at room temperature for 4 d. Silk-salt blocks were immersed in 90 % (v/v) methanol in UPW for 30 min to induce β-sheet formation (Tsukada et al., 1994) and dried at room temperature overnight. Silk-salt blocks were mounted in a precision cut-off machine (Accutom-5®, Struers GmbH Nederland, Maassluis, the Netherlands), and cut into discs of 3 mm height. NaCl was leached out in UPW for 2 d. UPW was replaced after 2 h, and then 2 × per day. Scaffolds were punched with a 5 mm diameter disposable biopsy punch and sterilized by autoclaving in phosphate buffered saline (PBS) at 121 °C for 20 min.

4.3.2.2   hMSC expansion, seeding onto scaffolds and osteoblastic differentiation

This study used human mesenchymal stromal cells (hMSC) at passage 5 that were isolated from human bone marrow (healthy male subject, 24 years of age) and characterized in a previous study (Hofmann et al., 2007). Cells were thawed, seeded at 2.5×10^3 cells/cm^2 and expanded for 6 d in control medium (DMEM, 10 % FBS, 1 % P/S) supplemented with 1 % NEAA and 1 ng/L bFGF. Scaffolds pre-wetted in control medium were seeded with 1 million hMSCs each in 20 µL control medium and incubated for 90 min at 37 °C. The constructs were then transferred to 4 custom-made spinner flask bioreactors (n = 4 per bioreactor) as described previously (Melke et al., 2018). Each bioreactor contained a magnetic stir bar and was placed on a magnetic stirrer plate (300 RPM, RTv5, IKA, Germany) in an incubator (37 °C, 5 % CO_2). Each bioreactor was filled with 5 mL osteogenic medium (control medium supplemented with 50 µg/mL L-ascorbic-acid-2-phosphate, 100 nM dexamethasone, 10 mM β-glycerophosphate) and medium was changed 3 times a week for 13 weeks. In this study the 3D mono-culture of hMSCs on SF scaffolds, differentiation into osteoblasts and matrix formation was designated as '3D osteoblast culture'.

4.3.2.3   Monocyte isolation from peripheral blood

A human peripheral blood buffy coat from a healthy anonymous volunteer who gave informed consent was obtained from the local blood donation centre (Sanquin, Nijmegen, the Netherlands). The buffy coats (~50 mL) was diluted to 180 mL in 0.6 % (w/v) sodium citrate in PBS adjusted to pH 7.2 at 4 °C (Citrate-PBS), after which the peripheral mononuclear cell fraction was isolated by carefully layering 30 mL diluted buffy coat onto 16 mL Lymphoprep™ iso-osmotic medium in 6 separate 50 mL centrifugal tubes, and centrifuging for 30 min with lowest brake and acceleration at 800 ×g at RT, as described previously (Bonito et al., 2019). Mononuclear cells were layered on top of the iso-osmotic layer, and were transferred to new tubes using a sterile Pasteur pipette. Isolated cells were washed (suspended in 50 mL Citrate-PBS and centrifuged for 10 min at 350 ×g) 5 × to remove all Lymphoprep™, diluted in freezing medium 1 (20 % FBS in RPMI-1640) and aliquoted into cryovials, 50 million cells in 750 µL per vial. Into each cryovial 750 µL freezing medium 2 (20 % dimethyl sulfoxide in freezing medium 1) was added and the cryovials were transferred to Nalgene® freezing containers overnight (-80 °C), before being transferred to liquid nitrogen tanks for long-term storage. Cells were taken out of liquid nitrogen and rapidly thawed before use without passaging. A purified monocyte fraction was isolated from the mononuclear cells using the negative selection MACS® Pan Monocyte Isolation Kit (Miltenyi Biotec) with LS columns according to the manufacturers' instructions. After magnetic separation, the cells were centrifuged for 10 min at 350 ×g,

resuspended in osteoclast control medium (RPMI-1640, 10 % FBS, 1 % P/S) and counted. The purified monocyte fraction will from now on be referred to as 'monocytes'.

4.3.2.4   2D osteoclast mono-culture

A 2D culture was conducted to show the differentiation potential of the monocytes and the resorption potential of the osteoclasts. To verify that the monocytes can form multinucleated tartrate-resistant acid phosphatase (TRAP) expressing and resorbing osteoclast-like cells, 0.25×10^6 monocytes per cm^2 (n = 4 per time point) were seeded in priming medium (osteoclast control medium + 50 ng/mL M-CSF) on 24-well Corning® Osteo Assay plates and regular tissue culture plastic 24-well tissue culture plates in monolayer (without scaffolds). Priming medium was replaced with osteoclastogenic medium (priming medium + 50 ng/mL RANKL) after 48 h. Osteoclastogenic medium was replaced 3 × per week for up to 19 d. This experiment was designated as '2D osteoclast mono-culture'.

4.3.2.5   2D Resorption assay

The Corning® Osteo Assay plate from the 2D osteoclast mono-culture was analysed for resorption according to the manufacturers' instructions. Cells were removed by incubation in 5 % bleach for 5 min, and their removal was confirmed with light microscopy. The plate was incubated with 5 % (w/v) aqueous silver nitrate for 30 min at room temperature in the dark, washed with UPW for 5 min, followed by 5 % (w/v) sodium carbonate in neutral buffered formalin for 4 min. The plate was dried at 50 °C for 1 h. Bright field images were taken with a Zeiss Axio Observer Z1 microscope.

4.3.2.6   Seeding monocytes onto tissue-engineered (pre-mineralized) constructs

Constructs which had been in culture for 13 weeks (3D osteoblast culture) were incised to allow monocyte seeding to the centre of the constructs. An incision of approximately 4 mm deep was made into the constructs at 1.5 mm height in the transverse plane, allowing the construct to fold partly open. Constructs were submersed for 1 h in priming medium. 1 million monocytes in 7.5 µL priming medium were seeded into the incision of the constructs and incubated for 180 min at 37 °C to allow the cells to attach. The constructs were then placed back into the bioreactors (n = 4 per bioreactor, one bioreactor per timepoint for histology and SEM, and one bioreactor that was scanned using µCT for the duration of the study). Each bioreactor was filled with 5 mL priming medium, resulting

in 1.25 mL of medium per construct. No stirring was applied. The 3D co-culture of osteoblasts with monocytes was designated as '3D co-culture'. Priming medium was replaced with osteoclastogenic medium (priming medium + 50 ng/mL RANKL) after 48h (De Vries et al., 2015). Osteoclastogenic medium was replaced 3 × per week for up to 22 d. Constructs were sacrificed at day 12, 18 and 25 for SEM, histology and immunohistochemistry. One bioreactor was used for µCT imaging of the co-culture.

4.3.2.7 *Micro-computed tomography imaging (µCT)*

µCT measurements were performed on a µCT100 imaging system (Scanco Medical, Brüttisellen, Switzerland) after 3, 4, 5 and 13 weeks of 3D osteoblast culture to monitor tissue mineralization. After 13 weeks, monocytes were seeded into the (now incised) constructs, and were scanned again after 4, 12 and 22 d of 3D co-culture to monitor mineralized tissue resorption. Scanning was performed at an isotropic nominal resolution of 17.2 µm, energy level was set to 45 kVp, intensity to 200 µA, 300 ms integration time and two-fold frame averaging, resulting in a computed tomography dose index (CTDI) in air of 230 mGy. A constrained Gaussian filter was applied to reduce part of the noise. Filter support was set to 1.0 and filter width sigma to 0.8 voxel. For all but the last 2 scans, a region of interest of 205 slices was selected within the bioreactor insert. This allowed to always scan the same regions of every scaffold and to limit the required scan time and thus x-ray exposure of the cells to 30 min per construct. For the last 2 scans, the whole construct was scanned to facilitate 3D registration, with a scan time of approximately 60 min per construct. Filtered greyscale images were segmented at a global threshold of 23 % of the maximal greyscale value and processed using image processing language (IPLFE v2.03, Scanco Medical AG) available on the PC supplied with the scanner. Unconnected objects smaller than 50 voxels were removed by component labelling (function: cl_nr_extract, min_number 50) and neglected for further analysis. Quantitative morphometry was performed using a Triangulation Metric Gobj DA Procedure (function: tri_da_metric, default settings) to assess the mineralized tissue volume of a region of interest of 205 slices per construct. 3D osteoblast culture quantitative µCT data was used as such, whereas 3D co-culture quantitative µCT data was transformed in such a way that the mineralized volumes of the first scan of each individual construct (d 4 of co-culture) was set to 100 %, and all successive scans were presented as percentages of change regarding the first scan. Rigid 3D registration was used to register the follow-up to the baseline image (images of day 22 and 12 respectively of the 3D co-culture) of the complete scans of the constructs (Ellouz et al., 2014). After registration, colour coding was used to label voxels only present at day 12 in blue (resorption), voxels only present at day 22 in orange (formation), and voxels present in both images in grey-purple (unaltered).

Unconnected objects smaller than 50 voxels were removed as before. The number of voxels for each colour was extracted by creating a histogram of all corresponding values (function: histo, screentab on, range from 0 to 123). Unaltered and resorbed voxels added together were used as 100 % baseline reference for each construct. Resorption, formation and unaltered volumes were expressed as percentage of the baseline. Background voxels were omitted from further analysis. All images shown are from component-labelled scans.

4.3.2.8   Histology

Constructs for histology and immunofluorescence were fixed in 10 % neutral buffered formalin for 24 h at 4 °C, dehydrated and embedded in paraffin (70, 80 and 96 % EtOH for 1.5 h each, 3 × 100 % EtOH for 1 h each, 2 × xylene for 1.5 h each, 2 × paraffin for 2 h each), sectioned vertically and cut into 10 µm thick sections and mounted on poly-L-lysine coated microscope slides. Sections were dewaxed and rehydrated (2 × 5 min Xylene, 3 × 100 %, 1 × 96 %, 70 % and 0 % EtOH in UPW for 2 min each). For overview, sections were stained with Haematoxylin and Eosin (H&E) (10 min Mayer's haematoxylin, 1 min acidified tap water, 5 min running tap water, 3 min Eosin Y, 1 min running tap water). To visualize mineralized tissue, sections were stained with von Kossa (30 min in 1 % aqueous silver nitrate (w/v) under UV light, rinsed with UPW, 5 min in 5 % sodium thiosulfate (w/v), rinsed with UPW, 5 min in nuclear fast red, rinsed in UPW). Stained sections were dehydrated (10 dips in 70 %, 90 % and 3 × 10 dips in 100 % EtOH in UPW, 2 × 3 min Xylene) and coverslipped with Entallan®.

4.3.2.9   Immunofluorescence

Sections were dewaxed and rehydrated as described before. Antigen retrieval was done on paraffin sections with citrate buffer at 95 °C for 20 min and left to cool back to RT. Cross-reactions were reduced by blocking with 10 % donkey serum for 30 min. Primary antibodies were diluted in PBS and incubated at 4 °C overnight. Sections were rinsed in PBS and incubated with secondary antibodies at RT for 1 h. Sections were labelled with DAPI for cell nuclei and with antibodies for osteoblast marker osterix, osteocyte marker sclerostin and osteoclast marker integrin β3 (CD61), which was chosen in favour of TRAP because of its specificity towards differentiated osteoclasts, while TRAP is present in osteoclast-like cells as well (Barbeck et al., 2017; Nakamura et al., 2007). The 2D osteoclast monoculture in plastic well-plates was immunofluorescently labelled for osteoclast marker TRAP, with TRITC-conjugated-Phalloidin to stain the actin cytoskeleton, and DAPI for cell nuclei to study multinucleation. Stained wells were imaged with a layer of

PBS on top with the Zeiss Axiovert 200M microscope, and sections were coverslipped with Mowiol® and imaged with the Leica TCS SP5X microscope. Antibodies are listed in Table 4.1.

4.3.2.10 Scanning electron microscopy (SEM)

Constructs for SEM were fixed at day 12 and 18 in 2,5 % glutaraldehyde for 24 h at 4 °C, dehydrated with a graded ethanol series (2 × 50 %, 70 % and 95 %, 3 × 100 % 10-15 min each) followed by a graded 1,1,1-Trimethyl-N-(trimethylsilyl)silanamine (HMDS)/ethanol series (1:2, 1:1, 2:1, 3 × 100 % HMDS 15 minutes each), dried at room temperature overnight and sputter coated with 5 nm gold (Q300TD, Quorum Technologies Ltd, Laughton, UK) prior to imaging with SEM (Quanta600, FEI Company, Eindhoven, the Netherlands) with spot size 3.0, 5.00 kV, working distance 10 mm).

4.3.2.11 TRAP quantification in supernatant

Supernatant medium samples were taken and stored at -80 °C at each medium change during the 3D co-culture (n = 4 per bioreactor) and the entire 2D osteoclast monoculture (n = 4 per group). 100 µL pNPP buffer (1 mg/mL para-nitrophenylphosphate (pNPP), 0.1 M sodium acetate, 0.1 % (v/v) triton-X-100 in PBS, first adjusted to pH 5.5, then supplemented with 30 µl/mL tartrate solution (Sigma Aldrich)) and 20 µL culture medium or nitrophenol standard in PBS were incubated in translucent 96-well plates at 37 °C. After 90 min, 100 µl 0.3M NaOH was added to stop the reaction. Absorbance was read at 405 nm to obtain TRAP enzyme activity. The resulting values were transformed to amount of transformed pNPP per minute.

4.3.2.12 Statistical analysis

Quantitative data is represented as average ± standard deviation (SD). Statistical analysis was performed using SPSS version 26 (IBM Corp, Armonk, NY, USA). Timepoints and groups that were statistically compared were tested for normality using the Shapiro-Wilk normality test and were normally distributed. Homogeneity of variance was assessed with the Levene's test for equality of variances. A repeated measures analysis of variances (ANOVA) was performed on the 3 consecutive scans with 205 slices each of the 3D co-culture. Paired-samples t-tests were used to compare total volume change between day 12 and 22 of the complete µCT scans, and the difference between quantified formation and resorption data. A one-way ANOVA with post-hoc Bonferroni correction for multiple

comparisons was used to compare differences between both culture surfaces and all relevant time points of the TRAP activity of cells seeded in 2D on plastic or Osteo Assay plates. Differences were considered statistically significant at a level of $p < 0.05$.

*Table 4.1. **Antibodies used for immunofluorescence.***

Antigen	Supplier	Cat. No	Conjugate	Species	Dilution
Osterix	Abcam	Ab22552	-	Rabbit	1:200
Sclerostin	ThermoFisher	PA5-37943	-	Goat	1:200
Integrin β3	Biorbyt	Orb248939	-	Mouse	1:100
TRAP	Santa-Cruz	Sc-30833	-	Goat	1:100
Anti-mouse IgG (H+L)	Jackson	715-545-150	Alexa488	Donkey	1:300
Anti-rabbit IgG (H+L)	Jackson	711-605-152	Alexa647	Donkey	1:300
Anti-goat IgG (H+L)	Invitrogen	A21432	Alexa555	Donkey	1:300
Anti-goat IgG (H+L)	Molecular Probes	A11055	Alexa488	Donkey	1:300

4.4   Results

4.4.1   hMSCs differentiate into osteoblasts and form mineralized tissue

hMSCs were seeded onto SF scaffolds and differentiated into mineralized matrix depositing osteoblasts for 13 weeks. Starting from week 3, mineralized matrix formation was monitored with consecutive μCT scans. Non-mineralized SF scaffolds were not visible on μCT images. Mineralization became detectable from week 4 onwards, and mineralization continued until week 13 (Fig. 4.1a). Mineralized volume increased over time to 17.62 ± 4.69 mm^3 at week 13 (Fig. 4.1b). A cross-section revealed that mineralized tissue was present throughout the construct (Fig. 4.1c). Tissue formation on the outside of the construct completely concealed the original porous architecture, which would have prevented cells seeded on top to penetrate into the construct and necessitated incising the construct to seed cells inside for the co-culture (Fig. 4.1d). An SEM image of an empty scaffold without any seeded cells is provided to illustrate the effect of osteoblastic tissue formation on the geometry of the construct (Fig. 4.1e).

4.4.2   Monocytes differentiate into resorbing TRAP expressing multinucleated osteoclasts in 2D

To verify that the primary monocytes were capable to differentiate into TRAP expressing, resorbing, multinucleated osteoclasts, monocytes were seeded in 2D on tissue culture plastic and on Osteo Assay plates to visualize resorption. On the plastic surface, multinucleated cells with more than 3 nuclei that express osteoclast marker TRAP with a

well-defined actin cytoskeleton were seen (Fig. 4.2a, image of day 12), indicating that they differentiated into osteoclast-like cells. During the differentiation from monocytes to osteoclasts, TRAP release increased until approximately day 12. Interestingly, cells cultured on Osteo Assay plates continued to release TRAP throughout the culture period, whereas cells cultured on plastic showed a rapid decrease in TRAP release over time after day 12 (Fig. 4.2b). The highest peak TRAP activities were 16.62 ± 0.92 μM pNPP / min / well at day 14 on the Osteo Assay surface and 14.88 ± 0.64 μM pNPP / min / well at day 12 on tissue culture plastic, but the difference was not statistically significant ($p = 0.173$). TRAP activity curves started to significantly deviate from each other from day 14 onward ($p < 0.001$). Cells were able to resorb parts of the mineralized layer (in black) creating resorption trails (in white) on Osteo Assay plates (Fig. 4.2c). At the first time point for the resorption assay (d 8), resorption was already visible. On later timepoints, more resorption was seen.
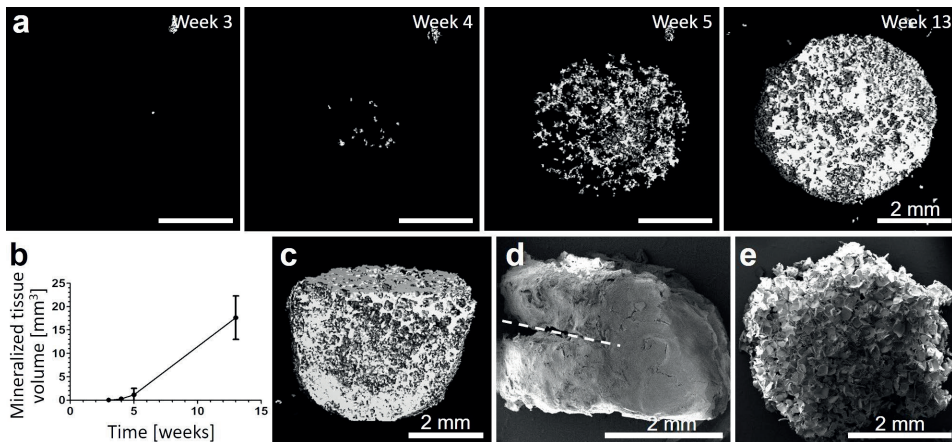
Fig. 4.1. **Formation of a mineralized matrix by osteoblasts on 3D SF scaffolds. (a)** *Non-mineralized SF scaffolds are not visible on µCT images. Mineralized matrix became detectable after 3 weeks of culture and increased in volume over time. Images are top-down views. Scale bars are 2 mm. **(b)** The mineralized tissue volume of the constructs continuously increased over time. (c) An inclined view on a digital cross-section of a µCT image shows the mineralized matrix distribution within a construct at week 13. (d) SEM example image of an SF scaffold after 9 weeks of osteoblast culture, showing that tissue formation completely concealed the pores of the SF scaffold, necessitating incising the construct to seed monocytes inside. A dashed line shows where the construct was incised for seeding. (e) SEM control image of an SF scaffold without any cells.*

4.4.3 Monocytes differentiate into resorbing TRAP expressing osteoclasts in 3D

Once a mineralized matrix was deposited by osteoblasts, monocytes were seeded into the centre of the construct by creating a transverse incision through the mineralized construct. The culturing environment was switched from an osteogenic medium with mechanical stimulation using a spinner flask bioreactor to a static environment with a medium inducing monocyte differentiation towards osteoclasts. The presence of resorbing osteoclast-like cells on the constructs was verified with SEM. Osteoclast-like cells were identified based on their size (> 50 µm in diameter) (Fig. 4.3a - b) and their proximity to what could be small resorption pits (Fig. 4.3a). The immediate surrounding area of the pits in Fig. 4.3a seemed morphologically different than the area surrounding it. Neither pits nor such areas were found on control constructs without seeded monocytes (Fig. 4.3c). Images of unseeded SF scaffolds illustrate the architecture of these scaffolds prior to the experiment (Fig. 4.3d + e). TRAP analysis in the supernatant showed an increasing release until day 12, followed by a continuous release of TRAP until the end of culture (Fig. 4.3f).

4.4.4 Histology confirms the presence of bone cells and mineralized matrix in 3D co-culture

Constructs for histological images were collected at day 12 to avoid a time point towards the end of the expected life expectancy of osteoclasts. The presence of cells throughout the construct was confirmed with H&E (Fig. 4.4a + d). Deposition of a mineralized matrix throughout the construct volume was confirmed with von Kossa staining (Fig. 4.4b + e) and has supported the threshold choice for the micro-CT analysis. The transverse incision for seeding monocytes can be seen in the histological images. The presence of osteoblast-like-, osteoclast-like- and osteocyte-like cells was confirmed with fluorescent staining of markers typical for the respective cell type (osterix, integrin β3 and sclerostin, respectively) (Fig. 4.4c + f). Osteoblast- and osteocyte-like cells were abundantly found throughout the construct, whereas only few integrin β3-positive osteoclast-like cells were detected. Classical morphological features of the cells could not be visualised as a result of creating 2D sections of a 3D tissue, where the odds of a cell lying precisely within the cutting plate are slim.
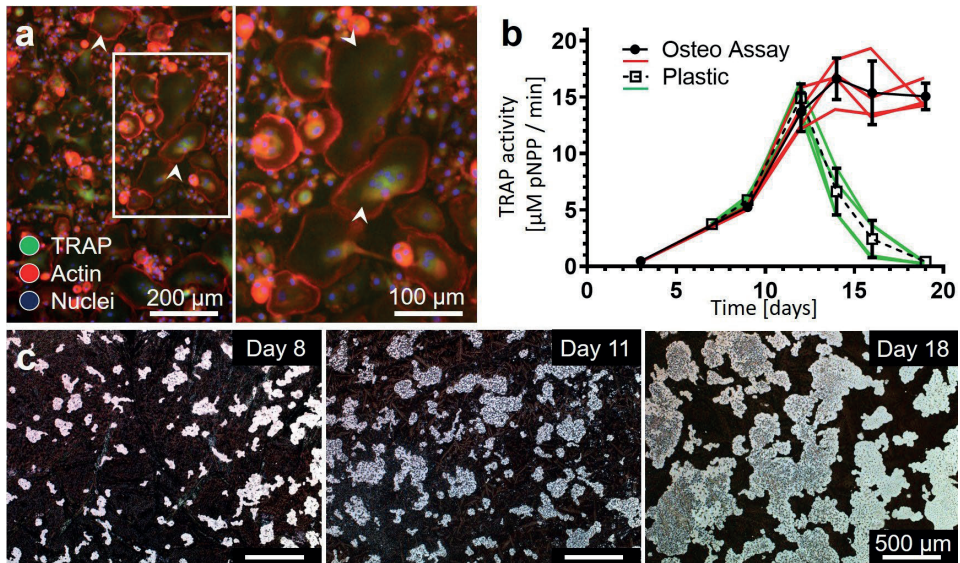
Fig. 4.2. **2D verification of the capability of monocytes to differentiate into functional osteoclast-like cells. (a)** *After a 12 day 2D culture on tissue culture plastic, TRAP-positive (green) multinucleated (blue) cells with a clearly defined actin cytoskeleton (red) could be distinguished. A magnified image is shown to verify the presence of multinucleated TRAP-positive cells, two of which are marked with white arrowheads in both the complete image and magnified panel. **(b)** TRAP release into the medium increased until approximately day 12, and was dependent of the surface. On a resorbable surface (Osteo Assay plate, average activity indicated by black line and circles, and individual samples as red lines), TRAP was expressed longer than on tissue culture plastic (average activity indicated by dotted line and hollow squares, individual lines in green). **(c)** The cells were capable of resorbing a resorbable surface, and the resorbed area increased over time. Unresorbed surfaces are stained black, whereas resorption trails are white (transparent).*
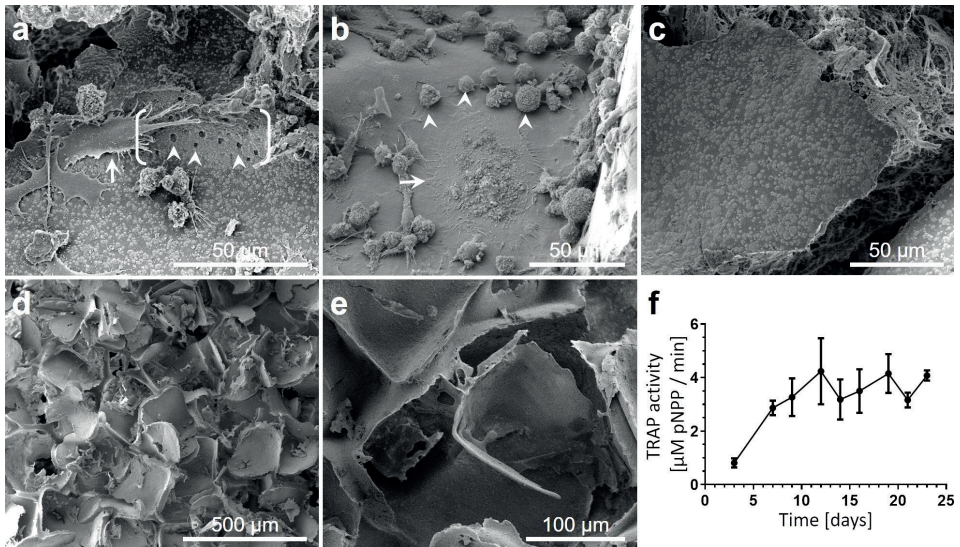
Fig. 4.3. **Osteoclasts created resorption pits and released TRAP on tissue-engineered 3D constructs.** *(a)* SEM image at day 12 of the 3D co-culture showing an osteoclast (arrow) and a series of pits (arrowheads, not all pits are marked) on the mineralized matrix. The surface in close proximity to the pits (within brackets) is morphologically different from the surrounding surface, suggesting the presence of a larger but flatter resorbed surface area, possibly an osteoclast trail. *(b)* SEM image at day 12 of the co-culture showing a flat osteoclast (arrow) and several round and smaller cells, possibly monocytes based on their size and morphology (arrowheads, not all cells are marked). *(c)* SEM image of a mineralized construct where no monocytes were seeded. *(d + e)* low and high magnification SEM images of an empty SF scaffold prior to seeding MSCs. *(f)* TRAP release in the 3D co-culture increased until approximately day 12 after the seeding of monocytes. From then on, TRAP activity stayed high until the end of the co-culture (day 23).
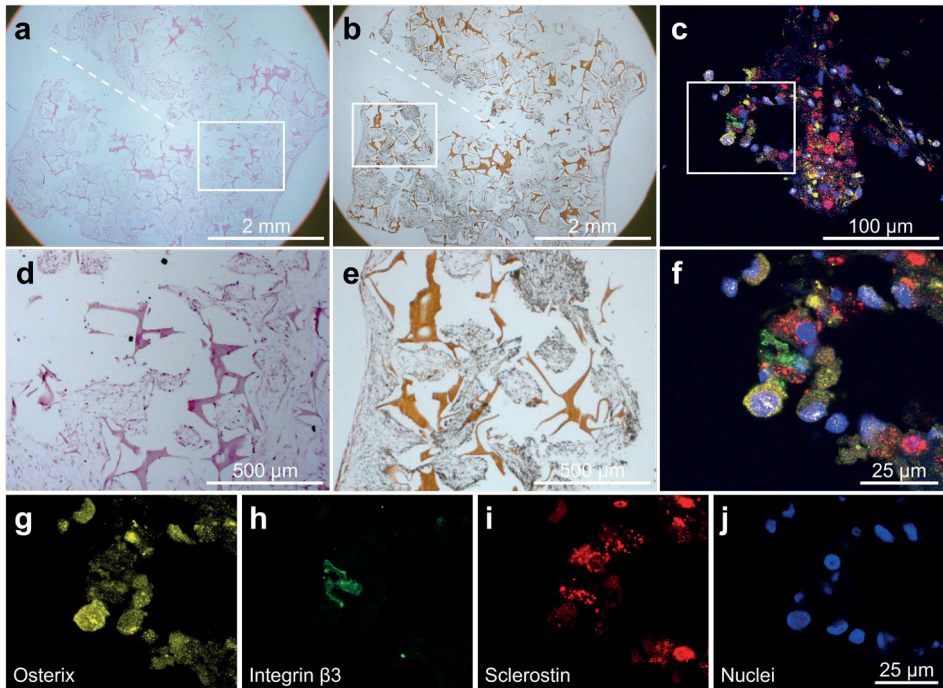
Fig. 4.4. **Cells expressing typical markers for osteoblasts, osteoclasts and osteocytes were present at day 12 of 3D osteoblast-osteoclast co-culture. (a + d)** *Haematoxylin and Eosin overview staining showing the presence of cells throughout the construct. A dashed line shows the incision for monocyte seeding.* **(b + e)** *Von Kossa staining revealing mineralized matrix formation (in black) and mineralized SF (in brown) throughout the whole scaffold. A dashed line shows the incision for monocyte seeding.* **(c + f, g - j)** *Fluorescent composite images and individual channels showing cells expressing typical bone cell markers: osterix (osteoblast marker, red), integrin β3 (osteoclast marker, green), and sclerostin (osteocyte marker, yellow). Nuclei stained with DAPI (blue).*

4.4.5 Formation and resorption of mineralized tissue were quantified in 3D co-culture

During the 3D osteoblast-osteoclast co-culture, the constructs were subjected to 3 additional successive µCT scans to monitor both mineralized tissue formation and resorption in parallel. The registration of the consecutive scans from day 12 and 22 after co-culture initiation revealed that both resorption (blue) and formation (orange) occurred in parallel throughout the construct volumes (Fig. 4.5a) Constructs were digitally sliced in halves to reveal the inside. Large areas coloured grey-purple indicate volumes that remained unchanged between scans. On the surfaces of the grey areas many resorption and formation events have taken place. The mineralized volume of the constructs increased on average by 8.35 ± 3.85 % ($p = 0.023$) from day 4 to 12 of the 3D co-culture (Fig. 4.5b). This confirmed that osteoblasts were continuing to deposit mineralized matrix although they were not in their preferred environment anymore, while the monocytes likely had not yet reached their functional osteoclastic state. From day 12 to 22, the total mineralized volume decreased on average by 7.19 ± 0.99 % ($p = 0.001$). This indicates a switch from mainly osteoblastic formation to mainly osteoclastic resorption of mineralized tissue in this period. Nevertheless, although there was overall a net resorptive effect, the formation of tissue still continued but was significantly lower ($p = 0.0017$) than the resorption (21.16 ± 1.18 % versus 29.06 ± 2.68 %, respectively) (Fig. 4.5c).

4.5 Discussion

The aim of this study was to establish a 3D co-culture in which the formation of a mineralized extracellular matrix by osteoblasts and its resorption by osteoclasts could be localized, visualized and quantified after the application of the corresponding biochemical cues. A 3D *in vitro* co-culture system comprising human cells was created in which osteoblasts seeded onto SF scaffolds formed a mineralized matrix and osteoclasts resorbed the mineralized tissue when exposed to the right environmental conditions. With µCT monitoring, the simultaneous formation and resorption process could be localized, quantified, and monitored. Cells performed as anticipated when stimulated with their corresponding biochemical cues. Osteoclasts were active for longer than expected when cultured on resorbable surfaces. While cell interaction was most likely occurring in parallel, the artificial environment with selected biochemical cues imposed on them was sufficient to steer the processes of formation and resorption into the desired direction.
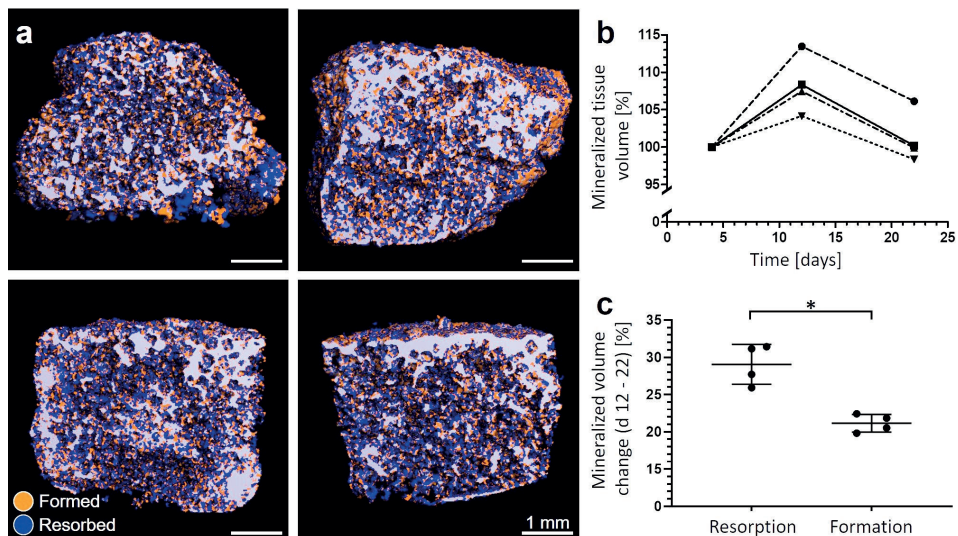
*Fig. 4.5. **Formation and resorption occurred simultaneously in the 3D osteoblast-osteoclast co-culture.** **(a)** 3D μCT images of 4 constructs were registered between days 12 and 22 of co-culture, digitally cross-sectioned and color-coded to visualize the formation (orange), resorption (dark blue), and unaltered regions (grey-purple). Depth of the 3D image creates shadows that make the areas deeper inside the constructs appear darker. **(b)** The overall remodeling balance switched from mainly formation to mainly resorption after 12 days of osteoclastic differentiation. Each line represents one construct. **(c)** Both formation and resorption are present between days 12 and 22 of co-culture, as determined by the voxel count per colour as percentage of the total number of voxels measured at d12. Both individual samples are plotted and their average +/- SD are plotted. The difference between formation and resorption is statistically significant (p = 0.0017).*

hMSCs differentiated towards osteoblasts, deposited a mineralized matrix over time in mono-culture, and continued to deposit mineralized matrix in co-culture. Matrix deposition was monitored with μCT, in a manner similar to what others have shown (Hagenmüller et al., 2007; Hofmann et al., 2013; Melke et al., 2018). Matrix deposition continued throughout the co-culture with monocytes, even after the medium was switched from osteogenic medium to osteoclastogenic medium and mechanical loading was stopped. While it has been shown previously that mechanical loading can promote mineralized matrix deposition both *in vivo* and *in vitro* (Klein-Nulend et al., 2013, 2012; Melke et al., 2018) an environment high in fluid flow does not represent the physiological environment of monocyte recruitment, attachment and differentiation into osteoclasts (Klein-Nulend et al., 2012; Kulkarni et al., 2012; Pathak et al., 2015). The continued mineralized matrix formation after the initiation of the co-culture until approximately day 12 could indicate that osteoblasts, once activated with the correct mechanical or biochemical stimuli, continue to deposit mineralized matrix even after these stimuli have been removed. This could occur as a result of factors liberated from the matrix or

expressed by the newly seeded monocytes that are now differentiating towards osteoclasts (Pang et al., 2013; Tang et al., 2009; Xian et al., 2012). Alternatively, osteoblasts could be responsible for the creation of the collagen framework and biochemical environment necessary for mineralization, but not required for the subsequent mineralization thereof (Samal et al., 2014). Between day 12 and 22 of co-culture, the overall mineralized tissue volume decreased and the overall remodeling balance switched from mainly formation to mainly resorption. The registration of consecutive scans allowed localizing and visualizing that both formation and resorption processes were present between day 12 and 22 of co-culture, confirming that they occurred in parallel.

A mineralized surface seems to prolong osteoclast activity beyond their expected lifespan of approximately 2 weeks (Owen and Reilly, 2018; Parfitt, 1994). Osteoclast activity was determined by measuring TRAP, a proteolytic enzyme secreted predominantly by osteoclasts which plays a role in osteoclastic activity (Hayman, 2008; Kirstein et al., 2006). TRAP samples were taken over time from the same cells, which allowed the determination of the moment of peak TRAP release. As TRAP release was elevated at day 7 in both the 2D and 3D culture, and resorption was visualized in the 2D mono-culture at day 8 after initiating the differentiation, it is reasonable to assume that osteoclasts had formed already before 7 d, which would result in a projected life expectancy of 21 d. As expected, TRAP release by cells cultured on plastic decreased sharply within 3 weeks of culture. However, the TRAP release of cells cultured on a mineralized surface in 2D or on constructs in 3D continued until the end of the experiment. This suggests that the presence of a mineralized surface is sufficient to prolong the osteoclastic activity, and perhaps to extend the lifespan of osteoclasts. In 3D, in addition to the presence of a mineralized surface, other factors could have contributed to the prolonged TRAP release, such as biochemical signals released by sclerostin-expressing cells (Atkins et al., 2009; Simonet et al., 1997; Wijenayaka et al., 2011) and osteoblasts (Matsuo and Irie, 2008). These findings are in line with the µCT data, further reinforcing the findings that resorption exceeded formation after 12 d in the osteoblast-osteoclast co-culture.

Large osteoclast-like cells (around 50 µm in diameter) were identified throughout the construct, most often in proximity to small pits. These pits are believed to be resorption pits and, although small in diameter, are within the range of sizes that others have reported in *in vitro* studies (Halai et al., 2014; Kleinhans et al., 2015; Varghese et al., 2006). Their morphology is different than the observed resorption in the 2D culture, where resorption presented itself as classical resorption trails with a width of approximately osteoclast size (50 µm) and larger. It is likely that larger areas of resorption are present on the 3D constructs, but do not have enough distinguishing features to confirm that they are truly resorption pits or trails. Similar difficulties arise when using extracellular bone

matrix of for example bovine origin (Kleinhans et al., 2015). Small distinct pits can be distinguished easily, but the larger the resorbed area and the less steep the slope of the pit, the harder it is to discern on a non-flat surface whether it is an actual resorbed area or whether the feature is part of the original construct architecture, which by itself is irregularly shaped. In Fig. 4.3a, the area surrounding the small pits seems to be structurally different from the surrounding surface, with a width similar to that of the osteoclast next to it, suggesting the area surrounding the pits could be a resorption trail. Identification of osteoblasts on the SEM images proved difficult due to the used methodology (Shah et al., 2019; Wierzchos et al., 2008). Their presence within the constructs was confirmed with histology.

The herein presented model contains the required cells to simulate bone crosstalk but has some limitations compared to natural bone. While the original porous scaffold mimics the geometry of trabecular bone, there are many aspects that do not accurately mimic bone tissue. There is no cortical bone, bone marrow or vasculature, and there is no systemic interaction with other tissues. Cells are introduced at discrete moments, whereas in bone there can be a continuous influx of cells in response to the correct biochemical cues. In the model, osteoblasts are introduced first to deposit mineralized matrix, followed by osteoclasts to resorb the deposited matrix. As a result, the phases of the bone remodeling cycle (resorption of damaged or old bone, followed by a reversal phase and formation of new bone) are actually reversed (Delaisse, 2014). Whereas in the bone remodeling cycle osteoblasts and osteoclasts are separated by a reversal phase, the current model provides the opportunity to manipulate and study osteoblasts, osteoclasts and their interactions together within the same environment at the same time.

3D *in vitro* co-cultures are subject to certain limitations. To answer patient-specific questions using trabecular bone-like bone structures requires a high number of well characterized cells (Buenzli and Sims, 2015) preferably from a single donor or patient (Evans et al., 2006). While well-characterized MSCs are available because these cells can be expanded (Ferrin et al., 2017; Ma et al., 2014), the number of monocytes available from a single blood donation is limited by the donated volume and dependent on donor characteristics and state of health (Yang et al., 2018). Monocytes cannot naturally be expanded (Jacome-Galarza et al., 2013), although exposure to M-CSF (without RANKL) has been reported to allow limited expansion, accelerated differentiation and survival of monocytes (Ross, 2006; Xu and Teitelbaum, 2013; Yamada et al., 2005), at the risk of developing an insensitivity to RANKL (De Vries et al., 2015). Large between-donor variation in activity and resorption is another issue in particular in the case of monocytes (Susa et al., 2004) that necessitates choosing one out of several tested donors.

Future research should focus on switching from an artificial to a more physiological environment where the present cells can produce sufficient cytokines by themselves to regulate formation and resorption activity between each other to the extent that these changes are large enough to be detected using μCT, as is the case *in vivo*. This may necessitate the development of a completely functional bone remodeling unit including osteocytes, requiring additional validation of their presence and function. In future experiments, biochemical bone turnover markers such as P1NP and CTx could be included to corroborate the volume-based μCT findings, and optimization of cell seeding techniques and culture durations could reduce variation and increase throughput of the system. Further validation of the use of μCT for these experiments should be conducted, specifically regarding the effect of radiation on cell survival and activity. Certain doses of radiation can negatively affect osteoblast function (Kraehenbuehl et al., 2010), and may affect monocytes and osteoclasts as well (Yang et al., 2012). Combined with the monitoring technology, this model could provide important information on the fine balance between formation and resorption rather than just looking at the overall increase and decrease of tissue volume. The presented co-culture system is a first step towards the development of a 3D *in vitro* model that could be used for fundamental research on bone remodeling and related bone diseases. It may have clinical relevance for patient-specific disease diagnosis, therapies or drug development when used with patient-derived cells.

4.6   Conclusion

This study shows that human monocytes can differentiate into osteoclasts when co-cultured with osteoblasts differentiated from hMSCs *in vitro*. In the co-culture, both cell types are simultaneously functional, osteoblasts form and osteoclasts resorb mineralized tissue. These processes can be quantified, visualized and localized using μCT. In this way, the effect of biochemical signals, drugs and other stimuli on bone crosstalk could be studied in a 3D *in vitro* model with unprecedented similarity to human *in vivo* bone remodeling.

Chapter 5

Tuning the resorption-formation balance in an *in vitro* 3D osteoblast-osteoclast co-culture model of bone

5

5.1 Abstract

The aim of the present study was to further improve an *in vitro* 3D osteoblast (OB) – osteoclast (OC) co-culture model of bone by tuning it towards states of formation, resorption, and equilibrium for their future applications in fundamental research, drug development and personalized medicine. This was achieved by varying culture medium composition and monocyte seeding density, the two external parameters that affect cell behavior the most. Monocytes were seeded at two seeding densities onto 3D silk-fibroin constructs pre-mineralized by MSC-derived OBs and were co-cultured in one of three different media (OC stimulating, Neutral and OB stimulating medium) for three weeks. Histology showed mineralized matrix after co-culture and OC markers in the OC medium group. Scanning Electron Microscopy showed large OC-like cells in the OC medium group. Micro-computed tomography showed increased formation in the OB medium group, equilibrium in the Neutral medium group and resorption in the OC medium group. Culture supernatant samples showed high early tartrate resistant acid phosphatase (TRAP) release in the OC medium group, a later and lower release in the Neutral medium group, and almost no release in the OB medium group. Increased monocyte seeding density showed a less-than-proportional increase in TRAP release and resorption in OC medium, while it proportionally increased TRAP release in Neutral medium without affecting net resorption. The 3D OB-OC co-culture model was effectively used to show an excess of mineral deposition using OB medium, resorption using OC medium, or an equilibrium using Neutral medium. All three media applied to the model may have their own distinct applications in fundamental research, drug development, and personalized medicine.

5.2   Introduction

Bone growth and homeostasis are regulated by bone forming osteoblasts (OBs), bone resorbing osteoclasts (OCs), and regulating osteocytes. These cells tightly regulate bone mass, bone strength and bone structure to continuously meet the requirements placed upon bone tissue. Disturbances to this balance can lead to diseases such as for example osteoporosis. While many treatment options are available for osteoporosis that can delay the progression of the disease, there is currently no cure to this degenerative disease (Bellido, 2014; Matsuo and Irie, 2008). Many of the biochemical actors in bone remodeling have been identified (Deschaseaux et al., 2010; Matsuo and Irie, 2008; Sims and Gooi, 2008), but much remains to be learned on the precise nature of the biochemical interplay orchestrating bone remodeling before osteoporosis can be treated or even cured as opposed to merely slowing down the degenerative nature of the disease.

Accurate, scalable, and translatable experimental models are needed to further study the mechanisms underlying bone remodeling. Options such as animal models are expensive, time consuming and far from scalable. They raise ethical concerns and often lead to poor translation from pre-clinical trials to clinical use (Burkhardt and Zlotnik, 2013; Contopoulos-Ioannidis et al., 2003; Swearengen, 2018). *In vitro* cell-culture models do not share those ethical concerns, can be developed into high-volume tests, and can use cells of various origins, including healthy human donors or even cells from patients suffering from bone diseases (Jemnitz et al., 2008; Langhans, 2018).

In vivo bone remodeling is a three-dimensional process where the cells from the basic multicellular unit (Frost, 1969) deposit and resorb three-dimensional volumes of bone tissue. This makes the use of 2D *in vitro* models (Amizuka et al., 1997; Marino et al., 2014) less appealing for studying bone remodeling, especially when cells in 2D monolayer often respond differently than in a 3D environment (Edmondson et al., 2014; Li and Kilian, 2015). Although usually easier to obtain, animal cells can respond differently than human cells (Jemnitz et al., 2008), possibly introducing errors due to interspecies differences. Consequently, to study remodeling and to quantify effects on both resorption and formation within the same model system, ideally a 3D environment is used in which at least both human OBs and OCs are co-cultured simultaneously (Owen and Reilly, 2018) and can interact freely with each other through both cell-cell contact and paracrine signaling (Matsuo and Irie, 2008).

3D OB-OC co-culture models exist (Hayden et al., 2014; Papadimitropoulos et al., 2011) where resorption and formation are studied using destructive techniques such as using for example Alizarin Red mineralized nodule staining (Rossi et al., 2018) or Scanning (Hayden et al., 2014) and Transmission (Domaschke et al., 2006) electron microscopy for

resorbed surface metrology. Longitudinal monitoring of bone remodeling offers the advantages of measuring changes within the same constructs over time and localizing where formation and resorption events take place within constructs. Longitudinal monitoring using micro-computed tomography (μCT) has been used in animal models before (Hagenmüller et al., 2007; Schulte et al., 2011a, 2011b), and was recently applied to monitor scaffold mineralization by mesenchymal stromal cell (MSC)-derived OBs (Melke et al., 2018) and subsequent OC resorption (S. Remmers et al., 2020). In these studies, the crosstalk occurring in the cultures was biochemically 'overruled' to obtain maximal formation and resorption. In a healthy *in vivo* situation, crosstalk between cells results in an equilibrium between formation and resorption, while bone diseases manifest as a disbalance between formation and resorption.

The aim of this study was to improve the earlier developed co-culture model by investigating how to steer the response of the co-culture model towards and away from resorption, formation, and equilibrium.

5.3   Materials and Methods

5.3.1   Materials

Human bone marrow was commercially purchased from Lonza (Walkersville, MD, USA), collected under their institutional guidelines and with written informed consent. A human buffy coat was obtained from Sanquin (Eindhoven, Netherlands) after review and approval of the study by the Sanquin ethics review board. The buffy coat was collected by Sanquin under their institutional guidelines and with written informed consent per Declaration of Helsinki. Antigen retrieval citrate buffer, RPMI-1640 medium, poly-L-lysine coated microscope slides and SnakeSkin Dialysis tubing (3.5 kDa molecular weight cut-off) were from Thermo Fisher Scientific (Breda, The Netherlands). Disposable biopsy punches were from Amstel Medical (Amstelveen, the Netherlands). Trypsin-EDTA (0.25 %) was from Lonza (Breda, The Netherlands). Dulbecco's modified Eagle media (DMEM low glucose + high glucose), non-essential amino acids (NEAA) and antibiotic/antimycotic (anti-anti) were from Life Technologies (Bleiswijk, The Netherlands). Fetal Bovine Serum (FBS, batch F7524-500ML / lot BCBV7611) was from Sigma Aldrich / Merck. Lymphoprep™ was from Axis-Shield (Oslo, Norway). MACS® Pan Monocyte Isolation Kit was from Miltenyi Biotec (Leiden, the Netherlands). Recombinant human basic fibroblast growth factor (bFGF), macrophage colony stimulating factor (M-CSF) and receptor activator of nuclear factor kappa-B ligand (RANKL) were from PeproTech (London, United Kingdom). *Bombyx mori L.* Silkworm cocoons were from Tajima Shoji Co., LTD. (Yokohama, Japan). Antibody Integrin β3

(Orb248939, Mouse, 1:100) was from Biorbyt (Cambridge, United Kingdom). Antibody tartrate resistant acid phosphatase (TRAP) (Sc-30833, Goat, 1:100) was from Santa-Cruz Biotechnology, Inc. (Heidelberg, Germany). Antibody Alexa488 (715-545-150, Donkey-anti-Mouse IgG (H+L), 1:300) was from Jackson ImmunoResearch (Cambridgeshire, United Kingdom). Antibody Alexa488 (A11055, Donkey-anti-Goat IgG (H+L), 1:300) was from Molecular Probes (Eugene, OR, USA). Thin bleach was from the local Jumbo grocery store (Stiphout, Netherlands). All other substances were of analytical or pharmaceutical grade and obtained from Sigma Aldrich / Merck (Zwijndrecht, The Netherlands).

5.3.2 Methods

5.3.2.1 *Monocyte isolation*

A human peripheral blood buffy coat from a healthy donor was obtained from the local blood donation center under informed consent. The buffy coat was processed in a similar manner as described previously (S. Remmers et al., 2020). The buffy coat was diluted to 180 mL in 0.6 % (w/v) sodium citrate in PBS adjusted to pH 7.2 at 4 °C (SC buffer), carefully layered onto Lymphoprep™ iso-osmotic medium and centrifuged at 800 × g for 30 min without brake and with minimal acceleration at RT. Mononuclear cells were washed 5 × with SC buffer to remove all Lymphoprep™, and cryogenically stored in liquid nitrogen until further use. Upon use, cells were thawed and used without passaging. A purified monocyte fraction was isolated from the thawed cells using the negative selection MACS® Pan Monocyte Isolation Kit (Miltenyi Biotec) with LS columns according to the manufacturers' instructions. After isolation, cells were resuspended in Neutral medium (Table 5.1). This purified monocyte fraction will from now on be referred to as 'monocytes'.

5.3.2.2 *2D OC culture and analysis*

To verify that the monocytes can form multinucleated TRAP expressing and resorbing OC-like cells, 0.25×10^6 monocytes per cm^2 (n = 4 per group) were seeded in monocyte priming medium (Table 5.1) on 24-well Corning® osteo assay plates and regular tissue culture plastic 24-well medium (Table 5.1) tissue culture plates in monolayer. Monocyte priming medium was replaced with OC or Neutral medium after 48 h. Medium was replaced 3 × per week for 14 d. The Corning® osteo assay plate was analyzed for resorption. Cells were removed using 5 % bleach for 5 min. The plate was washed with UPW and dried at 50 °C. Bright field images were taken with a Zeiss Axio Observer Z1 microscope and binarized with Matlab®. The 2D OC culture in plastic well-plates was

immunofluorescently labelled for OC markers (TRAP or Integrin β3), actin (TRITC-conjugated-Phalloidin) and nuclei (DAPI). Fluorescence images were taken with a Zeiss Axiovert 200M microscope. Supernatant culture medium samples were taken and stored at -80 °C at each medium change and analyzed for TRAP enzyme activity as described later for the 3D co-culture.

Table 5.1. **Media names, components and functions within the context of this study.**

Name	Components	Function
OB medium	DMEM low glucose 10 % FBS 1 % anti-anti 50 µg/mL L-ascorbic-acid-2-phosphate 100 nM dexamethasone 10 mM β-glycerophosphate	Osteogenic medium. One of three media compared during the co-culture. This medium was expected to further stimulate mineralized matrix deposition by OB.
Neutral medium	RPMI-1640 10 % FBS 1 % Anti-Anti	Unsupplemented medium. One of three media compared during the co-culture. This medium was expected to allow OB and OC crosstalk to control ongoing matrix deposition and resorption.
OC medium	RPMI-1640 10 % FBS 1 % Anti-Anti 50 ng/mL M-CSF 50 ng/mL RANKL	Osteoclastogenic medium. One of three media compared during the co-culture. This medium was expected to stimulate OC resorption.
MSC expansion medium	DMEM high glucose 10 % FBS 1 % anti-anti 1 % NEAA 1 ng/L bFGF	Used to expand MSCs prior to seeding onto scaffolds.
MSC seeding medium	DMEM high glucose 10 % FBS 1 % anti-anti	Unsupplemented medium that is used for MSC seeding onto scaffolds and prewetting of scaffolds.
Monocyte priming medium	RPMI-1640 10 % FBS 1 % Anti-Anti 50 ng/mL M-CSF	Used to prime monocytes during the first two days of culture which benefits osteoclastogenic differentiation.

5.3.2.3   Fabrication of silk fibroin scaffolds

Silk fibroin (SF) scaffolds were produced in a similar manner as described previously (Meinel et al., 2005; Melke et al., 2018; Nazarov et al., 2004; S. Remmers et al., 2020). Unless stated otherwise, solutions used were ultra-pure water (UPW) or dissolved in UPW. Cocoons from the *Bombyx mori L.* silkworm were degummed by boiling in 0.2 M Na_2CO_3 twice for 1 h, rinsed (boiling UPW) followed by 10 × washing (cold UPW). After overnight drying the silk was dissolved in 9 M LiBr (10 % w/v) at 55 °C for 1 h and filtered through a 5 μm filter after cooling to RT. The filtered silk solution was dialyzed for 36 h using SnakeSkin Dialysis Tubing. UPW was refreshed at 1, 3, 12, and 24 h. The dialyzed solution was frozen (-80 °C), lyophilized and dissolved to a 17 % (w/v) solution in 1,1,1,3,3,3-Hexafluoro-2-propanol (HFIP). 1 mL silk-HFIP was added to 2.5 g NaCl (granule size between 250-300 μm) in a Teflon container and was allowed to dry at RT for at least 4 d. β-sheet formation (Tsukada et al., 1994) was induced by immersion in 90 % (v/v) methanol for 30 min. Silk-salt blocks were dried at RT overnight and cut into 3 mm discs using a precision cut-off machine (Accutom-5®, Struers GmbH Nederland, Maassluis, the Netherlands). NaCl was leached out in UPW which was refreshed after 2, 12, 24 and 36 h. Scaffolds were punched with a biopsy punch (5 mm) and sterilized by autoclaving (20 min at 121 °C) in phosphate buffered saline (PBS). Scaffolds were pre-wetted in mesenchymal stromal cell (MSC) seeding medium (Table 5.1) prior to use.

5.3.2.4   Construct mineralization by MSC-derived OBs

The human MSCs used in this study were previously isolated from human bone marrow and characterized (Hofmann et al., 2007). Briefly, 2.5×10^3 cells/cm^2 (passage 5) were seeded and expanded for 6 d in MSC expansion medium (Table 5.1). 1×10^6 MSCs in 20 μL MSC seeding medium were seeded onto each pre-wetted scaffold and incubated for 90 min at 37 °C. The cell-seeded scaffolds are from now on referred to as constructs. These constructs were then transferred to 8 custom-made spinner flask bioreactors (n = 4 per bioreactor) containing magnetic stir bars (Melke et al., 2018; S. Remmers et al., 2020) that were filled with 5 mL OB medium (Table 5.1). Each bioreactor was placed in an incubator (37 °C, 5 % CO_2) on a magnetic stirrer plate (RTv5, IKA, Germany) rotating at 300 RPM (Melke et al., 2018). Medium was changed 3 times a week for 11 weeks. This culture is from now on referred to as '3D OB monoculture', and the currently present cells are from now on referred to as OBs.

5.3.2.5 Initiation of 3D co-culture on pre-mineralized constructs

Constructs which had been in culture for 11 weeks with osteogenically stimulated MSCs (from now on referred to as OBs) were incised with a 4 mm deep incision in the transverse plane to allow seeding to the center of the constructs. 1 million (M) monocytes, 1.5 M monocytes or no monocytes in 7.5 μL monocyte priming medium (Table 5.1) were seeded into the incision of constructs pre-wetted in monocyte priming medium. All constructs were incubated for 180 min at 37 °C to facilitate cell attachment. Then, all constructs were placed back into the bioreactors (n = 4 per bioreactor) with 5 mL monocyte priming medium per bioreactor. No stirring was applied during the co-culture to better stimulate monocyte attachment and differentiation (Klein-Nulend et al., 2012; Kulkarni et al., 2012; Pathak et al., 2015). The 3D co-culture of OBs with monocytes will be referred to as '3D co-culture'. The 3D co-cultures were primed in monocyte priming medium for 48 h (De Vries et al., 2015; Hayes and Zoon, 1993). Monocyte priming medium was replaced after 48 h with one of three media for the remainder of the culture: OB medium, Neutral medium, or OC medium (Table 5.1). This resulted in bioreactors with constructs seeded with 0 M monocytes cultured in OB and OC medium, 1 M monocytes cultured in OB, OC and Neutral medium, and 1.5 M monocytes cultured in OB, OC and Neutral medium. Medium was replaced 3 × per week for 21 d.

5.3.2.6 μCT imaging

μCT images were taken on a μCT100 imaging system (Scanco Medical, Brüttisellen, Switzerland) every week except week 2 of the 3D OB monoculture to monitor tissue mineralization. After 11 weeks, co-culture was initiated and the scanning frequency was increased to twice per week (isotropic nominal resolution:17.2 μm, energy level: 45 kVp, intensity: 200 μA, integration time: 300 ms, two-fold frame averaging, computed tomography dose index (CTDI) in air: 230 mGy (S. Remmers et al., 2020). A constrained Gaussian filter was applied to reduce noise (Filter support: 1.0, filter width sigma: 0.8 voxel). A fixed region of interest (RoI) of 205 slices was selected within each bioreactor. This ensured that the same RoI of every scaffold was scanned each time and limited the required scan time and radiation exposure to 30 min per scan. At the start of the co-culture, this RoI was reassessed for each bioreactor to contain as much of the constructs as possible, and this exact RoI of 205 slices was used for the remainder of the co-culture. Segmentation was done at a global threshold of 23 % of the max greyscale value. Image processing language (IPLFE v2.03, Scanco Medical AG) was used to further process the images. Component labelling was used to remove unconnected objects < 50 voxels. These were neglected from further analysis. The mineralized tissue volume of the RoI was assessed using quantitative morphometry. 3D OB monoculture quantitative μCT data was used as

measured, whereas 3D co-culture quantitative µCT data was normalized to the mineralized volumes of the first scan of each individual construct during the co-culture (d 4 of co-culture) counting that volume as 100 %. All successive scans were presented as relative volume with respect to this first scan. Rigid 3D registration was used to register the follow-up (d 7) to the baseline image (d 4) of the 3D co-culture (Ellouz et al., 2014). Color coding was used to label resorption (blue), formation (orange) and unaltered regions (grey). Unconnected objects < 100 voxels were removed as before using component labelling for registered images only.

5.3.2.7   Histology

At the end of the culture, constructs were fixed in 10 % neutral buffered formalin for 24 h at 4 °C. Fixed constructs were dehydrated with an EtOH and xylene series (1.5-2 h per step) and embedded in paraffin. 10 µm thick vertical sections were mounted on poly-L-lysine coated microscope slides. Sections were dewaxed and rehydrated with a Xylene and EtOH to UPW series. These sections were used for histology and immunofluorescence. Sections were stained with von Kossa staining to visualize calcium phosphate deposition (30 min in 1 % aqueous silver nitrate (w/v) under UV light, rinsed with UPW, 5 min in 5 % sodium thiosulfate (w/v), rinsed with UPW, 5 min in nuclear fast red, rinsed in UPW). To visualize calcium deposition, sections were stained for Alizarin Red (2 min in 2 % Alizarin Red in H_2O, pH 4.2). Stained sections were dehydrated using EtOH (von Kossa) or acetone (Alizarin Red) to Xylene and coverslipped with Entallan®. Bright field images were taken with a Zeiss Axio Observer Z1 microscope.

5.3.2.8   Immunofluorescence

Sections were prepared, dewaxed, and rehydrated as for histology. After antigen retrieval (citrate buffer at 95 °C for 20 min, then slowly cooled back to RT), cross-reactivity was blocked (10 % donkey serum for 30 min). Primary antibodies were incubated at 4 °C overnight, and secondary antibodies were incubated at RT for 1 h. Sections were labelled for OC marker (integrin β3) (Barbeck et al., 2017; Nakamura et al., 2007), actin (TRITC-conjugated-Phalloidin) and nuclei (DAPI). Sections were coverslipped with Mowiol® and imaged with a Leica TCS SP5X microscope.

5.3.2.9 Scanning electron microscopy (SEM)

Constructs for SEM were fixed using glutaraldehyde (2,5 % for 24 h at 4 °C), dehydrated with a graded EtOH series followed by a graded 1,1,1-Trimethyl-N-(trimethylsilyl)silanamine (HMDS)/ethanol series, dried overnight at RT and sputter coated with 5 nm gold (Q300TD, Quorum Technologies Ltd, Laughton, UK). Sputter coated constructs were imaged with SEM (Quanta600, FEI Company, Eindhoven, the Netherlands, spot size 3.0, 5.00 kV, working distance 10 mm).

5.3.2.10 Tartrate-resistant acid phosphatase (TRAP) quantification in supernatant

Supernatant medium samples were taken and stored at -80 °C just before each medium change (n = 4 technical replicates per bioreactor, or 1 sample from each well). 20 μL of the supernatant medium samples or nitrophenol standard in PBS were incubated in translucent 96-well plates at 37 °C for 90 min with 100 μL para-nitrophenylphosphate (pNPP) buffer (1 mg/mL pNPP, 0.1 M sodium acetate, 0.1 % (v/v) triton-X-100 in PBS adjusted to pH 5.5 supplemented with 30 μl/mL tartrate solution). The reaction was stopped with 100 μl 0.3 M NaOH. TRAP enzyme activity was determined by measuring absorbance at 405 nm and recalculated to pNPP transformation per minute.

5.3.2.11 Statistical analysis

Quantitative data is represented as mean ± standard deviation (SD) and was analyzed using GraphPad Prism version 8. Data used for statistical analysis was tested for normality using the Shapiro-Wilk normality test and was normally distributed. Groups were compared using a Two-Way Analysis of Variances (ANOVA). Trends within groups over time were compared using a Repeated Measures ANOVA. Planned comparisons within groups were: volume increase within the 1st week of co-culture, volume decrease starting after the 1st week, TRAP release increase starting in the 1st week, TRAP release decrease starting after the 2nd week. Bonferroni post-hoc correction was used to account for multiple comparisons in all other comparisons. Geisser-Greenhouse correction was used to account for unequal variances. Differences were considered statistically significant at a level of $p < 0.05$. SDs that were much larger than others within the same dataset were tested with Grubbs test for outliers against other SDs within the dataset. If an SD was positively identified, the underlying data was searched for outliers. Statistical analyses were rerun with the identified datapoint replaced with the mean of the remaining datapoints. If this led to different significances, then figures show a '+' indicating a relevant outlier. The original (unchanged) dataset is shown in all figures regardless of the outcome, but the

results of both analyses are described. Grubbs test was used for the TRAP results of 1 M monocytes seeded in both OC medium and Neutral medium, timepoints of d 7 and d 16 respectively. Notable significant effects are numbered in the results section and in the figures using unique sequential numbering preceded by an asterisk throughout the study for easy referencing between texts and figures.

5.4   Results

5.4.1   Verification of osteoclastogenesis in 2D

Monocytes were cultured in 2D to verify their capability to differentiate into multinucleated TRAP expressing resorbing cells. Monocytes cultured in OC medium continuously released increasing amounts of TRAP into the culture supernatant over a period of 14 d ending at 2.84 ± 0.29 μmol/min, whereas those cultured in Neutral medium released lower quantities of TRAP even at the peak of 1.37 ± 0.08 μmol/min at d 7 (difference with OC group at d 7: 0.54 μmol/min, $p = 0.0089$, *1) after which the release of TRAP decreased again (Fig. 5.1a). After 14 d on Osteo Assay plates, cells cultured in OC medium showed extensive resorption, whereas those cultured in Neutral medium showed only minimal traces of resorption (Fig. 5.1b + c). Fluorescence imaging revealed that cells cultured in OC medium developed into large multinucleated cells with clearly defined actin rings, expressing OC markers TRAP (Fig. 5.1d) and integrin-β3 (Fig. 5.1f), although TRAP was also expressed in unfused monocytes. In Neutral medium some clusters of nuclei are seen, possibly small multinucleated cells that developed as a result of 2-day priming (Fig. 5.1e). Most monocytes in the Neutral medium group expressed TRAP like those in the OC medium group, whereas integrin-β3 was expressed almost exclusively in multinucleated cells and was not found in cells cultured in Neutral medium (Fig. 5.1g). These results confirm that the monocytes used in this study were able to differentiate into multinucleated TRAP expressing and resorbing OCs in 2D.

5.4.2   Mineralized matrix is deposited onto SF scaffolds

hMSCs were seeded onto SF scaffolds (Fig. 5.2a + b) and differentiated into mineralized matrix depositing MSC-derived OBs for 11 weeks. Matrix deposition was monitored using μCT for each individual construct until the start of co-culture (Fig. 5.2c + d). Non-mineralized SF scaffolds were not detectable with the used μCT settings. Already after 6 d, 0.002 ± 0.003 mm^3 of mineralized matrix was detected with μCT. Mineralized matrix deposition continued steadily throughout the culture duration and throughout the construct reaching a mean mineralized volume of 9.67 ± 2.42 mm^3 on d 69.
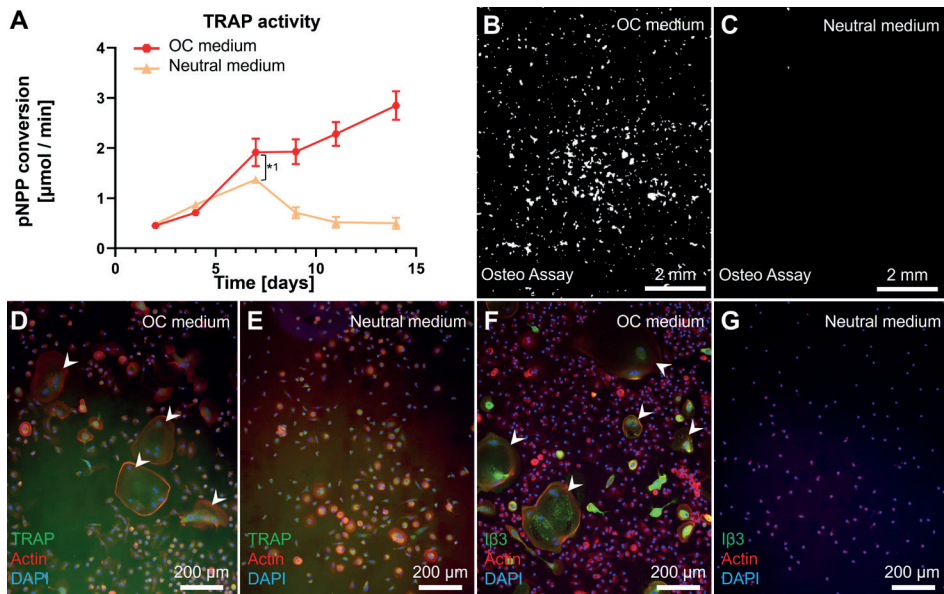
Fig. 5.1. **Monocytes can differentiate into TRAP expressing resorbing cells in 2D mono-culture. (A)** *TRAP release by monocytes cultured in OC medium or Neutral medium. Both groups showed an initial increase of TRAP release, but only the osteoclastogenically stimulated group kept releasing more TRAP after d 7.* **(B)** *Resorption of Osteo Assay plate surfaces after 14 d of culture in OC medium or* **(C)** *Neutral medium. Images are binarized light microscopy images of the center of the well. Resorption was present in the OC medium group, whereas resorption in the Neutral medium group was negligible.* **(D)** *Multinucleated (blue) TRAP (green) expressing cells (white arrowheads) with a clearly defined actin ring (red) were seen when cultured with OC medium, whereas monocytes cultured in Neutral medium* **(E)** *mostly remained uninuclear and only lightly expressed TRAP.* **(F)** *Integrin β3 (green) was expressed almost exclusively in multinucleated cells (white arrowhead) in a culture with OC medium, whereas monocytes cultured in Neutral medium* **(G)** *did not express Integrin β3 at all.*
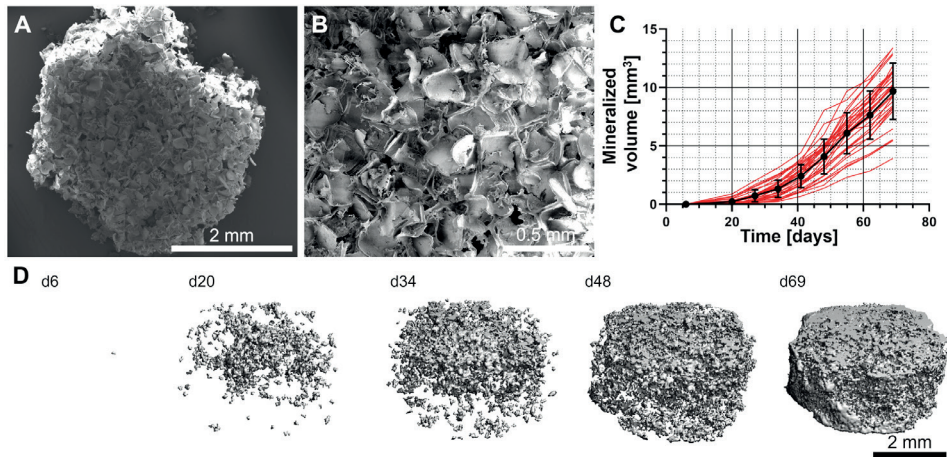
*Fig. 5.2. **Mineralized matrix deposition over time onto SF scaffolds.** (A) Top view of a freshly prepared SF scaffold. (B) Higher magnification view revealing the highly porous nature of the scaffolds. (C) µCT monitoring confirmed continuous mineralized matrix deposition and an increase in mineralized volume during the entire culture duration. Individual construct volumes are shown in red; the mean ± SD are shown in black. (D) The volumetric distribution and growth of an individual construct over time.*
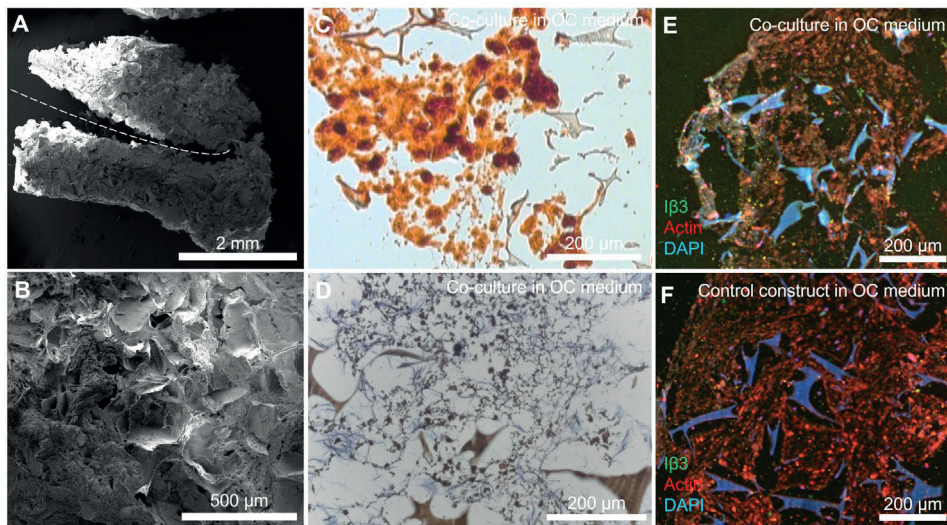
*Fig. 5.3. **Construct morphology and histology after co-culture.** (A) Mineralized constructs were sectioned in the transverse plane to seed the monocytes. The incision is marked with a dashed line. (B) After co-culture, ECM deposition into the pores of the construct was visible on SEM images. (C) Alizarin Red staining confirmed the presence of calcium throughout the constructs after co-culture in OC medium. (D) Von Kossa staining confirmed the deposition of (calcium) phosphates throughout the constructs after co-culture in OC medium. (E) Immunofluorescence for Integrin β3 (green), actin (red) and nuclei (blue) revealed the presence of OC marker Integrin β3 even after 21 d of co-culture in constructs cultured in OC medium. (F) Immunofluorescence for Integrin β3 (green), actin (red) and nuclei (blue) on a control construct without monocytes, cultured in OC medium.*
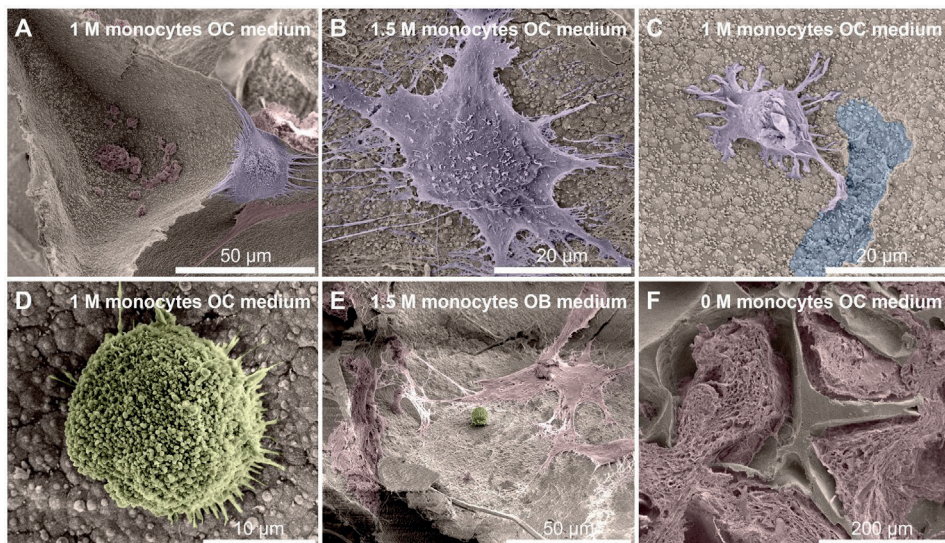
*Fig. 5.4. **Cells and tissue after co-culture.** (**A**) An OC on the edges of a pore, with likely remnants of MSC-derived cells and ECM at the bottom of the pore. (**B**) OC with many filopodia stretching out in all directions. (**C**) Small OC-like cell moving away from a resorption trail. Its OC lineage is recognizable by the 'frizzled' appearance on the top surface like that of the OC in panels A and B, which contrasts with the smoother surface of MSC-derived cells and ECM that is marked in red in for example panels A and E. (**D**) Close-up of a monocyte. Round cells such as these were only found in constructs onto which monocytes were seeded and not on unseeded control constructs, regardless of media type. (**E**) A lone monocyte amidst deposited MSC-derived cells and/or ECM. (**F**) Overview image of the native SF scaffold structure that has been filled with ECM. Images are digitally enhanced SEM images. OC are colored purple, monocytes are colored yellow, resorption trails are colored blue, MSC/OB derived ECM (possibly including cells) is colored red.*

5.4.3 Histology and SEM show calcium phosphates and ECM after co-culture

An incision in the transverse plane (Fig. 5.3a) was used to deliver cells to the center of the mineralized construct. This seeding strategy was chosen because otherwise, the deposited (mineralized) tissue (Fig. 5.3b) could have prevented the subsequently seeded monocytes from penetrating deeper into the construct if seeded on the outside surface. Alizarin Red (Fig. 5.3c) and von Kossa (Fig. 5.3d) stainings showed that calcium phosphate deposits are abundantly present in the ECM in all groups at the end of co-culture.

5.4.4   Confirmation of osteoclastogenesis on mineralized constructs

Immunofluorescence imaging revealed the presence of OC marker integrin-β3 in constructs cultured in OC medium even after 3 weeks of co-culture while the marker was absent in constructs without seeded monocytes (Fig. 5.3e + f). SEM images were taken after 3 weeks of co-culture to investigate the presence of monocytes and OCs (Fig. 5.4). Only in the groups cultured in OC medium, large OC-like cells were identified (Fig. 5.4a + b), sometimes in the presence of what could be resorption trails (Fig. 5.4c). Small round monocyte-like cells were also identified in all groups in which monocytes were seeded (Fig. 5.4d + e). MSC-produced extracellular matrix was present abundantly throughout all constructs, often completely filling pores in the SF scaffolds (Fig. 5.4f).

5.4.5   Co-culture media affects the amount TRAP release

Monocytes were co-cultured with OBs on constructs in one of three media: OC medium, Neutral medium, or OB medium. As expected, TRAP release (Fig. 5.5a) over time was highest in the group cultured in OC medium (1.58 ± 0.20 μmol/min at d 14). TRAP release in the OC medium group was significantly higher than in the Neutral medium group from d 7 to d 18 ($p < 0.05$ for all timepoints, d 7 only after outlier correction, *3). TRAP release in the Neutral medium group increased compared to the group cultured to OB medium only after 11 d ($p = 0.04$ at d 14, $p = 0.02$ at d 16 after outlier correction, $p = 0.99$ with outlier, *2), but TRAP release in the Neutral medium group followed a clear linear trend ($p = 0.0185$). This suggested that differentiation towards OCs and onset of increased TRAP release occurred later in the Neutral medium group than in the OC medium group. Remarkably, monocytes cultured in unfavorable OB medium still released TRAP into the medium, as it is structurally higher than the 'baseline' TRAP measurement of constructs onto which no monocytes were seeded ($p < 0.05$ at each timepoint).
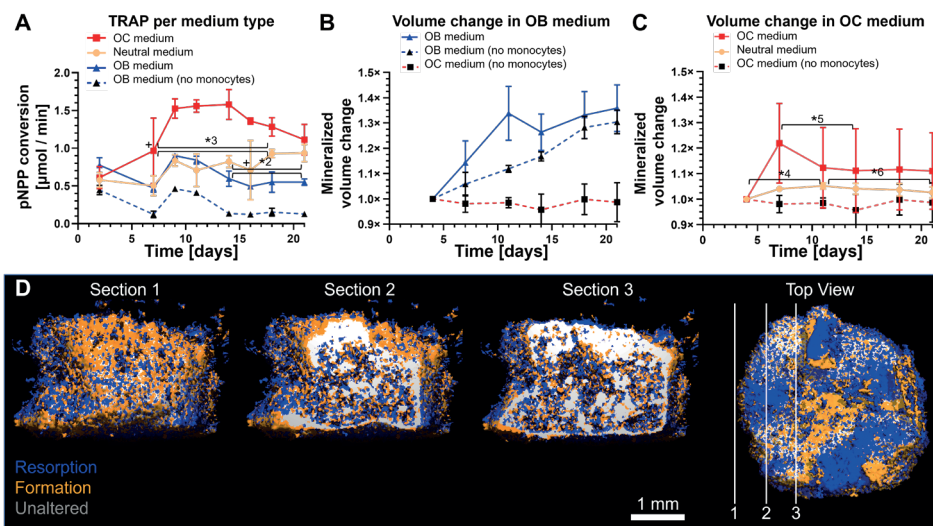
5

Fig. 5.5. *Medium composition affects TRAP activity, mineralized tissue formation and resorption activity in co-culture in 1 M seeded monocytes groups.* **(A)** *TRAP release of the 1 M monocytes groups. Co-cultures in OC medium showed highest TRAP release, followed by those cultured using Neutral medium and OB medium. The 0 M group in OB medium serves as reference.* **(B)** *Mineralized volume increased in OB medium with or without co-culture, but no longer increased in OC medium without monocytes.* **(C)** *Mineralized volume change of constructs of co-culture in OC or Neutral medium. There was no resorption without monocytes. With monocytes, mineralized volume increased in the first few days, and then decreased. The OC medium group showed a large and early decrease in volume, while the Neutral medium group showed a small but steady decrease in volume until the end of culture. The OC medium (no monocytes) group is identical in panels B and C and is for reference.* **(D)** *Three sections of the same registered scans of d 4 and d 7 of co-culture construct cultured in OC medium show many resorption (blue) and formation (orange) events on the pore surfaces, while the inside of the SF structure of the construct remains mostly unchanged (grey). The locations of the sections within the construct are shown on the top view.*

5.4.6   Co-culture medium affects mineralized matrix volume

Mineralized volume was measured over time with µCT and normalized relative to the measurement at d 4 of co-culture. As expected from the mineralization curve before co-culture (Fig. 5.2c), the amount of mineralized volume in constructs cultured in OB medium both with and without seeded monocytes increased for another 3 weeks (Fig. 5.5b). With exception of d 11 ($p = 0.025$), the volume change per timepoint between these groups were not significantly different suggesting that the mere presence of monocytes did not influence OB activity. Switching from OB medium to OC medium or Neutral medium seemingly ended this trend regardless of monocyte presence (Fig. 5.5c). The presence of monocytes seemed to prolong mineralized matrix deposition by a few days, but this effect was only statistically significant for the co-culture in Neutral medium ($p = 0.0035$, *4) and not for the co-culture in OC medium ($p = 0.064$), likely because of the large

SDs withing this group. In all individual constructs of the OC medium group, there was a significant decrease in mineralized volume between d 7 and d 14 (9.12 % decrease, p = 0.003, *5), suggesting differentiation and peak OC resorption activity happened in this period. In the Neutral medium group, a smaller but gradual decrease in mineralized volume was seen between d 11 and d 21 (2.5 % decrease, p = 0.018, *6). Formation and resorption occurred both on the inside and the outside of the constructs. An example µCT image registration shows the difference between d 4 and d 7 in a co-culture in OC medium (Fig. 5.5d).

5.4.7 Monocyte seeding density affects TRAP release but not resorptive activity

Monocytes were seeded at a density of either 1 M or 1.5 M cells per construct. A higher seeding density led to a seemingly higher TRAP release (Fig. 5.6a + c), but these differences were only significant in the group cultured in Neutral medium (Fig. 5.6c) ($p < 0.05$ for all timepoints, d 16 only after outlier correction, *7) suggesting that the presence of more neighboring monocytes contributed to differentiation by giving more chances for cell fusion and subsequent TRAP release when no OC supplements were present. An excess of OC factors (Fig. 5.6a) partially bypassed the need to have many neighboring cells as it resulted in higher TRAP expression in the group seeded with only 1 M monocytes.

In line with the TRAP results, the effects of seeding density did not result in significant differences in resorption between the groups cultured in OC medium ($p > 0.05$ at each timepoint) (Fig. 5.6b), although there was a slight downward trend in mineralized volume (indicating resorption) in both the 1 M monocytes (d 7 to d 11, p = 0.008, *8) and the 1.5 M monocytes (d 11 to d 21, p = 0.019, *9) group. This was not seen in the control group. In the groups cultured in Neutral medium (Fig. 5.6d), mineralized volume in the 1 M and 1.5 M monocytes group was significantly different from the control group without monocytes only at d 11 (1 M: p = 0.0023, 1.5 M: p = 0.0123, *10), around the time where OC are expected to become active as shown by TRAP results. Other than this there were no significant differences between groups. Both the 1 M monocytes group (5.2 % increase, p = 0.0035, *11) and the 1.5 M monocytes group (4.5 % increase, p = 0.043, *11) slightly but significantly increased in mineralized volume during the first 11 d of co-culture suggesting again that monocytes briefly stimulate mineralization. The constructs of the 1 M monocytes group slightly but continuously decrease in volume from d 11 until d 21 (p = 0.018, *12) as shown earlier in Fig. 5.5d.
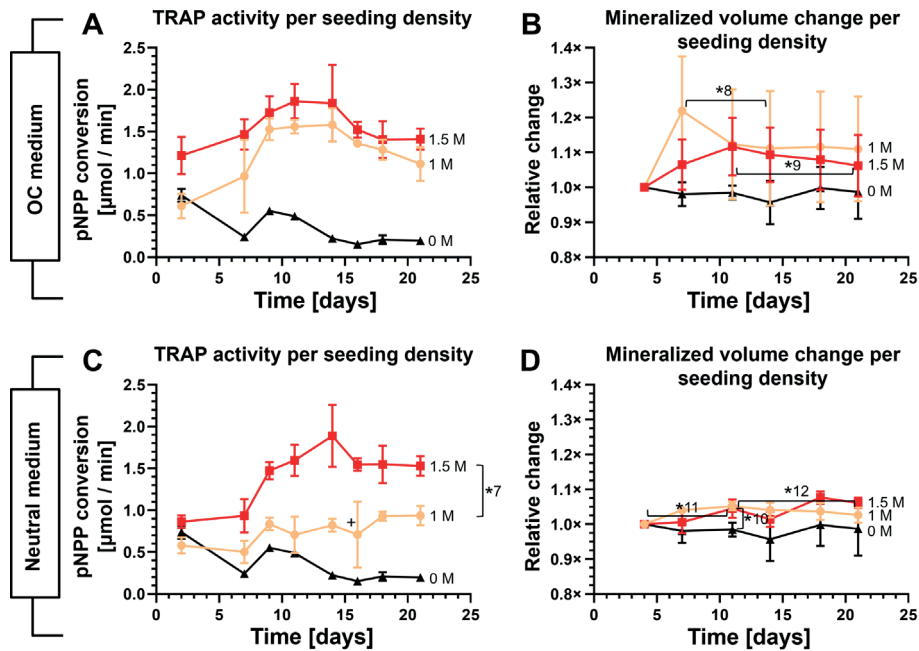
Fig. 5.6. **TRAP release and resorption during co-culture at different seeding densities in different media. (A)** *TRAP release of all monocyte seeding densities cultured in OC medium. TRAP expression was higher in constructs with 1.5 M than in those with 1 M monocytes seeded, but not significantly.* **(B)** *Mineralized volume change of all monocyte seeding densities cultured in OC medium. The control constructs showed no net change in mineralized volume. Both monocyte seeding densities increased in mineralized volume, followed by a downward trend in mineralized volume.* **(C)** *TRAP release of all monocyte seeding densities cultured in Neutral medium. The co-cultures with 1.5 M monocytes showed more TRAP release than the co-cultures with 1 M monocytes.* **(D)** *Mineralized volume change in co-cultures cultured in Neutral medium. The mineralized volume of the 1 M and 1.5 M groups increased significantly until d 11. The 1 M group steadily decreased in volume from d 11 to the end of co-culture. Note that the 0 M and 1 M lines from all panels of this figure were also shown in Fig. 5.5. The unseeded controls in Fig. 5.6A and B were cultured in OC medium and are show as a reference in these figures only.*

98 | P a g e

5.5   Discussion

If 3D OB-OC co-culture models are to be used for fundamental research, drug development or personalized medicine, it is imperative that these models can demonstrate (im)balanced matrix formation and resorption. Our earlier work has shown that both formation and resorption can be monitored within 3D constructs in co-culture (S. Remmers et al., 2020). Ideally, the model allows to investigate remodeling both in equilibrium or out of balance situations, mimicking a healthy state or a diseased state, respectively. It has previously been shown that both medium composition (Mather, 1998; Shahdadfar et al., 2005) and cell seeding density (Kozbial et al., 2019) affect intercellular communication, maturation, differentiation and cell activity. In this study, different media compositions and seeding densities were used to tune the direction and amount of remodeling to a state of equilibrium, forced formation and forced resorption.

5.5.1   Co-culture in OB medium resulted in continued matrix deposition

Co-culture in OB medium resulted in continued matrix deposition, which seemed unaffected by the presence of monocytes. This was expected because the co-culture of this group was provided with an excess of osteogenic supplements, effectively overruling OC signaling that could affect mineralized matrix deposition. At the same time, the TRAP measurements suggested that there was only a 'basal' expression of TRAP by monocytes (S. Remmers et al., 2020) and minimal OC differentiation ongoing (Hayman, 2008; Kirstein et al., 2006). This was in line with what was expected based on the bone remodeling cycle, where a resorption phase precedes a reversal phase (Delaisse, 2014) followed by a formation phase to repair the resorbed area. If OB stimulation simulates the formation phase, there would be no direct need for a new resorption phase, and OBs would not want to stimulate additional osteoclastogenesis. *In vivo*, this task is attributed to the osteocytes (Bellido, 2014; Bonewald, 2011). While the current study did not attempt to prove their presence, earlier work has shown indications of osteocyte-like cells in similar culture conditions (S. Remmers et al., 2020). The model with OB medium could be used to investigate the maximum mineralizing capacity of different cell donors (such as osteoporotic patients) within the context of the model.

5.5.2   Monocyte presence prolonged OB mineralized matrix deposition

In both Neutral and OC medium, when monocytes were present, there was ongoing mineralized matrix deposition in the first 11 d. Compared to OB medium however, the

mineralization curve was flattened. This curve was absent in the group where no monocytes were seeded. This indicated that in the absence of osteogenic supplements, the presence of monocytes was able to marginally support further mineralization. The net effect of this activity dissipated after d 11, as monocytes started to differentiate into OCs and became capable of resorbing matrix, which likely resulted in formation and resorption masking each other's changes in mineralized volume. This was further demonstrated by the µCT registrations revealing both resorption and formation occurring simultaneously. This confirmed that the model using Neutral or OC medium can be used to monitor both resorption and formation in co-culture simultaneously.

5.5.3 In OC medium, resorption initiated faster than in Neutral medium

The OC medium group had a large increase in resorption during week 2 of co-culture while the mineralized volume in Neutral medium decreased much slower over the remaining culture period. This is in line with the TRAP release results that showed a similar peak for the OC medium during week 2 of co-culture while the Neutral medium group gradually released increasing amounts of TRAP over time. The early increased TRAP release and faster onset of resorption in the OC medium group likely resulted from more OCs generated by an excess of osteoclastic supplements, which is in line with the identification of OC-like cells and resorption trails in SEM images especially in this group (Halai et al., 2014; Kleinhans et al., 2015; Varghese et al., 2006). Cell behavior in the Neutral medium group relied solely on the interaction with the matrix and on OB-OC crosstalk since no OC supplements supporting OC differentiation were added. Nevertheless, a slow build-up of TRAP release and by extension OC differentiation took place, although it did not reach the same level as in the OC medium group. This confirmed that when OC medium is used, monocytes are forcefully steered towards osteoclastogenesis, whereas Neutral medium allows exclusively OB-OC crosstalk and basic medium components (Ansari et al., 2022) to regulate remodeling. The model using OC medium would be suitable to study the maximum resorptive capacity of the applied cells, such as cells from osteoporotic patients. The model using Neutral medium provides a near-equilibrium situation under control of OB-OC communication, and open to external manipulation. Using Neutral medium, the model could be used to study the effect of drugs or other biochemical compounds on formation and resorption of donor cells, such as cells from osteoporotic patients.

5.5.4   Increased seeding density led to an increase in TRAP release

Seeding density has been shown to affect the extent of intercellular communication, maturation and the fusion towards OCs (Kozbial et al., 2019). The TRAP results from the neutral medium groups were as expected; a more than 50 % increase in TRAP release with a peak that occurred earlier in the 1.5 M monocytes group. The increased monocyte seeding density likely also facilitated an increase in cell-fusion events (Song et al., 2019) although these were not directly measured in this study. The groups cultured in OC medium did not respond the same way. The increased TRAP release by the 1 M monocytes group was as expected, but the 1.5 M monocytes group did not increase its TRAP release proportionally. Instead, the 1 M and 1.5 M monocytes groups released almost equal amounts of TRAP, and coincidently approximately similar amounts as the 1.5 M monocytes group in Neutral medium. This could indicate that there is a maximum amount of TRAP that these cells can release, and that this amount was reached in both media. It could also mean that there was a maximum to the number of cells close to the surface of the constructs, and that remaining cells did not attach, detached again, or migrated further into the construct where TRAP diffusion into the culture supernatant could be more difficult (Leddy et al., 2004; Offeddu et al., 2020).

5.5.5   Seeding density affected resorption in OC medium, but not in Neutral medium.

After an initial differentiation phase from monocytes into OCs, resorption of mineralized volume exceeded formation in the OC medium groups. Interestingly, this switch was observed a little earlier in the 1 M monocytes group than in the 1.5 M group but continued for much longer in the 1.5 M group. In the Neutral medium group, resorption was less apparent, although there was resorption in the 1 M seeded group. One explanation of the higher resorption at lower seeding density group would be that the limited amount of osteoclastogenic signaling molecules released by OB were shared by a higher number of seeded cells of which fewer achieved the necessary threshold to differentiate into resorbing OCs (Song et al., 2019), although TRAP results do not directly support this hypothesis. Furthermore, the earlier shown mineralized matrix deposition could be masking low the levels of resorption, essentially creating again an equilibrium situation in tissue remodeling. This indicates that using a higher monocyte seeding density in OC medium leads to a less-than-proportionate increase in TRAP release and possibly an increase in resorption. Using a higher seeding density with OC medium could be useful if a model is needed that favors resorption above formation. Using a higher seeding density with Neutral medium increases TRAP release proportionally without forcing the model

into a state of net resorption, which could be useful to study the reaction of OC in a state of equilibrium. However, these conclusions are only valid for cells of this particular donor, because there may be a large variation in activity and resorption between donors (Susa et al., 2004). Until models are further qualified and validated to work with variable cell numbers and cells with unknown activity, it is strongly recommended to use well characterized monocytes (Buenzli and Sims, 2015).

5.5.6 Osteoclasts exceeded their predicted lifespan

The TRAP results showed that OCs exceeded their expected lifespan of 2 weeks (Parfitt, 1994). Others have recently shown similar findings. Jacome-Galarza *et al.* showed that parabiont labelled OC were seen up to 24 weeks after parabiont separation (Jacome-Galarza et al., 2019). They propose that OC are long-lived but need to acquire new nuclei from circulating blood cells. McDonald *et al.* showed that OC can 'recycle' into smaller cells called osteomorphs that can relocate through the bloodstream and re-fuse in the presence of soluble RANKL (McDonald et al., 2021). Both support the notion that OC can, under some circumstances, indeed die or disappear after 2 weeks, but that with the proper environment it is possible to have active OCs in co-culture for longer than 2 weeks. As in our 2D results, we have shown that in the 3D co-culture monocyte-like cells are present during the entire culture duration. These cells could serve as nuclei-donors as described by Jacome-Galarza to prolong the life of existing OCs and could contain next to monocytes also osteomorphs as described by McDonald to generate new OCs elsewhere in the constructs. These results underline that there is still much to be investigated about the lifespan of OCs.

5.5.7 Limitations and future research

The 3D *in vitro* OB-OC co-culture has certain limitations. *In vitro* differentiation of OB and OC precursors is largely dependent on using the correct supplements and media, but these are different for OBs and OCs. Differentiation within the co-culture is thus a compromise between multiple media, and an optimal medium has not been determined yet (Remmers et al., 2021). OC precursors are typically available in limited quantities and cannot be expanded (Jacome-Galarza et al., 2013), and OCs have a life limited life expectancy. This poses challenges regarding experiment size and duration. Increasing resolution (decreasing voxel size) of μCT measurements results in more accurate measurements, at the cost of increased scanning duration and radiation exposure of the cells which may

affect both OBs (Kraehenbuehl et al., 2010) and OCs (Yang et al., 2012) and their function, especially when performing repeated measurements on the same cells.

Future research should focus on refining the herein presented 3D co-culture model and three media to reflect specific states of health and disease (Ross and Wilson, 2014), possibly by introducing patient cells instead of healthy cells, thereby replicating the response of the model on diseases such as osteoporosis. This could pave the way for developing an invaluable tool for fundamental research, drug development and personalized medicine.

5.6   Conclusion

This study shows that the current 3D OB-OC co-culture model can be tuned towards pronouncing either matrix deposition, matrix resorption, or a state of equilibrium by applying one of three culture media. OB medium resulted in continued matrix deposition overshadowing any ongoing resorption, while OC medium forced the differentiation of monocytes towards OCs and resulted in resorption after a period of continuing mineralization. Neutral medium contained neither the osteogenic nor osteoclastogenic supplements and was shown to be closely mimicking a situation of equilibrium, facilitating the study of intricate cell-cell interaction and the result thereof on resorption and formation. The 3D OB-OC co-culture model can be used with either of the three media as an *in vitro* co-culture model of human bone formation and resorption for various applications in fundamental research, drug development and personalized medicine.

5

Chapter 6

General Discussion

6

6.1   Introduction

Bone is a highly dynamic tissue with both mechanical and metabolic functions. As the mechanical demands placed upon bones change, bones adapt and optimize their structure and strength by removing obsolete or damaged tissue and producing new or stronger tissue when and where needed. The process of bone remodeling involves among others bone forming osteoblasts, bone resorbing osteoclasts and regulating osteocytes. In healthy tissue, bone formation and resorption are in equilibrium, but in diseases such as osteoporosis this equilibrium is disturbed (Feng and McDonald, 2011). Despite the many treatment options available (Bellido, 2014; Matsuo and Irie, 2008) targeting a variety of players in this biochemical process (Deschaseaux et al., 2010; Matsuo and Irie, 2008; Sims and Gooi, 2008), osteoporosis remains a degenerative disease that can merely be slowed down.

To study the intricate mechanisms underlying bone remodeling and disease, osteoblast-osteoclast co-culture models have been developed. However, these commonly use animal cells which can respond differently than human cells (Jemnitz et al., 2008). While bone remodeling is a 3D process, these studies are often conducted in 2D because of the many advantages regarding to experimental cost, duration and complexity. However, cells in 2D respond differently than in 3D (Edmondson et al., 2014; Li and Kilian, 2015). Finally, the most potent analytical techniques require the sacrifice of culture samples. The main drawback thereof is that any temporal information about formation and resorption within each culture sample is lost, leaving only the quantification of material at each time point as opposed to changes within samples with regard to previous time points.

This led to the aim of this thesis, which was to develop a human 3D osteoblast-osteoclast co-culture model in which both bone formation and resorption could be monitored over time.

6.2   Main findings and implications

While osteoblasts have been reliably cultured in both 2D and 3D environments in the past, including the functionality of osteoclasts into these culture conditions proved difficult. After many experiments with irreproducible results, it became apparent that culture conditions favorable for osteoclasts were essential for obtaining functional osteoclastic resorption. Remarkably, culture conditions and analytical techniques varied tremendously in published literature. A systematic map was constructed by systematically identifying and analyzing all available osteoblast-osteoclast co-culture

studies and extracting these culture condition and analytical techniques. This systematic map is presented in **Chapter 2**.

The systematic map provided a structured overview of both 2D and 3D co-culture analytical techniques, the latter of which were of particular interest for developing a 3D osteoblast-osteoclast co-culture model. Techniques suitable for monitoring resorption in 3D were µCT imaging (Hagenmüller et al., 2007) and supernatant analysis techniques such as NTx (Rossi et al., 2018) and CTx (Krishnan et al., 2014), with only µCT capable of visualization within 3D cultures themselves. Formation in 3D could be quantified non-destructively with either supernatant CICP analysis (Boanini et al., 2015) or, similar to resorption, with µCT imaging, making this the preferred choice for monitoring and visualizing both formation and resorption. Both osteoblast and osteoclast activity (alkaline phosphatase and tartrate resistant acid phosphatase respectively) were commonly measured using either pNPP-based or immunoenzymatic assays, both of which could be used non-destructively on supernatant samples. The systematic map showed that mesenchymal stromal cell-derived osteoblasts and monocyte-derived osteoclasts were the best candidates for obtaining relevant numbers of healthy human cells, with the possibility of replacing them with cells of patients for developing a personalized model if required. The map also revealed that there was no consensus whatsoever on seeding density and medium composition, especially in 3D studies.

The large variation in culture medium composition and cell seeding densities was surprising, considering that culture medium content (Mather, 1998; Shahdadfar et al., 2005) and cell seeding density (Kozbial et al., 2019) both greatly affect osteoclastogenesis. **Chapter 3** describes a 2D study conducted to develop a better understanding of the effect of seeding density and osteoclastic supplement concentration on osteoclastogenesis from monocytes and PBMCs, which was essential for introducing osteoclasts into a 3D co-culture model. This study showed that there was a clear relationship between osteoclastic supplement concentration and both the number and size of osteoclasts and osteoclastic resorption. Increasing seeding densities also led to more and larger osteoclasts, but due to experimental constraints only to more resorption in PBMCs. Remarkably though, TRAP release did not correlate to osteoclastic resorptive activity, although it seemed to correlate with osteoclast number instead (Halleen et al., 2006).

Building upon these findings, **Chapter 4** describes the proof-of-concept that formation and resorption can be monitored using µCT in a 3D co-culture. In this study, MSC-derived osteoblasts deposited mineralized matrix onto a porous silk-fibroin scaffold for 13 weeks, after which monocytes were introduced to initiate a co-culture. Osteoclastic supplements were used at a concentration in agreement with the results from **Chapter 3** and co-culture

6

conditions used were in agreement with those identified in **Chapter 2** to direct the differentiation of the cells towards osteoclastogenesis, which resulted in resorption and formation occurring in parallel during the co-culture phase, and even leading to a decrease in total mineralized volume. Using image registration on sequential μCT images, individual resorption and formation events could be visualized, localized, and quantified. While this proved that these culture conditions resulted in formation and resorption in a 3D co-culture and μCT could be used to monitor these events, remodeling was not in equilibrium nor was it regulated from within the co-culture. Instead, the processes of formation and resorption were controlled externally through supplements in the culture media, overruling the intricate biochemical interplay between cells required for such a model to serve as a tool for fundamental research, drug testing or personalized medicine.

In **Chapter 5**, the 3D co-culture model of **Chapter 4** was further improved by tuning the response thereof towards formation, resorption and equilibrium. The main challenge of the 3D osteoblast-osteoclast co-culture consisted not of achieving osteoblastic mineralization, but of introducing functionally competent osteoclasts capable of resorbing relevant volumes of mineralized tissue detectable by μCT. Thus, the osteoclastic aspect of the model required further finetuning to on one hand maximize the attainable resorptive capacity within the model, and on the other hand present a state of equilibrium open to respond to any internal or external stimuli. To investigate this, monocytes were seeded at different seeding densities, and the co-cultures were cultured with one of three culture media: an osteoclast-stimulating, a neutral or an osteoblast-stimulating medium. Culture in the osteoblast-stimulating medium resulted in continued matrix deposition, proving that mineralization could still take place in co-culture, and showing that the co-culture itself did not influence the osteoblasts' capacity to deposit mineralized matrix. Osteoclast-stimulating medium resulted in resorption, in a similar manner as in **Chapter 4** as expected. Here, more seeded monocytes led to a slightly higher TRAP release, which according to **Chapter 3** correlated with an increase in osteoclast number and to more resorption. The culture in neutral medium showed TRAP release indicative of osteoclast presence, formation and resorption events in μCT registration indicative of ongoing remodeling, but hardly any change in total mineralized volume, closely mimicking a state of equilibrium. The 3D osteoblast-osteoclast co-culture model presented in this thesis thus was shown capable of reaching a state of near-equilibrium, and with the correct stimuli capable of showing an excess of either resorption or formation. Although the stimuli used in this study were not based on physiological conditions or disease models, this study proves that the 3D co-culture model in equilibrium can respond to biochemical stimuli, having the capacity to show a quantifiable effect of a stimulus on resorption and formation.

The 3D osteoblast-osteoclast co-culture model presented in this thesis can be used as an *in vitro* co-culture model of human bone remodeling and can be further developed for various applications in fundamental research, drug development and personalized medicine.

6.3 Remaining Challenges and future work

6.3.1 Experimental optimization and limitations

The dependency on human primary cells is tied to certain practical challenges. Because human osteoblasts and osteoclasts cannot easily be extracted from healthy donors in the required numbers, they must be generated from available precursor cells. These precursors must differentiate into the required cell types, usually within the final culture environment, adding an additional layer of complexity to the model. *In vitro* differentiation is largely dependent on supplying the correct biochemical signals, usually through specialized media composition. However, the requirements for differentiation are different for osteoblasts and osteoclasts, creating a conflicting situation that must result in a compromise between the various media components required by the cells. An optimal co-culture medium has not been determined yet (Remmers et al., 2021), and may very well be dependent on specific donor characteristics.

The between-donor variation of monocytes and osteoclasts greatly limits translation of experimental results (Flanagan and Massey, 2003; Susa et al., 2004) to the general population. Any experimental results can be the result of chance, being applicable only to cells of one donor in one particular experimental setting. The same experimental setup with cells from different donors may lead to inexplicably different results. Similarly, any results that are obtained can only reliably be translated to the cell donor itself. This is not necessarily an issue if the research question is of a 'personalized' nature related to that specific donor or patient, but severely limits the translational value of such results to make claims about osteoclast biology in general. Repeating the experiments with cells from a large number of independent donors or even pooling cell populations from multiple donors only partially solves this, because the subject of translation in the clinic will still be a single person or patient with his or her own cell characteristics. Only when a predictor is identified that can account for this between-donor variation, will the translation of results be dramatically improved.

6.3.2 Extending the effective duration of co-culture

One of the main limitations of *in vitro* osteoclast cultures is their short lifespan of approximately 2 weeks (Manolagas and Parfitt, 2010; Parfitt, 1994), especially combined

with their complex manner of differentiation and inability to expand *in vitro* (Jacome-Galarza et al., 2013). Remarkably, this lifespan was exceeded in **Chapter 5**. Recently, others have shown similar findings. One study proposed that osteoclasts are in fact long-lived, but need to acquire new nuclei from other cells to extend their life-span (Jacome-Galarza et al., 2019). Another study showed that osteoclasts can recycle into so-called osteomorphs to relocate and re-fuse elsewhere in the body (McDonald et al., 2021). This suggests that using the right conditions, it should be possible to extend the duration of cultures involving osteoclasts. How this could be achieved *in vitro* remains to be elucidated. Until then, the only way to extend an osteoblast-osteoclast co-culture with human primary cells would be to replenish the culture with fresh monocytes capable of differentiating into new osteoclasts, and potentially serving as nucleus-donors for existing osteoclasts.

Alternatively, it is possible to use immortalized cell lines such as murine RAW 264.7 (Collin-Osdoby and Osdoby, 2012) or human THP-1 (Ke et al., 2019) to extend osteoclast life-span. While convenient, this option has several major drawbacks. The extended lifespan is a deviation from the *in vivo* situation where osteoclasts are still considered short-lived. Using an animal cell-line introduces additional concerns regarding the translation from animal cells to the human situation (Burkhardt and Zlotnik, 2013; Contopoulos-Ioannidis et al., 2003). Finally, monocyte and osteoclast experiments have shown a large between-donor variation (Flanagan and Massey, 2003; Susa et al., 2004), which is neglected when using a cell line. And finally, the shift from using healthy cells to using patient cells cannot be made, because cell lines for individual patients do not exist.

6.3.3   Inclusion of osteocytes and bone lining cells into the model

While earlier iterations of the mineralized silk-fibroin constructs (Melke et al., 2018) and the first 3D osteoblast-osteoclast co-culture (S. Remmers et al., 2020) have suggested the presence of osteocyte-like cells, the model presented in this thesis was not validated to contain functional osteocytes. Given the role that osteocytes play in bone remodeling (Bonewald, 2011), but also the role they play in regulating osteoclastogenesis (Xiong et al., 2015), this is a considerable limitation of the model. Similar concerns can be raised about the role bone lining cells play in coupling resorption and formation (Everts et al., 2002). While it is possible that osteoblasts eventually differentiate into osteocyte- or bone lining-like cells, this is at this moment still a welcome but unintentional side effect. Proper introduction of either or even both additional cell types into the model is desired but considering the experimental challenges and limitations of maintaining a mere two different cell types in functionally competent states, this poses a considerable challenge that has yet to be overcome.

6.3.4 Validation of the model to simulate *in vivo* conditions

The work in this thesis describes the development of a co-culture model of bone remodeling where certain stimuli manifest as changes in formation or resorption. The concept was proven to work in **Chapter 7** with osteoclastic supplements RANKL and M-CSF as stimuli, but the model has not been validated using physiologically relevant stimuli yet (Liao et al., 2021). The next step to further develop and validate this model is to apply other stimuli to the model which are physiologically relevant and compare these to the *in vivo* situation (Mollentze et al., 2021). This could be a type of mechanical loading to simulate exercise, or certain drugs or cytokines known to affect bone remodeling *in vivo* such as bisphosphonates.

6.3.5 Using patient cells for disease research and drug effectiveness

The 3D osteoblast-osteoclast co-culture model presented in this thesis replicates the assumed healthy state of anonymous donors. This is well-suited for fundamental research on bone cells and bone remodeling, but not necessarily applicable to study bone diseases such as osteoporosis. Replacing both cell types with cells from ideally a single diseased donor (Evans et al., 2006) would facilitate fundamental research on the corresponding disease state (Ross and Wilson, 2014). This is particularly interesting from a personalized medicine point of view, as the same model can be used to test the response of diseased cells to a variety of drugs or drug combinations. This way the drug effectiveness for a single patient can be evaluated or predicted to optimize treatment plans and prevent or reduce treatment courses of ineffective drugs. For using the model as a predictive tool in a clinical setting, it has to be further developed in to a faster, lower-cost and higher-throughput tool, because in its current state, the time required, cost and manual labor needed make it vastly unsuitable for routine clinical prediction (Sieberath et al., 2020). One of the major challenges to overcome in developing this model into a clinical tool is to efficiently obtain both precursor cell types from the patient. While monocytes were obtained from peripheral blood, the mesenchymal stromal cells used in this model were isolated from bone marrow, which requires a more invasive procedure. Under normal conditions, a type of mesenchymal stromal cells circulates in the blood in extremely low numbers but could be extracted after using a mobilization procedure (Park et al., 2019; Xu and Li, 2014). Other points for improvement could be off-the-shelf availability of (mineralized) constructs to reduce the duration of the culture, construct size reduction to reduce the amount of cells needed, and (partially) automated culture and analysis techniques to reduce the cost of manual labor.

6.3.6   Towards tissue-engineered bone for healing critical-sized defects

The first thing that comes to mind when thinking about tissue engineering (Langer and Vacanti, 1993) in the context of bone is its application in healing critical-sized bone defects. Autologous bone grafts are still considered the gold standard of bone regeneration and repair (Brown and Cruess, 1982; Habibovic and de Groot, 2007), but drawbacks such as donor site morbidity and limited availability prevent wide-spread use thereof. Synthetic or lab-grown grafts do not have these drawbacks. While the idea of implanting live tissue engineered bone is incredible, the transition from such novel techniques into routine clinical applications on a large scale has still not taken place (Henkel et al., 2013). Most discoveries disappear into the 'valley of death' because of the immense funding required for design and manufacturing, pre-clinical studies and clinical trials (Hollister, 2009). Acquiring regulatory approval becomes more challenging, time consuming and expensive as the products become more complex and contain more biological elements, with most tissue engineered products being regulated as class III medical devices or drugs (Ratcliffe, 2007). Even if a product passes these challenges, the product must still be accepted by surgeons and insurance companies as a viable alternative considering practicality, functionality and cost. Although never intended for that purpose, the model presented in this thesis is vastly unsuitable for clinical implantation because it uses a myriad of animal or human-derived components such as silkworm-derived silk, fetal bovine serum, various bacteria-derived culture supplements and anonymous human donor cells, each possibly adding years to the development and approval processes.

Instead of implanting the full-blown scaffold-biomolecule-cell tissue engineering triad (O'Brien, 2011), many other approaches are being developed based around the concept of osteoinductivity (Urist, 1965). Many materials including calcium Phosphate (Yuan et al., 2001a), titanium (Fujibayashi et al., 2004) and glass (Van Gestel et al., 2015; Yuan et al., 2001b) have shown various degrees of osteoconductivity and osteoinductivity, a process largely dependent on materials having a porous macro- and microstructure and having a chemical composition that can calcify *in situ* or already contains calcium phosphate (Habibovic and de Groot, 2007). These materials and technologies can be further functionalized by manipulating the surface architecture to mimic those occurring in nature (Honig et al., 2020) or specifically control the inflammatory response (Vassey et al., 2020). These materials can be combined with for example calcium phosphate coatings to improve bioactivity (Nandakumar et al., 2013), sucrose to improve tissue ingrowth (Lodoso-Torrecilla et al., 2018), or they can be implanted with ions such as Cu^{2+} to reduce infections (Cordeiro et al., 2022) or Co^{2+} to stimulate neovascularization (Birgani et al., 2016). The diverse development of these cell-free implantable materials for bone regeneration has shown promising results. Such materials can generally be produced faster, easier and cheaper for clinical use than those with embedded cells such as our

model and will have less trouble obtaining regulatory approval. Once approved, they are likely more practical to integrate into routine clinical use and are more easily adopted by surgeons and insurance companies.

6.4 Conclusion

This thesis provides an unprecedented amount of readily accessible information on osteoblast-osteoclast co-cultures, culminating in the development of a human *in vitro* 3D osteoblast-osteoclast co-culture model of bone remodeling in which formation and resorption can be monitored over time non-destructively. The model is capable of pronouncing states of near-equilibrium, resorption, and formation after application of the correct stimuli. The 3D osteoblast-osteoclast co-culture model presented in this thesis can be used as an *in vitro* co-culture model of human bone remodeling and can be further developed for various applications in fundamental research, drug development and personalized medicine.

6

Bibliography

Amizuka, N., Takahashi, N., Udagawa, N., Suda, T., Ozawa, H., 1997. An ultrastructural study of cell-cell contact between mouse spleen cells and calvaria-derived osteoblastic cells in a co-culture system for osteoclast formation. Acta Histochem Cytochem 30, 351–362.

Ansari, S., Ito, K., Hofmann, S., 2022. Alkaline Phosphatase Activity of Serum Affects Osteogenic Differentiation Cultures. ACS Omega 7, 12724–12733. https://doi.org/10.1021/acsomega.1c07225

Antonov, A.S., Antonova, G.N., Munn, D.H., Mivechi, N., Lucas, R., Catravas, J.D., Verin, A.D., 2011. αVβ3 integrin regulates macrophage inflammatory responses via PI3 kinase/Akt-dependent NF-κB activation. J Cell Physiol 226, 469–476. https://doi.org/10.1002/jcp.22356

Armour, K.J., van 't Hof, R.J., Armour, K.E., Torbergsen, A.C., Del Soldato, P., Ralston, S.H., 2001. Inhibition of bone resorption in vitro and prevention of ovariectomy-induced bone loss in vivo by flurbiprofen nitroxybutylester (HCT1026). Arthritis Rheum 44, 2185–2192.

Atkins, G.J., Welldon, K.J., Halbout, P., Findlay, D.M., 2009. Strontium ranelate treatment of human primary osteoblasts promotes an osteocyte-like phenotype while eliciting an osteoprotegerin response. Osteoporos Int 20, 653–664. https://doi.org/10.1007/s00198-008-0728-6

Barbeck, M., Booms, P., Unger, R., Hoffmann, V., Sader, R., Kirkpatrick, C.J., Ghanaati, S., 2017. Multinucleated giant cells in the implant bed of bone substitutes are foreign body giant cells-New insights into the material-mediated healing process. J Biomed Mater Res Part A 105, 1105–1111. https://doi.org/10.1002/jbm.a.36006

Bellido, T., 2014. Osteocyte-driven bone remodeling. Calcif Tissue Int 94, 25–34. https://doi.org/10.1007/s00223-013-9774-y

Bellver, M., Del Rio, L., Jovell, E., Drobnic, F., Trilla, A., 2019. Bone mineral density and bone mineral content among female elite athletes. Bone 127, 393–400. https://doi.org/10.1016/j.bone.2019.06.030

Berg, S., Kutra, D., Kroeger, T., Straehle, C.N., Kausler, B.X., Haubold, C., Schiegg, M., Ales, J., Beier, T., Rudy, M., Eren, K., Cervantes, J.I., Xu, B., Beuttenmueller, F., Wolny, A., Zhang, C., Koethe, U., Hamprecht, F.A., Kreshuk, A., 2019. ilastik: interactive machine learning for (bio)image analysis. Nat Methods 16, 1226–1232. https://doi.org/10.1038/s41592-019-0582-9

Birgani, Z.T., Fennema, E., Gijbels, M.J., De Boer, J., Van Blitterswijk, C.A., Habibovic, P., 2016. Stimulatory effect of cobalt ions incorporated into calcium phosphate coatings on neovascularization in an in vivo intramuscular model in goats. Acta Biomater 36, 267–276. https://doi.org/10.1016/j.actbio.2016.03.031

Bitar, M., Brown, R.A., Salih, V., Kidane, A.G., Knowles, J.C., Nazhat, S.N., 2008. Effect of cell density on osteoblastic differentiation and matrix degradation of biomimetic dense collagen scaffolds. Biomacromolecules 9, 129–135. https://doi.org/10.1021/bm701112w

Boanini, E., Torricelli, P., Sima, F., Axente, E., Fini, M., Mihailescu, I.N., Bigi, A., 2015. Strontium and zoledronate hydroxyapatites graded composite coatings for bone prostheses. J Colloid Interface Sci 448, 1–7.

7

Bonewald, L.F., 2011. The amazing osteocyte. J Bone Miner Res 26. https://doi.org/10.1002/jbmr.320

Bongio, M., Lopa, S., Gilardi, M., Bersini, S., Moretti, M., 2016. A 3D vascularized bone remodeling model combining osteoblasts and osteoclasts in a CaP nanoparticle-enriched matrix. Nanomedicine (London, England) 11, 1073–91. https://doi.org/10.2217/nnm-2015-0021

Bonito, V., de Kort, B., Bouten, C., Smits, A., 2019. Cyclic strain affects macrophage cytokine secretion and ECM turnover in electrospun scaffolds. Tissue Eng Part A 25, 1310–1325. https://doi.org/10.1089/ten.TEA.2018.0306

Bose, S., Roy, M., Bandyopadhyay, A., 2012. Recent advances in bone tissue engineering scaffolds. Trends Biotechnol. https://doi.org/10.1016/j.tibtech.2012.07.005

Boskey, A.L., 2007. Mineralization of Bones and Teeth. Elements 3, 385–391. https://doi.org/10.2113/GSELEMENTS.3.6.385

Brouwers, J.E.M., Lambers, F.M., Gasser, J.A., Van Rietbergen, B., Huiskes, R., 2008. Bone degeneration and recovery after early and late bisphosphonate treatment of ovariectomized wistar rats assessed by in vivo micro-computed tomography. Calcif Tissue Int 82, 202–211. https://doi.org/10.1007/s00223-007-9084-3

Brown, K.L., Cruess, R.L., 1982. Bone and cartilage transplantation in orthopaedic surgery. A review. J Bone Joint Surg Am 64, 270–279.

Buckley, K.A., Chan, B.Y., Fraser, W.D., Gallagher, J.A., 2005. Human osteoclast culture from peripheral blood monocytes: phenotypic characterization and quantitation of resorption. Methods Mol Med 107, 55–68.

Buckley, K.A., Hipskind, R.A., Gartland, A., Bowler, W.B., Gallagher, J.A., 2002. Adenosine triphosphate stimulates human osteoclast activity via upregulation of osteoblast-expressed receptor activator of nuclear factor-kappa B ligand. Bone 31, 582–590.

Buenzli, P.R., Sims, N.A., 2015. Quantifying the osteocyte network in the human skeleton. Bone 75, 144–150. https://doi.org/10.1016/j.bone.2015.02.016

Burkhardt, A.M., Zlotnik, A., 2013. Translating translational research: mouse models of human disease. Cell Mol Immunol 10, 373–4. https://doi.org/10.1038/cmi.2013.19

Chambers, T.J., 1982. Osteoblasts release osteoclasts from calcitonin-induced quiescence. J Cell Sci 57, 247–260.

Chan, E.K.M., Darendeliler, M.A., Petocz, P., Jones, A.S., 2004. A new method for volumetric measurement of orthodontically induced root resorption craters. Eur J Oral Sci 112, 134–139. https://doi.org/10.1111/j.1600-0722.2004.00118.x

Clarke, M.S.F., Sundaresan, A., Vanderburg, C.R., Banigan, M.G., Pellis, N.R., 2013. A three-dimensional tissue culture model of bone formation utilizing rotational co-culture of human adult osteoblasts and osteoclasts. Acta Biomater 9, 7908–7916. https://doi.org/10.1016/j.actbio.2013.04.051

Collin-Osdoby, P., Osdoby, P., 2012. RANKL-mediated osteoclast formation from murine RAW 264.7 cells. Methods Mol Biol (Clifton, NJ) 816, 187–202. https://doi.org/10.1007/978-1-61779-415-5_13

Contopoulos-Ioannidis, D.G., Ntzani, E., Ioannidis, J.P.A., 2003. Translation of highly promising basic science research into clinical applications. Am J Med 114, 477–84.

Cordeiro, J.M., Barão, V.A.R., de Avila, E.D., Husch, J.F.A., Yang, F., van den Beucken, J.J.J.P., 2022. Tailoring Cu2+-loaded electrospun membranes with antibacterial ability for guided bone regeneration. Biomater Adv 139. https://doi.org/10.1016/j.bioadv.2022.212976

Davidov, M., 1967. Histochemical detection of alkaline phosphatase by means of naphthol phosphate AS-MX in association with fast blue salt BB in the large acinous glands - PubMed. Nauchni Tr Viss Med Inst Sofiia 46, 13–18.

de Vries, R.B.M., Hooijmans, C.R., Langendam, M.W., van Luijk, J., Leenaars, M., Ritskes-Hoitinga, M., Wever, K.E., 2015. A protocol format for the preparation, registration and publication of systematic reviews of animal intervention studies. Evidence-based Preclin Med 2, e00007. https://doi.org/10.1002/ebm2.7

De Vries, T.J., El Bakkali, I., Kamradt, T., Schett, G., Jansen, I.D.C., D'Amelio, P., 2019. What are the peripheral blood determinants for increased osteoclast formation in the various inflammatory diseases associated with bone loss? Front Immunol 10, 1–12. https://doi.org/10.3389/fimmu.2019.00505

De Vries, T.J., Schoenmaker, T., Aerts, D., Grevers, L.C., Souza, P.P.C., Nazmi, K., van de Wiel, M., Ylstra, B., Lent, P.L. Van, Leenen, P.J.M., Everts, V., 2015. M-CSF priming of osteoclast precursors can cause osteoclastogenesis-insensitivity, which can be prevented and overcome on bone. J Cell Physiol 230, 210–25. https://doi.org/10.1002/jcp.24702

de Wildt, B.W.M., Ansari, S., Sommerdijk, N.A.J.M., Ito, K., Akiva, A., Hofmann, S., 2019. From bone regeneration to three-dimensional in vitro models: tissue engineering of organized bone extracellular matrix. Curr Opin Biomed Eng. https://doi.org/10.1016/j.cobme.2019.05.005

Delaisse, J.-M., 2014. The reversal phase of the bone-remodeling cycle: cellular prerequisites for coupling resorption and formation. BoneKEy reports 3, 561. https://doi.org/10.1038/bonekey.2014.56

Deschaseaux, F., Pontikoglou, C., Sensebe, L., 2010. Bone regeneration: the stem/progenitor cells point of view. J Cell Mol Med 14, 103–115. https://doi.org/10.1111/j.1582-4934.2009.00878.x

Dirckx, N., Van Hul, M., Maes, C., 2013. Osteoblast recruitment to sites of bone formation in skeletal development, homeostasis, and regeneration. Birth Defects Res C Embryo Today 99, 170–191. https://doi.org/10.1002/bdrc.21047

Domaschke, H., Gelinsky, M., Burmeister, B., Fleig, R., Hanke, T., Reinstorf, A., Pompe, W., Rösen-Wolff, A., 2006. In vitro ossification and remodeling of mineralized collagen I scaffolds. Tissue Eng 12, 949–58. https://doi.org/10.1089/ten.2006.12.949

Edmondson, R., Broglie, J.J., Adcock, A.F., Yang, L., 2014. Three-dimensional cell culture systems and their applications in drug discovery and cell-based biosensors. Assay Drug Dev Technol 12, 207–18. https://doi.org/10.1089/adt.2014.573

Ellouz, R., Chapurlat, R., van Rietbergen, B., Christen, P., Pialat, J.-B., Boutroy, S., 2014. Challenges in longitudinal measurements with HR-pQCT: Evaluation of a 3D registration method to improve bone microarchitecture and strength measurement reproducibility. Bone 63, 147–157. https://doi.org/10.1016/j.bone.2014.03.001

Engvall, E., Perlmann, P., 1971. Enzyme-linked immunosorbent assay (ELISA) quantitative assay of immunoglobulin G. Immunochemistry 8, 871–874. https://doi.org/10.1016/0019-2791(71)90454-X

Evans, C.E., Mylchreest, S., Andrew, J.G., 2006. Age of donor alters the effect of cyclic hydrostatic pressure on production by human macrophages and osteoblasts of sRANKL, OPG and RANK. BMC Musculoskelet Disord 7, 21. https://doi.org/10.1186/1471-2474-7-21

Everts, V., Delaissé, J.M., Korper, W., Jansen, D.C., Tigchelaar-Gutter, W., Saftig, P., Beertsen, W., 2002. The Bone Lining Cell: Its Role in Cleaning Howship's Lacunae and Initiating Bone Formation. J Bone Miner Res 17, 77–90. https://doi.org/10.1359/jbmr.2002.17.1.77

Feng, X., McDonald, J.M., 2011. Disorders of Bone Remodeling. Annu Rev Pathol 6, 121–145. https://doi.org/10.1146/annurev-pathol-011110-130203

Ferrin, I., Beloqui, I., Zabaleta, L., Salcedo, J.M., Trigueros, C., Martin, A.G., 2017. Isolation, Culture, and Expansion of Mesenchymal Stem Cells, in: Methods in Molecular Biology (Clifton, N.J.). p. : 177-190. https://doi.org/10.1007/978-1-4939-6921-0_13

Flanagan, A.M., Massey, H.M., 2003. Generating human osteoclasts in vitro from bone marrow and peripheral blood. Methods Mol Med 80, 113–128. https://doi.org/10.1385/1-59259-366-6:113

Frost, H.M., 1969. Tetracycline-based histological analysis of bone remodeling. Calcif Tissue Res 3, 211–37. https://doi.org/10.1007/bf02058664

Fujibayashi, S., Neo, M., Kim, H.M., Kokubo, T., Nakamura, T., 2004. Osteoinduction of porous bioactive titanium metal. Biomaterials 25, 443–450. https://doi.org/10.1016/S0142-9612(03)00551-9

Goers, L., Freemont, P., Polizzi, K.M., 2014. Co-culture systems and technologies: taking synthetic biology to the next level. J R Soc Interface / R Soc 11. https://doi.org/10.1098/rsif.2014.0065

Golub, E.E., Boesze-Battaglia, K., 2007. The role of alkaline phosphatase in mineralization. Curr Opin Orthop. https://doi.org/10.1097/BCO.0b013e3282630851

Graves, D.T., Jiang, Y., Valente, A.J., 1999. The expression of monocyte chemoattractant protein-1 and other chemokines by osteoblasts. Front Biosci a J virtual Libr 4, D571-80.

Gruber, H.E., Ivey, J.L., Thompson, E.R., Chesnut, C.H., Baylink, D.J., 1986. Osteoblast and osteoclast cell number and cell activity in postmenopausal osteoporosis. Miner Electrolyte Metab 12, 246–254.

Gstraunthaler, G., Seppi, T., Pfaller, W., 1999. Impact of culture conditions, culture media volumes, and glucose content on metabolic properties of renal epithelial cell cultures: Are renal cells in tissue culture hypoxic? Cell Physiol Biochem 9, 150–172. https://doi.org/10.1159/000016312

Habibovic, P., de Groot, K., 2007. Osteoinductive biomaterials—properties and relevance in bone repair. J Tissue Eng Regen Med 1, 25–32. https://doi.org/10.1002/term.5

Hagenmüller, H., Hofmann, S., Kohler, T., Merkle, H.P., Kaplan, D.L., Vunjak-Novakovic, G., Müller, R., Meinel, L., 2007. Non-invasive time-lapsed monitoring and quantification of engineered bone-like tissue. Ann Biomed Eng 35, 1657–67. https://doi.org/10.1007/s10439-007-9338-2

Halai, M., Ker, A., Meek, R.D., Nadeem, D., Sjostrom, T., Su, B., McNamara, L.E., Dalby, M.J., Young, P.S., 2014. Scanning electron microscopical observation of an osteoblast/osteoclast co-culture on micropatterned orthopaedic ceramics. J Tissue Eng 5, 2041731414552114. https://doi.org/10.1177/2041731414552114

Halleen, J.M., Tiitinen, S.L., Ylipahkala, H., Fagerlund, K.M., Väänänen, H.K., 2006. Tartrate-resistant acid phosphatase 5b (TRACP 5b) as a marker of bone resorption. Clin Lab 52, 499–509.

Halleen, J.M., Ylipahkala, H., Alatalo, S.L., Janckila, A.J., Heikkinen, J.E., Suominen, H., Cheng, S., Vaananen, H.K., 2002. Serum tartrate-resistant acid phosphatase 5b, but not 5a, correlates with other markers of bone turnover and bone mineral density. Calcif Tissue Int 71, 20–25. https://doi.org/10.1007/s00223-001-2122-7

Hammerl, A., Diaz Cano, C.E., De-Juan-Pardo, E.M., van Griensven, M., Poh, P.S.P., 2019. A Growth Factor-Free Co-Culture System of Osteoblasts and Peripheral Blood Mononuclear Cells for the Evaluation of the Osteogenesis Potential of Melt-Electrowritten Polycaprolactone Scaffolds. Int J Mol Sci 20.

Hayden, R.S., Fortin, J., Harwood, B., Subramanian, B., Quinn, K.P., Georgakoudi, I., Kopin, A.S., Kaplan, D.L., 2014. Cell-tethered ligands modulate bone remodeling by osteoblasts and osteoclasts. Adv Funct Mater 24, 472–479. https://doi.org/10.1002/adfm.201302210

Hayes, M.P., Zoon, K.C., 1993. Priming of human monocytes for enhanced lipopolysaccharide responses: Expression of alpha interferon, interferon regulatory factors, and tumor necrosis factor. Infect Immun 61, 3222–3227. https://doi.org/10.1128/iai.61.8.3222-3227.1993

Hayman, A.R., 2008. Tartrate-resistant acid phosphatase (TRAP) and the osteoclast/immune cell dichotomy. Autoimmunity 41, 218–223. https://doi.org/10.1080/08916930701694667

Hayman, A.R., Jones, S.J., Boyde, A., Foster, D., Colledge, W.H., Carlton, M.B., Evans, M.J., Cox, T.M., 1996. Mice lacking tartrate-resistant acid phosphatase (Acp 5) have disrupted endochondral ossification and mild osteopetrosis. Dev (Cambridge, England) 122, 3151–62.

Hayman, A.R., Macary, P., Lehner, P.J., Cox, T.M., 2001. Tartrate-resistant acid phosphatase (Acp 5): Identification in diverse human tissues and dendritic cells. J Histochem Cytochem 49, 675–683. https://doi.org/10.1177/002215540104900601

Heinemann, C., Heinemann, S., Bernhardt, A., Lode, A., Worch, H., Hanke, T., 2010. In vitro osteoclastogenesis on textile chitosan scaffold. Eur Cell Mater 19, 96–106.

Heinemann, C., Heinemann, S., Worch, H., Hanke, T., 2011. Development of an osteoblast/osteoclast co-culture derived by human bone marrow stromal cells and human monocytes for biomaterials testing. Eur Cell Mater 21, 80–93.

Henkel, J., Woodruff, M.A., Epari, D.R., Steck, R., Glatt, V., DIckinson, I.C., Choong, P.F.M., Schuetz, M.A., Hutmacher, D.W., 2013. Bone Regeneration Based on Tissue Engineering Conceptions-A 21st Century Perspective. Bone Res. https://doi.org/10.4248/BR201303002

Henriksen, K., Karsdal, M.A., Taylor, A., Tosh, D., Coxon, F.P., 2012. Generation of human osteoclasts from peripheral blood. Methods Mol Biol (Clifton, NJ) 816, 159–75. https://doi.org/10.1007/978-1-61779-415-5_11

Hikita, A., Iimura, T., Oshima, Y., Saitou, T., Yamamoto, S., Imamura, T., 2015. Analyses of bone modeling and remodeling using in vitro reconstitution system with two-photon microscopy. Bone 76, 5–17.

Hofmann, S., Hagenmüller, H., Koch, A.M., Müller, R., Vunjak-Novakovic, G., Kaplan, D.L., Merkle, H.P., Meinel, L., 2007. Control of in vitro tissue-engineered bone-like structures using human mesenchymal stem cells and porous silk scaffolds. Biomaterials 28, 1152–1162. https://doi.org/10.1016/j.biomaterials.2006.10.019

Hofmann, S., Hilbe, M., Fajardo, R.J., Hagenmüller, H., Nuss, K., Arras, M., Müller, R., von Rechenberg, B., Kaplan, D.L., Merkle, H.P., Meinel, L., 2013. Remodeling of tissue-engineered bone structures in vivo. Eur J Pharm Biopharm 85, 119–29. https://doi.org/10.1016/j.ejpb.2013.02.011

Hollister, S.J., 2009. Scaffold engineering: A bridge to where? Biofabrication. https://doi.org/10.1088/1758-5082/1/1/012001

Holmes, A., Brown, R., Shakesheff, K., 2009. Engineering tissue alternatives to animals: applying tissue engineering to basic research and safety testing. Regen Med 4, 579–592. https://doi.org/10.2217/rme.09.26

Honig, F., Vermeulen, S., Zadpoor, A.A., de Boer, J., Fratila-Apachitei, L.E., 2020. Natural architectures for tissue engineering and regenerative medicine. J Funct Biomater. https://doi.org/10.3390/JFB11030047

Husch, J.F.A., Stessuk, T., Den Breejen, C., Van Den Boom, M., Leeuwenburgh, S.C.G., Van Den Beucken, J.J.J.P., 2021. A Practical Procedure for the in Vitro Generation of Human Osteoclasts and Their Characterization. Tissue Eng - Part C Methods 27, 421–432. https://doi.org/10.1089/ten.tec.2021.0122

Jacome-Galarza, C.E., Lee, S.-K., Lorenzo, J.A., Aguila, H.L., 2013. Identification, characterization, and isolation of a common progenitor for osteoclasts, macrophages, and dendritic cells from murine bone marrow and periphery. J bone Miner Res Off J Am Soc Bone Miner Res 28, 1203–13. https://doi.org/10.1002/jbmr.1822

Jacome-Galarza, C.E., Percin, G.I., Muller, J.T., Mass, E., Lazarov, T., Eitler, J., Rauner, M., Yadav, V.K., Crozet, L., Bohm, M., Loyher, P.L., Karsenty, G., Waskow, C., Geissmann, F., 2019. Developmental origin, functional maintenance and genetic rescue of osteoclasts. Nature 568, 541–545. https://doi.org/10.1038/s41586-019-1105-7

Janckila, A.J., Takahashi, K., Sun, S.Z., Yam, L.T., 2001. Naphthol-ASBI phosphate as a preferred substrate for tartrate-resistant acid phosphatase isoform 5b. J Bone Miner Res 16, 788–793. https://doi.org/10.1359/jbmr.2001.16.4.788

Jemnitz, K., Veres, Z., Monostory, K., Kóbori, L., Vereczkey, L., 2008. Interspecies differences in acetaminophen sensitivity of human, rat, and mouse primary hepatocytes. Toxicol In Vitro 22, 961–967. https://doi.org/10.1016/j.tiv.2008.02.001

Jolly, J.J., Chin, K.-Y., Farhana, M.F.N., Alias, E., Chua, K.H., Hasan, W.N.W., Ima-Nirwana, S., 2018. Optimization of the Static Human Osteoblast/Osteoclast Co-culture System. Iran J Med Sci 43, 208–213.

Jones, G.L., Motta, A., Marshall, M.J., El Haj, A.J., Cartmell, S.H., 2009. Osteoblast: osteoclast co-cultures on silk fibroin, chitosan and PLLA films. Biomaterials 30, 5376–5384.

Kadow-Romacker, A., Duda, G.N., Bormann, N., Schmidmaier, G., Wildemann, B., 2013. Slight changes in the mechanical stimulation affects osteoblast- and osteoclast-like cells in co-culture. Transfus Med Hemother 40, 441–447. https://doi.org/10.1159/000356284

Karsdal, M.A., Martin, T.J., Bollerslev, J., Christiansen, C., Henriksen, K., 2007. Are nonresorbing osteoclasts sources of bone anabolic activity? J Bone Min Res 22, 487–494. https://doi.org/10.1359/jbmr.070109

Kasoju, N., Bora, U., 2012. Silk Fibroin in Tissue Engineering. Adv Healthc Mater 1, 393–412. https://doi.org/10.1002/adhm.201200097

Kaunitz, J.D., Yamaguchi, D.T., 2008. TNAP, TrAP, ecto-purinergic signaling, and bone remodeling. J Cell Biochem 105, 655–662. https://doi.org/10.1002/jcb.21885

Ke, D.X., Banerjee, D., Bose, S., 2019. In Vitro Characterizations of Si4+ and Zn2+ Doped Plasma Sprayed Hydroxyapatite Coatings Using Osteoblast and Osteoclast Coculture. Acs Biomater Sci Eng 5, 1302–1310.

Kim, M.S., Magno, C.L., Day, C.J., Morrison, N.A., 2006. Induction of chemokines and chemokine receptors CCR2b and CCR4 in authentic human osteoclasts differentiated with RANKL and osteoclast like cells differentiated by MCP-1 and RANTES. J Cell Biochem 97, 512–518. https://doi.org/10.1002/jcb.20649

Kim, Y.H., Yoon, D.S., Kim, H.O., Lee, J.W., 2012. Characterization of different subpopulations from bone marrow-derived mesenchymal stromal cells by alkaline phosphatase expression. Stem Cells Dev 21, 2958–2968. https://doi.org/10.1089/scd.2011.0349

Kirstein, B., Chambers, T.J., Fuller, K., 2006. Secretion of tartrate-resistant acid phosphatase by osteoclasts correlates with resorptive behavior. J Cell Biochem 98, 1085–1094. https://doi.org/10.1002/jcb.20835

Klein-Nulend, J., Bacabac, R.G., Bakker, A.D., 2012. Mechanical loading and how it affects bone cells: the role of the osteocyte cytoskeleton in maintaining our skeleton. Eur Cell Mater 24, 278–291.

Klein-Nulend, J., Bakker, A.D., Bacabac, R.G., Vatsa, A., Weinbaum, S., 2013. Mechanosensation and transduction in osteocytes. Bone 54, 182–190. https://doi.org/10.1016/j.bone.2012.10.013

Kleinhans, C., Schmid, F.F., Schmid, F. V, Kluger, P.J., 2015. Comparison of osteoclastogenesis and resorption activity of human osteoclasts on tissue culture polystyrene and on natural extracellular bone matrix in 2D and 3D. J Biotechnol 205, 101–110. https://doi.org/10.1016/j.jbiotec.2014.11.039

Kleiveland, C.R., 2015. Peripheral blood mononuclear cells, in: The Impact of Food Bioactives on Health: In Vitro and Ex Vivo Models. Springer International Publishing, pp. 161–167. https://doi.org/10.1007/978-3-319-16104-4_15

Kozbial, A., Bhandary, L., Murthy, S.K., 2019. Effect of monocyte seeding density on dendritic cell generation in an automated perfusion-based culture system. Biochem Eng J 150. https://doi.org/10.1016/j.bej.2019.107291

Kraehenbuehl, T.P., Stauber, M., Ehrbar, M., Weber, F., Hall, H., Muller, R., 2010. Effects of muCT radiation on tissue engineered bone-like constructs. Biomed Tech 55, 245–250. https://doi.org/10.1515/BMT.2010.031

Krishnan, V., Vogler, E.A., Sosnoski, D.M., Mastro, A.M., 2014. In vitro mimics of bone remodeling and the vicious cycle of cancer in bone. J Cell Physiol 229, 453–462.

Kristensen, H.B., Andersen, T.L., Marcussen, N., Rolighed, L., Delaisse, J.M., 2014. Osteoblast recruitment routes in human cancellous bone remodeling. Am J Pathol 184, 778–789. https://doi.org/10.1016/j.ajpath.2013.11.022

Kulkarni, R.N., Bakker, A.D., Everts, V., Klein-Nulend, J., 2012. Mechanical loading prevents the stimulating effect of IL-1β on osteocyte-modulated osteoclastogenesis. Biochem Biophys Res Commun 420, 11–16. https://doi.org/10.1016/j.bbrc.2012.02.099

Kyllönen, L., Haimi, S., Mannerström, B., Huhtala, H., Rajala, K.M., Skottman, H., Sándor, G.K., Miettinen, S., 2013. Effects of different serum conditions on osteogenic differentiation of human adipose stem cells in vitro. Stem Cell Res Ther 4, 17. https://doi.org/10.1186/scrt165

Lacey, D.L., Timms, E., Tan, H.L., Kelley, M.J., Dunstan, C.R., Burgess, T., Elliott, R., Colombero, A., Elliott, G., Scully, S., Hsu, H., Sullivan, J., Hawkins, N., Davy, E., Capparelli, C., Eli, A., Qian, Y.X., Kaufman, S., Sarosi, I., Shalhoub, V., Senaldi, G., Guo, J., Delaney, J., Boyle, W.J., 1998. Osteoprotegerin ligand is a cytokine that regulates osteoclast differentiation and activation. Cell 93, 165–76.

Lalande, A., Roux, S., Denne, M.A., Stanley, E.R., Schiavi, P., Guez, D., De Vernejoul, M.C., 2001. Indapamide, a thiazide-like diuretic, decreases bone resorption in vitro. J Bone Min Res 16, 361–370.

Langenbach, F., Handschel, J., 2013. Effects of dexamethasone, ascorbic acid and β-glycerophosphate on the osteogenic differentiation of stem cells in vitro. Stem Cell Res Ther. https://doi.org/10.1186/scrt328

Langer, R., Vacanti, J.P., 1993. Tissue engineering. Science 260, 920–926. https://doi.org/10.1126/science.8493529

Langhans, S.A., 2018. Three-dimensional in vitro cell culture models in drug discovery and drug repositioning. Front Pharmacol. https://doi.org/10.3389/fphar.2018.00006

Leddy, H.A., Awad, H.A., Guilak, F., 2004. Molecular diffusion in tissue-engineered cartilage constructs: Effects of scaffold material, time, and culture conditions. J Biomed Mater Res - Part B Appl Biomater 70, 397–406. https://doi.org/10.1002/jbm.b.30053

Lee, E.J., Kim, J.L., Gong, J.H., Park, S.H., Kang, Y.H., 2015. Inhibition of osteoclast activation by phloretin through disturbing α v β 3 integrin-c-Src pathway. BioMed Res Int 2015. https://doi.org/10.1155/2015/680145

Lees, R.L., Sabharwal, V.K., Heersche, J.N.M., 2001. Resorptive state and cell size influence intracellular pH regulation in rabbit osteoclasts cultured on collagen-hydroxyapatite films. Bone 28, 187–194. https://doi.org/10.1016/S8756-3282(00)00433-6

Lequin, R.M., 2005. Enzyme immunoassay (EIA)/enzyme-linked immunosorbent assay (ELISA). Clin Chem 51, 2415–2418. https://doi.org/10.1373/clinchem.2005.051532

Li, Y., Kilian, K.A., 2015. Bridging the gap: from 2D cell culture to 3D microengineered extracellular matrices. Adv Healthc Mater 4, 2780–96. https://doi.org/10.1002/adhm.201500427

Liao, C.C., Wu, C.Y., Lin, M.H., Hsieh, F.K., Hsu, L.T., Chang, S.Y., Chen, K.J., Huang, H.T., Hsu, H.C., Lin, C.H., Lin, P.J., Lai, H.M., Kojima, H., Todo, H., Lin, S.J., Li, J.H., Chen, W., 2021. Validation study of a new reconstructed human epidermis model EPiTRI for in vitro skin irritation test according to OECD guidelines. Toxicol In Vitro 75. https://doi.org/10.1016/j.tiv.2021.105197

Lindner, U., Kramer, J., Rohwedel, J., Schlenke, P., 2010. Mesenchymal stem or stromal cells: Toward a better understanding of their biology? Transfus Med Hemotherapy. https://doi.org/10.1159/000290897

Lodoso-Torrecilla, I., van Gestel, N.A.P., Diaz-Gomez, L., Grosfeld, E.C., Laperre, K., Wolke, J.G.C., Smith, B.T., Arts, J.J., Mikos, A.G., Jansen, J.A., Hofmann, S., van den Beucken, J.J.J.P., 2018. Multimodal pore formation in calcium phosphate cements. J Biomed Mater Res - Part A 106, 500–509. https://doi.org/10.1002/jbm.a.36245

Loomer, P.M., Ellen, R.P., Tenenbaum, H.C., 1998. Osteogenic and osteoclastic cell interaction: development of a co-culture system. Cell Tissue Res 294, 99–108.

Lord, D.K., Cross, N.C.P., Bevilacqua, M.A., Rider, S.H., Gorman, P.A., Groves, A. V., Moss, D.W., Sheer, D., Cox, T.M., 1990. Type 5 acid phosphatase: Sequence, expression and chromosomal localization of a differentiation-associated protein of the human macrophage. Eur J Biochem 189, 287–293. https://doi.org/10.1111/j.1432-1033.1990.tb15488.x

Ma, J., Both, S.K., Yang, F., Cui, F.-Z., Pan, J., Meijer, G.J., Jansen, J.A., van den Beucken, J.J.J.P., 2014. Concise review: cell-based strategies in bone tissue engineering and regenerative medicine. Stem cells Transl Med 3, 98–107. https://doi.org/10.5966/sctm.2013-0126

Manolagas, S.C., 2000. Birth and death of bone cells: basic regulatory mechanisms and implications for the pathogenesis and treatment of osteoporosis. Endocr Rev 21, 115–37. https://doi.org/10.1210/edrv.21.2.0395

Manolagas, S.C., Parfitt, A.M., 2010. What old means to bone. Trends Endocrinol Metab. https://doi.org/10.1016/j.tem.2010.01.010

Marino, S., Logan, J.G., Mellis, D., Capulli, M., 2014. Generation and culture of osteoclasts. Bonekey Rep 3, 570. https://doi.org/10.1038/bonekey.2014.65

Mather, J.P., 1998. Making informed choices: Medium, serum, and serum-free medium how to choose the appropriate medium and culture system for the model you wish to create. Methods Cell Biol 57, 19–30. https://doi.org/10.1016/s0091-679x(08)61569-1

Matsuo, K., Irie, N., 2008. Osteoclast-osteoblast communication. Arch Biochem Biophys 473, 201–209. https://doi.org/10.1016/j.abb.2008.03.027

McDonald, M.M., Khoo, W.H., Ng, P.Y., Xiao, Y., Zamerli, J., Thatcher, P., Kyaw, W., Pathmanandavel, K., Grootveld, A.K., Moran, I., Butt, D., Nguyen, A., Warren, S., Biro, M., Butterfield, N.C., Guilfoyle, S.E., Komla-Ebri, D., Dack, M.R.G., Dewhurst, H.F., Logan, J.G., Li, Y., Mohanty, S.T., Byrne, N., Terry, R.L., Simic, M.K., Chai, R., Quinn, J.M.W., Youlten, S.E., Pettitt, J.A., Abi-Hanna, D., Jain, R., Weninger, W., Lundberg, M., Sun, S., Ebetino, F.H., Timpson, P., Lee, W.M., Baldock, P.A., Rogers, M.J., Brink, R., Williams, G.R., Bassett, J.H.D., Kemp, J.P., Pavlos, N.J., Croucher, P.I., Phan, T.G., 2021. Osteoclasts recycle via osteomorphs during RANKL-stimulated bone resorption. Cell 184, 1330-1347.e13. https://doi.org/10.1016/j.cell.2021.02.002

Meinel, L., Fajardo, R., Hofmann, S., Langer, R., Chen, J., Snyder, B., Vunjak-Novakovic, G., Kaplan, D., 2005. Silk implants for the healing of critical size bone defects. Bone 37, 688–698. https://doi.org/10.1016/j.bone.2005.06.010

Melke, J., 2019. Environmental stimuli for controlled bone tissue engineering applications. Eindhoven University of Technology.

Melke, J., Midha, S., Ghosh, S., Ito, K., Hofmann, S., 2016. Silk fibroin as biomaterial for bone tissue engineering. Acta Biomater. https://doi.org/10.1016/j.actbio.2015.09.005

Melke, J., Zhao, F., van Rietbergen, B., Ito, K., Hofmann, S., 2018. Localisation of mineralised tissue in a complex spinner flask environment correlates with predicted wall shear stress level localisation. Eur Cell Mater 36, 57–68. https://doi.org/10.22203/eCM.v036a05

Mollentze, J., Durandt, C., Pepper, M.S., 2021. An in Vitro and in Vivo Comparison of Osteogenic Differentiation of Human Mesenchymal Stromal/Stem Cells. Stem Cells Int. https://doi.org/10.1155/2021/9919361

Montagutelli, X., 2015. Animal models are essential to biological research: issues and perspectives. Futur Sci OA 1. https://doi.org/10.4155/FSO.15.63

Motiur Rahman, M., Takeshita, S., Matsuoka, K., Kaneko, K., Naoe, Y., Sakaue-Sawano, A., Miyawaki, A., Ikeda, K., 2015. Proliferation-coupled osteoclast differentiation by RANKL: Cell density as a determinant of osteoclast formation. Bone 81, 392–399. https://doi.org/10.1016/j.bone.2015.08.008

Nakamura, I., Duong, L.T., Rodan, S.B., Rodan, G.A., 2007. Involvement of αvβ3 integrins in osteoclast function. J Bone Miner Metab 25, 337–344. https://doi.org/10.1007/s00774-007-0773-9

Nandakumar, A., Barradas, A., de Boer, J., Moroni, L., van Blitterswijk, C., Habibovic, P., 2013. Combining technologies to create bioactive hybrid scaffolds for bone tissue engineering. Biomatter 3. https://doi.org/10.4161/biom.23705

Nazarov, R., Jin, H.-J., Kaplan, D.L., 2004. Porous 3-D scaffolds from regenerated silk fibroin. Biomacromolecules 5, 718–726. https://doi.org/10.1021/bm034327e

O'Brien, F.J., 2011. Biomaterials & scaffolds for tissue engineering. Mater Today 14, 88–95. https://doi.org/10.1016/S1369-7021(11)70058-X

Offeddu, G.S., Mohee, L., Cameron, R.E., 2020. Scale and structure dependent solute diffusivity within microporous tissue engineering scaffolds. J Mater Sci Mater Med 31, 1–11. https://doi.org/10.1007/s10856-020-06381-x

Ouzzani, M., Hammady, H., Fedorowicz, Z., Elmagarmid, A., 2016. Rayyan-a web and mobile app for systematic reviews. Syst Rev 5, 210. https://doi.org/10.1186/s13643-016-0384-4

Owen, R., Reilly, G.C., 2018. In vitro Models of Bone Remodelling and Associated Disorders. Front Bioeng Biotechnol 6, 134. https://doi.org/10.3389/FBIOE.2018.00134

Pang, H., Wu, X.H., Fu, S.L., Luo, F., Zhang, Z.H., Hou, T.Y., Li, Z.Q., Chang, Z.Q., Yu, B., Xu, J.Z., 2013. Co-culture with endothelial progenitor cells promotes survival, migration, and differentiation of osteoclast precursors. Biochem Biophys Res Commun 430, 729–734. https://doi.org/10.1016/j.bbrc.2012.11.081

Papadimitropoulos, A., Scherberich, A., Guven, S., Theilgaard, N., Crooijmans, H.J., Santini, F., Scheffler, K., Zallone, A., Martin, I., 2011. A 3D in vitro bone organ model using human progenitor cells. Eur Cell Mater 21, 445–58.

Parfitt, A.M., 1994. Osteonal and hemi-osteonal remodeling: The spatial and temporal framework for signal traffic in adult human bone. J Cell Biochem 55, 273–286. https://doi.org/10.1002/jcb.240550303

Parfitt, A.M., 1977. The cellular basis of bone turnover and bone loss. A rebuttal of the osteocytic resorption, bone flow theory. Clin Orthop NO. 127, 236–247.

Park, J.K., Askin, F., Giles, J.T., Halushka, M.K., Rosen, A., Levine, S.M., 2012. Increased Generation of TRAP Expressing Multinucleated Giant Cells in Patients with Granulomatosis with Polyangiitis. PLoS ONE 7, e42659. https://doi.org/10.1371/journal.pone.0042659

Park, Y.K., Heo, S.J., Koak, J.Y., Park, G.S., Cho, T.J., Kim, S.K., Cho, J., 2019. Characterization and differentiation of circulating blood mesenchymal stem cells and the role of phosphatidylinositol 3-kinase in modulating the adhesion. Int J Stem Cells 12, 265–278. https://doi.org/10.15283/ijsc18136

Paschos, N.K., Brown, W.E., Eswaramoorthy, R., Hu, J.C., Athanasiou, K.A., 2015. Advances in tissue engineering through stem cell-based co-culture. J Tissue Eng Regen Med 9, 488–503. https://doi.org/10.1002/term.1870

Pathak, J.L., Bravenboer, N., Luyten, F.P., Verschueren, P., Lems, W.F., Klein-Nulend, J., Bakker, A.D., 2015. Mechanical loading reduces inflammation-induced human osteocyte-to-osteoclast communication. Calcif Tissue Int 97, 169–78. https://doi.org/10.1007/s00223-015-9999-z

Perrotti, V., Nicholls, B.M., Horton, M.A., Piattelli, A., 2009. Human osteoclast formation and activity on a xenogenous bone mineral. J Biomed Mater Res A 90, 238–246. https://doi.org/10.1002/jbm.a.32079

Pittenger, M.F., Mackay, A.M., Beck, S.C., Jaiswal, R.K., Douglas, R., Mosca, J.D., Moorman, M.A., Simonetti, D.W., Craig, S., Marshak, D.R., 1999. Multilineage potential of adult human mesenchymal stem cells. Science 284, 143–7.

Place, T.L., Domann, F.E., Case, A.J., 2017. Limitations of oxygen delivery to cells in culture: An underappreciated problem in basic and translational research. Free Radic Biol Med. https://doi.org/10.1016/j.freeradbiomed.2017.10.003

Ratcliffe, A., 2007. Industrial approaches in tissue engineering, Translational Approaches in Tissue Engineering and Regenerative Medicine. Artech.

Remmers, S., Mayer, D., Melke, J., Ito, K., Hofmann, S., 2020. Measuring mineralised tissue formation and resorption in a human 3d osteoblast-osteoclast co-culture model. Eur Cell Mater 40, 189–202. https://doi.org/10.22203/eCM.v040a12

Remmers, S.J.A., de Wildt, B.W.M., Vis, M.A.M., Spaander, E.S.R., de Vries, R.B.M., Ito, K., Hofmann, S., 2021. Osteoblast-osteoclast co-cultures: A systematic review and map of available literature. PLoS ONE 16, e0257724. https://doi.org/10.1371/journal.pone.0257724

Remmers, S.J.A., van der Heijden, F.C., de Wildt, B.W.M., Ito, K., Hofmann, S., 2023a. Tuning the resorption-formation balance in an in vitro 3D osteoblast-osteoclast co-culture model of bone. Bone Reports 18, 101646. https://doi.org/10.1016/j.bonr.2022.101646

Remmers, S.J.A., van der Heijden, F.C., Ito, K., Hofmann, S., 2023b. The effects of seeding density and osteoclastic supplement concentration on osteoclastic differentiation and resorption. Bone Reports 18, 101651. https://doi.org/10.1016/j.bonr.2022.101651

Remmers, S.J.A., Wildt, B.W.M., Vis, M.V.A., Spaander, E.S.R., de Vries, R., Hofmann, S., Ito, K., 2020. Osteoblast-osteoclast co-culture models of bone-remodelling: A systematic review protocol [WWW Document]. https://doi.org/10.5281/ZENODO.3969441

Ross, F.P., 2006. M-CSF, c-Fms, and signaling in osteoclasts and their precursors. Ann N Y Acad Sci 1068, 110–116. https://doi.org/10.1196/annals.1346.014

Ross, N.T., Wilson, C.J., 2014. In vitro clinical trials: The future of cell-based profiling. Front Pharmacol 5 MAY. https://doi.org/10.3389/fphar.2014.00121

Rossi, E., Mracsko, E., Papadimitropoulos, A., Allafi, N., Reinhardt, D., Mehrkens, A., Martin, I., Knuesel, I., Scherberich, A., 2018. An In Vitro Bone Model to Investigate the Role of Triggering Receptor Expressed on Myeloid Cells-2 in Bone Homeostasis. Tissue Eng Part C Methods 24, 391–398.

Rucci, N., Zallone, A., Teti, A., 2019. Isolation and generation of osteoclasts, in: Methods in Molecular Biology. Humana Press Inc., pp. 3–19. https://doi.org/10.1007/978-1-4939-8997-3_1

Rumpler, M., Würger, T., Roschger, P., Zwettler, E., Sturmlechner, I., Altmann, P., Fratzl, P., Rogers, M.J., Klaushofer, K., 2013. Osteoclasts on bone and dentin in vitro: mechanism of trail formation and comparison of resorption behavior. Calcif Tissue Int 93, 526–39. https://doi.org/10.1007/s00223-013-9786-7

Salamanna, F., Maglio, M., Borsari, V., Giavaresi, G., Aldini, N.N., Fini, M., 2016. Peripheral Blood Mononuclear Cells Spontaneous Osteoclastogenesis: Mechanisms Driving the Process and Clinical Relevance in Skeletal Disease. J Cell Physiol 231, 521–530. https://doi.org/10.1002/jcp.25134

Samal, S.K., Dash, M., Declercq, H.A., Gheysens, T., Dendooven, J., Voort, P. Van Der, Cornelissen, R., Dubruel, P., Kaplan, D.L., 2014. Enzymatic mineralization of silk scaffolds. Macromol Biosci 14, 991–1003. https://doi.org/10.1002/mabi.201300513

Schindelin, J., Arganda-Carreras, I., Frise, E., Kaynig, V., Longair, M., Pietzsch, T., Preibisch, S., Rueden, C., Saalfeld, S., Schmid, B., Tinevez, J.Y., White, D.J., Hartenstein, V., Eliceiri, K., Tomancak, P., Cardona, A., 2012. Fiji: An open-source platform for biological-image analysis. Nat Methods. https://doi.org/10.1038/nmeth.2019

Schneider, C.A., Rasband, W.S., Eliceiri, K.W., 2012. NIH Image to ImageJ: 25 years of image analysis. Nat Methods. https://doi.org/10.1038/nmeth.2089

Schroder, H.C., Wang, X.H., Wiens, M., Diehl-Seifert, B., Kropf, K., Schlossmacher, U., Muller, W.E., 2012. Silicate modulates the cross-talk between osteoblasts (SaOS-2) and osteoclasts (RAW 264.7 cells): inhibition of osteoclast growth and differentiation. J Cell Biochem 113, 3197–3206.

Schulte, F.A., Lambers, F.M., Kuhn, G., Muller, R., 2011a. In vivo micro-computed tomography allows direct three-dimensional quantification of both bone formation and bone resorption parameters using time-lapsed imaging. Bone 48, 433–442. https://doi.org/10.1016/j.bone.2010.10.007

Schulte, F.A., Lambers, F.M., Webster, D.J., Kuhn, G., Muller, R., 2011b. In vivo validation of a computational bone adaptation model using open-loop control and time-lapsed micro-computed tomography. Bone 49, 1166–1172. https://doi.org/10.1016/j.bone.2011.08.018

Shah, F.A., Ruscsák, K., Palmquist, A., 2019. 50 years of scanning electron microscopy of bone—a comprehensive overview of the important discoveries made and insights gained into bone material properties in health, disease, and taphonomy. Bone Res 7, 15. https://doi.org/10.1038/s41413-019-0053-z

Shahdadfar, A., Frønsdal, K., Haug, T., Reinholt, F.P., Brinchmann, J.E., 2005. In Vitro Expansion of Human Mesenchymal Stem Cells: Choice of Serum Is a Determinant of Cell Proliferation, Differentiation, Gene Expression, and Transcriptome Stability. Stem Cells 23, 1357–1366. https://doi.org/10.1634/stemcells.2005-0094

Shetty, S., Kapoor, N., Bondu, J., Thomas, N., Paul, T., 2016. Bone turnover markers: Emerging tool in the management of osteoporosis. Indian J Endocrinol Metab. https://doi.org/10.4103/2230-8210.192914

Sheu, T.J., Schwarz, E.M., Martinez, D.A., O'Keefe, R.J., Rosier, R.N., Zuscik, M.J., Puzas, J.E., 2003. A phage display technique identifies a novel regulator of cell differentiation. J Biol Chem 278, 438–443. https://doi.org/10.1074/jbc.M208292200

Sibonga, J.D., 2013. Spaceflight-induced bone loss: Is there an Osteoporosis Risk? Curr Osteoporos Rep 11, 92–98. https://doi.org/10.1007/s11914-013-0136-5

Sieberath, A., Bella, E. Della, Ferreira, A.M., Gentile, P., Eglin, D., Dalgarno, K., 2020. A comparison of osteoblast and osteoclast in vitro co-culture models and their translation for preclinical drug testing applications. Int J Mol Sci. https://doi.org/10.3390/ijms21030912

Simonet, W.S., Lacey, D.L., Dunstan, C.R., Kelley, M., Chang, M.S., Lüthy, R., Nguyen, H.Q., Wooden, S., Bennett, L., Boone, T., Shimamoto, G., DeRose, M., Elliott, R., Colombero, A., Tan, H.L., Trall, G., Sullivan, J., Davy, E., Bucay, N., Renshaw-Gegg, L., Hughes, T.M., Hill, D., Pattison, W., Campbell, P., Sander, S., Van, G., Tarpley, J., Derby, P., Lee, R., Boyle, W.J., 1997. Osteoprotegerin: A novel secreted protein involved in the regulation of bone density. Cell 89, 309–319. https://doi.org/10.1016/S0092-8674(00)80209-3

Sims, N.A., Gooi, J.H., 2008. Bone remodeling: Multiple cellular interactions required for coupling of bone formation and resorption. Semin Cell Dev Biol 19, 444–451. https://doi.org/10.1016/j.semcdb.2008.07.016

Song, C., Yang, X., Lei, Y., Zhang, Z., Smith, W., Yan, J., Kong, L., 2019. Evaluation of efficacy on RANKL induced osteoclast from RAW264.7 cells. J Cell Physiol 234, 11969–11975. https://doi.org/10.1002/jcp.27852

Suda, T., Takahashi, N., Udagawa, N., Jimi, E., Gillespie, M.T., Martin, T.J., 1999. Modulation of osteoclast differentiation and function by the new members of the tumor necrosis factor receptor and ligand families. Endocr Rev. https://doi.org/10.1210/edrv.20.3.0367

Susa, M., Luong-Nguyen, N.-H., Cappellen, D., Zamurovic, N., Gamse, R., 2004. Human primary osteoclasts: in vitro generation and applications as pharmacological and clinical assay. J Transl Med 2, 6. https://doi.org/10.1186/1479-5876-2-6

Swearengen, J.R., 2018. Choosing the right animal model for infectious disease research. Anim Model Exp Med 1, 100–108. https://doi.org/10.1002/ame2.12020

Takahashi, N., Akatsu, T., Udagawa, N., Sasaki, T., Yamaguchi, A., Moseley, J.M., Martin, T.J., Suda, T., 1988. Osteoblastic cells are involved in osteoclast formation. Endocrinology 123, 2600–2. https://doi.org/10.1210/endo-123-5-2600

Takahashi, N., Udagawa, N., Suda, T., 1999. A New Member of Tumor Necrosis Factor Ligand Family, ODF/OPGL/TRANCE/RANKL, Regulates Osteoclast Differentiation and Function. Biochem Biophys Res Commun 256, 449–455. https://doi.org/10.1006/bbrc.1999.0252

Tang, Y., Wu, X., Lei, W., Pang, L., Wan, C., Shi, Z., Zhao, L., Nagy, T.R., Peng, X., Hu, J., Feng, X., Van Hul, W., Wan, M., Cao, X., 2009. TGF-β1–induced migration of bone mesenchymal stem cells couples bone resorption with formation. Nat Med 15, 757–765. https://doi.org/10.1038/nm.1979

Teitelbaum, S.L., 2000. Bone resorption by osteoclasts. Science 289, 1504–8.

Teti, A., Grano, M., Colucci, S., Cantatore, F.P., Loperfido, M.C., Zallone, A.Z., 1991. Osteoblast-osteoclast relationships in bone resorption: osteoblasts enhance osteoclast activity in a serum-free co-culture system. Biochem Biophys Res Commun 179, 634–640.

Thomas, D.W., Burns, J., Audette, J., Adam Carroll, Dow-Hygelund, C., Hay, M., 2016. Clinical Development Success Rates 2006-2015.

Toyosaki-Maeda, T., Takano, H., Tomita, T., Tsuruta, Y., Maeda-Tanimura, M., Shimaoka, Y., Takahashi, T., Itoh, T., Suzuki, R., Ochi, T., 2001. Differentiation of monocytes into multinucleated giant bone-resorbing cells: Two-step differentiation induced by nurse-like cells and cytokines. Arthritis Res 3, 306–310. https://doi.org/10.1186/ar320

Tsukada, M., Gotoh, Y., Nagura, M., Minoura, N., Kasai, N., Freddi, G., 1994. Structural changes of silk fibroin membranes induced by immersion in methanol aqueous solutions. J Polym Sci Part B Polym Phys 32, 961–968. https://doi.org/10.1002/polb.1994.090320519

Udagawa, N., Takahashi, N., Akatsu, T., Tanaka, H., Sasaki, T., Nishihara, T., Koga, T., Martin, T.J., Suda, T., 1990. Origin of osteoclasts: mature monocytes and macrophages are capable of differentiating into osteoclasts under a suitable microenvironment prepared by bone marrow-derived stromal cells. Proc Natl Acad Sci U S A 87, 7260–4. https://doi.org/10.1073/pnas.87.18.7260

Urist, M.R., 1965. Bone: Formation by autoinduction. Science 150, 893–899. https://doi.org/10.1126/science.150.3698.893

van der Valk, J., Bieback, K., Buta, C., Cochrane, B., Dirks, W.G., Fu, J., Hickman, J.J., Hohensee, C., Kolar, R., Liebsch, M., Pistollato, F., Schulz, M., Thieme, D., Weber, T., Wiest, J., Winkler, S., Gstraunthaler, G., 2018. Fetal Bovine Serum (FBS): Past - Present - Future. ALTEX 35, 99–118. https://doi.org/10.14573/altex.1705101

Van Gestel, N.A.P., Geurts, J., Hulsen, D.J.W., Van Rietbergen, B., Hofmann, S., Arts, J.J., 2015. Clinical Applications of S53P4 Bioactive Glass in Bone Healing and Osteomyelitic Treatment: A Literature Review. BioMed Res Int. https://doi.org/10.1155/2015/684826

Varghese, B.J., Aoki, K., Shimokawa, H., Ohya, K., Takagi, Y., 2006. Bovine deciduous dentine is more susceptible to osteoclastic resorption than permanent dentine: results of quantitative analyses. J Bone Miner Metab 24, 248–54. https://doi.org/10.1007/s00774-005-0679-3

Vassey, M.J., Figueredo, G.P., Scurr, D.J., Vasilevich, A.S., Vermeulen, S., Carlier, A., Luckett, J., Beijer, N.R.M., Williams, P., Winkler, D.A., de Boer, J., Ghaemmaghami, A.M., Alexander, M.R., 2020. Immune Modulation by Design: Using Topography to Control Human Monocyte Attachment and Macrophage Differentiation. Adv Sci 7. https://doi.org/10.1002/advs.201903392

Vaughan, A., Guilbault, G.G., Hackney, D., 1971. Fluorometric methods for analysis of acid and alkaline phosphatase. Anal Chem 43, 721–724. https://doi.org/10.1021/ac60301a001

Vis, M.A.M., Ito, K., Hofmann, S., 2020. Impact of Culture Medium on Cellular Interactions in in vitro Co-culture Systems. Front Bioeng Biotechnol 8, 911. https://doi.org/10.3389/fbioe.2020.00911

Wiedmann-Al-Ahmad, M., Gutwald, R., Lauer, G., Hübner, U., Schmelzeisen, R., 2002. How to optimize seeding and culturing of human osteoblast-like cells on various biomaterials. Biomaterials 23, 3319–3328. https://doi.org/10.1016/S0142-9612(02)00019-4

Wierzchos, J., Falcioni, T., Kiciak, A., Woliński, J., Koczorowski, R., Chomicki, P., Porembska, M., Ascaso, C., 2008. Advances in the ultrastructural study of the implant–bone interface by backscattered electron imaging. Micron 39, 1363–1370. https://doi.org/10.1016/j.micron.2008.01.022

Wijenayaka, A.R., Kogawa, M., Lim, H.P., Bonewald, L.F., Findlay, D.M., Atkins, G.J., 2011. Sclerostin stimulates osteocyte support of osteoclast activity by a RANKL-dependent pathway. PLoS ONE 6, e25900. https://doi.org/10.1371/journal.pone.0025900

Wu, S., Liu, X., Yeung, K.W.K., Liu, C., Yang, X., 2014. Biomimetic porous scaffolds for bone tissue engineering. Mater Sci Eng R Reports. https://doi.org/10.1016/j.mser.2014.04.001

Xian, L., Wu, X., Pang, L., Lou, M., Rosen, C.J., Qiu, T., Crane, J., Frassica, F., Zhang, L., Rodriguez, J.P., Jia, X., Yakar, S., Xuan, S., Efstratiadis, A., Wan, M., Cao, X., 2012. Matrix IGF-1 maintains bone mass by activation of mTOR in mesenchymal stem cells. Nat Med 18, 1095–1101. https://doi.org/10.1038/nm.2793

Xiong, J., Piemontese, M., Onal, M., Campbell, J., Goellner, J.J., Dusevich, V., Bonewald, L., Manolagas, S.C., O'Brien, C.A., 2015. Osteocytes, not osteoblasts or lining cells, are the main source of the RANKL required for osteoclast formation in remodeling bone. PLoS ONE 10. https://doi.org/10.1371/journal.pone.0138189

Xu, F., Teitelbaum, S.L., 2013. Osteoclasts: New Insights. Bone Res 1, 11–26. https://doi.org/10.4248/BR201301003

Xu, L., Li, G., 2014. Circulating mesenchymal stem cells and their clinical implications. J Orthop Transl.

https://doi.org/10.1016/j.jot.2013.11.002

Yamada, N., Tsujimura, T., Ueda, H., Hayashi, S.-I., Ohyama, H., Okamura, H., Terada, N., 2005. Down-regulation of osteoprotegerin production in bone marrow macrophages by macrophage colony-stimulating factor. Cytokine 31, 288–297. https://doi.org/10.1016/j.cyto.2005.03.009

Yang, B., Zhou, H., Zhang, X.-D., Liu, Z., Fan, F.-Y., Sun, Y.-M., 2012. Effect of radiation on the expression of osteoclast marker genes in RAW264.7 cells. Mol Med reports 5, 955–8. https://doi.org/10.3892/mmr.2012.765

Yang, Jing, Qiao, M., Li, Y., Hu, G., Song, C., Xue, L., Bai, H., Yang, Jie, Yang, X., 2018. Expansion of a population of large monocytes (atypical monocytes) in peripheral blood of patients with acute exacerbations of chronic obstructive pulmonary diseases. Mediators Inflamm 2018, 1–13. https://doi.org/10.1155/2018/9031452

Yasuda, H., Shima, N., Nakagawa, N., Yamaguchi, K., Kinosaki, M., Mochizuki, S., Tomoyasu, A., Yano, K., Goto, M., Murakami, A., Tsuda, E., Morinaga, T., Higashio, K., Udagawa, N., Takahashi, N., Suda, T., 1998. Osteoclast differentiation factor is a ligand for osteoprotegerin/osteoclastogenesis-inhibitory factor and is identical to TRANCE/RANKL. Proc Natl Acad Sci U S A 95, 3597–602.

Yoshida, H., Hayashi, S.-I., Kunisada, T., Ogawa, M., Nishikawa, S., Okamura, H., Sudo, T., Shultz, L.D., Nishikawa, S.-I., 1990. The murine mutation osteopetrosis is in the coding region of the macrophage colony stimulating factor gene. Nature 345, 442–444. https://doi.org/10.1038/345442a0

Young, P.S., Tsimbouri, P.M., Gadegaard, N., Meek, R., Dalby, M.J., 2015. Osteoclastogenesis/osteoblastogenesis using human bone marrow-derived cocultures on nanotopographical polymer surfaces. Nanomedicine (London, England) 10, 949–57. https://doi.org/10.2217/nnm.14.146

Yuan, H., De Bruijn, J.D., Li, Y., Feng, J., Yang, Z., De Groot, K., Zhang, X., 2001a. Bone formation induced by calcium phosphate ceramics in soft tissue of dogs: A comparative study between porous α-TCP and β-TCP. J Mater Sci Mater Med 12, 7–13. https://doi.org/10.1023/A:1026792615665

Yuan, H., De Bruijn, J.D., Zhang, X., Van Blitterswijk, C.A., De Groot, K., 2001b. Bone induction by porous glass ceramic made from Bioglass® (45S5). J Biomed Mater Res 58, 270–276. https://doi.org/10.1002/1097-4636(2001)58:3<270::AID-JBM1016>3.0.CO;2-2

Zhu, S., Ehnert, S., Rouß, M., Häussling, V., Aspera-Werz, R.H., Chen, T., Nussler, A.K., 2018. From the clinical problem to the basic research—co-culture models of osteoblasts and osteoclasts. Int J Mol Sci 19. https://doi.org/10.3390/ijms19082284

Curriculum Vitae

Stefan Remmers was born on 23-11-1989 in Tilburg. After finishing the Gymnasium in 2008 at the St.-Willibrord Gymnasium in Deurne, the Netherlands, he studied Biomedical Sciences at the Radboud University in Nijmegen, the Netherlands. He concluded his Bachelor thesis at the Orthopedic Research Laboratory in Nijmegen where he used Finite Element modelling to study the design of meniscus prostheses. During his Master's in Biomedical Sciences, he did an externship in Heidelberg, Germany at the Universitätsklinikum Heidelberg, studying the mechanobiology of uniaxial strain on mesenchymal stromal cells. During his final year, he participated in an 'Honours Master Programme' at the Radboud Honours Academy, in which he studied 'The Future of Healthcare' with a year-long international interdisciplinary thinktank. In 2014, he graduated within the Biomaterials group at the Radboud University on the development of antibacterial nanofiber membranes and wound dressings. In the same year he supervised the 'class of 2015' of his former Honours Programme and started a PhD project within the department of Biomedical Engineering at the Eindhoven University of Technology in Eindhoven, the Netherlands of which the results are presented in this dissertation. In 2015, he won the 'best oral presentation' award at the Netherlands Society for Biomaterals and Tissue Engineering annual meeting. In 2019 he was awarded a ZonMW research grant to conduct a systematic review as part of the 'Meer Kennis Minder Dieren' program. Since 2020 he is employed at ASML in the DUV System Integration group, where he works on developing some of the most complex machines found on planet earth.

List of Publications

9.1 Publication related to this thesis

Remmers, S.J.A., Mayer, D., Melke, J., Ito, K., Hofmann, S., 2020. Measuring mineralised tissue formation and resorption in a human 3d osteoblast-osteoclast co-culture model. Eur Cell Mater 40, 189–202. https://doi.org/10.22203/eCM.v040a12

Remmers, S.J.A., de Wildt, B.W.M., Vis, M.A.M., Spaander, E.S.R., de Vries, R.B.M., Ito, K., Hofmann, S., 2021. Osteoblast-osteoclast co-cultures: A systematic review and map of available literature. PLoS ONE 16, e0257724. https://doi.org/10.1371/journal.pone.0257724

Remmers, S.J.A., van der Heijden, F.C., de Wildt, B.W.M., Ito, K., Hofmann, S., 2023. Tuning the resorption-formation balance in an in vitro 3D osteoblast-osteoclast co-culture model of bone. Bone Reports 18, 101646. https://doi.org/10.1016/j.bonr.2022.101646

Remmers, S.J.A., van der Heijden, F.C., Ito, K., Hofmann, S., 2023. The effects of seeding density and osteoclastic supplement concentration on osteoclastic differentiation and resorption. Bone Reports 18, 101651. https://doi.org/10.1016/j.bonr.2022.101651

9.2 Other publications

Song, J., Remmers, S.J.A., Shao, J., Kolwijck, E., Walboomers, X.F., Jansen, J.A., Leeuwenburgh, S.C.G., Yang, F. Antibacterial effects of electrospun chitosan/poly(ethylene oxide) nanofibrous membranes loaded with chlorhexidine and silver. Nanomedicine Nanotechnology, Biol Med 12, 1357–1364 (2016). https://doi.org/10.1016/j.nano.2016.02.005

Remmers, S.J.A., Song, J. & Yang, F. Development and characterization of an antibacterial electrospun nanofiber wound dressing. Radboud Ann Med Students 1, 15–21 (2015)

9

Acknowledgements

This great journey has finally come to an end. I could never have done this without the help and support of many people, and I want to take this opportunity to thank them.

Dear Sandra, thank you for everything. I have learned so much in the last years and having you as promotor most definitely helped a lot. You cared not only about the work, but at least just as much about the people doing the work. Even when I lost faith in myself, you were able to convince me that I had it in me to finish this thesis. And guess what: You were right! Dear Keita, the last three years I've been working on this thesis from home in the evenings and weekends exclusively, which made any type of communication and discussion a lot more challenging than it should have been. I was always pleasantly surprised that no matter on what day and at what time, I usually got a thorough response to my questions way sooner than expected.

I would also like to thank the committee members for reading and evaluating this thesis and accepting to be on my committee. Dear Pamela, Jan, Jenneke, Chris and Jeroen. Thank you so much for helping me complete the final phase of my PhD.

I would like to thank all the other people that facilitated or helped me do my research. I could not have done it with you. My co-authors: Dominik, Freek, Johanna, Bregje, Michelle, Rob, and Eva. Thanks for helping me do awesome science and writing these manuscripts with me. Bert, Janneke, Wendy, Evelien, Moniek, Ginny, Yuana, Sylvia, Marina, Marloes, Jurgen, Mark and Manon, thank you for all the help and support. To all office mates from Gem-Z 4.12: Anne, Bart, Bente, Dina, Dylan, Elias, Irene, Jordy, Laura, Marjan, Nicole, Maike, Marc, Mathieu, Pim, Renate Ronald, (andere) Stefan, Suzanne, Talita, Thomas, Willeke. And thank you to all others OPB and BMT people I that I did not mention by name.

10

And of course, I could not have done this without the support of my friends and family. Above all, my parents: Chris and Cornelli. Without your continuous support I would never have made it through the Gymnasium, Bachelor, Master and finally the PhD. Thanks for always supporting my choices, always helping me when I needed help, and just for always being there. Maarten, little brother. Despite all the stress from recent years, you still decided to step into my footsteps and do a PhD as well. I hope it goes smoother for you than it did for me. Thanks for being there when I did my PhD. I'll try to return the favor! Joren, by now we've known each other for 20 years already! Time really flies by. Thanks for showing interest in my work sometimes (well, most of the times really) from half a world apart. Luckily distance does not matter for playing online video games. You may not know much about this topic, but I'm still glad to have you as my paranymph! And Dominik, my second paranymph and co-author of my first publication of my PhD, I'm glad we stayed in touch after you returned back to Austria, and hope that we get to reach that 20-year milestone as well. My parents-in-law: Henk and Francis. You already thought I was crazy for torturing myself with doing a PhD when I was still getting paid to do it, let alone continuing for another 3 years in my own personal time during the weekends. Looking back, I agree, but I'm glad I finished it anyway. Although it was unfortunate to lose all those weekends, I did actually enjoy doing it, believe it or not.

To all my friends from all the bands: no matter what happened, music was always my way to blow off steam. Literally. Whether it was on trumpet, flugelhorn, trombone or sousaphone, music has always been and will always be the biggest highlight of my week. A special shoutout to harmonie Musis Sacrum Bakel, fanfare de Vooruitgang Stiphout, and above all, my friends at Doe Mar Wa Bakel. With this thesis finally done, many of you will be seeing more of me again.

And finally, Carlijn. The PhD has been a constant factor in our lives for most of our time together. While it started out OK, we've both had to overcome some serious issues related to physical and mental health. I know that especially the last three years have not been easy for you. Working 7 days a week to get those manuscripts published and eventually this thesis finished next to a full-time job, and even working longer hours in the weekends has put some serious strain on our relationship. Combined with all the other stuff going on this was no fun at all, but we made it. Thanks for sticking with me, and I promise that from now on, we can finally enjoy our lives without this constant pressure of the PhD above our heads.

And with that, this thesis is finished and the PhD over. That leaves me with just three more words to say, which by the time this sentence is read, are hopefully true:

Dr. Remmers out.